

Title	Sugar matrices in stabilization of bioactives by dehydration
Authors	Zhou, Yankun
Publication date	2013
Original Citation	Zhou, Y. 2013. Sugar matrices in stabilization of bioactives by dehydration. PhD Thesis, University College Cork.
Type of publication	Doctoral thesis
Rights	© 2013, Yankun Zhou - http://creativecommons.org/licenses/by-nc-nd/3.0/
Download date	2025-07-03 23:36:07
Item downloaded from	https://hdl.handle.net/10468/1027



UCC

University College Cork, Ireland
Coláiste na hOllscoile Corcaigh

Ni mOllscoil na hÉireann, Corcaigh

THE NATIONAL UNIVERSITY OF IRELAND

Coláiste na hOllscoile, Corcaigh

UNIVERSITY COLLEGE CORK



Sugar Matrices in Stabilization of Bioactives by Dehydration

A Thesis Submitted to School of Food and Nutritional Sciences, in
Fulfillment of the Requirements for the Degree of Doctor of Philosophy

Presented by

Yankun Zhou

B.Sc. in Food Science and Technology (University College Cork)

B.Sc. in Food Science and Engineering (Beijing Technology and Business University)

Under the Supervision of

Professor Yrjö H. Roos

March, 2013

DEDICATION

To my parents with love

ACKNOWLEDGEMENTS

On a day in September, 2008, I got the offer of PhD study in School of Food and Nutritional Sciences, University College Cork, from Professor Roos. That day was my 22nd birthday. Till now I still think the offer is one of the best presents I have ever received, and it has also changed my life dramatically.

I got the opportunity of doing research under one of the best experts in food materials science area; I was shown that one great scientist should be sensitive to see through the superficial to reach the core of the results and able to explain them; I learnt the ways of constructing small scientific observations into a meaningful whole piece; I was taught that the paper may not be perfect but one could always try his/her best to approach the perfection; I was encouraged to attend international conferences and to present my results in front of my peers in food science; I got the chance to meet people and to make friends worldwide. All but not limited to the above experiences that I have gained, I attribute them to my kind and professional supervisor, Professor Roos, who has not only opened me a door to scientific research but also inspired me in being a patient, helpful, and encouraging person to other people. I would like to give my sincere acknowledgement to Professor Roos for all that he has done to make me a better person professionally and mentally.

I am grateful to the external examiner Professor Stephan Drusch and to the internal examiner Dr. Thomas O'Connor for their detailed discussion on the research carried out. Their comments and suggestions have contributed to improve the quality of the present work and are greatly appreciated.

I would also like to thank Food Institutional Research Measure (FIRM) of the Department of Agriculture, Food and the Marine, Ireland for providing financial support on the "Bioactives Advanced Stabilization (BAS)" project (08RDC695), my tuition fees, conference travel, and scholarship.

Many thanks to the technicians and staff, in particular Dr. Kamrul Haque, Mr. Dave Waldron, Mr. Eddie Beatty, Mr. Donal Humphreys, and Mr. Jim McNamara, in the School of Food and Nutritional Sciences and Dr. Fatma Farag in the School of Pharmacy, for their kind help with the accesses to instruments and the guidance in operations.

Like doing any other thing, the joyful moments during my PhD are accompanied with difficulties. I appreciate the friendships I have received, which have made my PhD journey easier and unforgettable. Special thanks to my lab mates and friends Dr. Nattiga Silalai, Dr. Leonardo Cornacchia, and Ms. Naritchaya Potes, for their kindness and making me feel part of a family. To Amy Tran, Marie-Cécile Cuxac, Brian Mc Grath, Yinong Tian, Joyue Zhang, and Like Mao, thanks for listening to my worries and cheering me up. To my friends in China, “Bandon 15”, and Badminton club, thanks for helping me release all the stresses from work.

Finally, I would like to thank my loving family. I met my husband, Shilei, almost the same time as I started my PhD. He has always been patient and supportive through the difficult periods when I lost my motivation and confidence. He has witnessed and also been involved in my mental and psychological growth during my pursuit of this PhD. When six years ago I came to Ireland, I chose a life far away from my parents. However, their love and support have never faded away with the physical distance. My parents have made my life beautiful and full of possibilities. I feel happy and grateful of being their daughter.

“Thank you!” to everyone who joined my PhD journey and walked me here.

ABSTRACT

Development of functional foods with bioactive components requires component stability in foods and ingredients. Stabilization of sensitive bioactive components can be achieved by entrapment or encapsulation of these components in solid food matrices. Sugars are typical structure-forming materials which form an amorphous glass-like continuous phase. The bioactive components may exist within the continuous phase or in dispersed particles in the matrices and become protected from external stresses. The present study addressed the physical properties of the matrices and their effects on the stability of the bioactive components during storage.

Lactose or trehalose was used as the glass-forming material for the entrapment of hydrophilic vitamins (ascorbic acid or thiamine hydrochloride) or the encapsulation of oil particles containing a hydrophobic vitamin (α -tocopherol). In the delivery of hydrophobic components, milk protein isolate (MPI), soy protein isolate (SPI), or whey protein isolate (WPI) were used as emulsifiers and, in some cases, applied in excess amount to form matrices together with sugars. Dehydrated amorphous structures with bioactive components were produced by freezing and freeze-drying. The sugar-based dehydrated systems were characterized for water sorption and crystallization behavior using a gravimetric method, for glass transition and instant crystallization temperatures using Differential Scanning Calorimetry (DSC), for emulsion particle size and charge using light scattering Mastersizer or Zetasizer, and for retention of the bioactive components at various water activities and temperatures using spectrophotometer.

Experimental results in the present study indicated that: (i) lactose and trehalose showed similar water sorption and glass transition but very different crystallization behavior as pure sugars; (ii) the presence of hydrophilic vitamins and proteins contributed to the water sorption of sugar-based mixture systems; (iii) the glass transition of sugar-based systems was slightly affected by the presence of other components in anhydrous systems but followed closely that of sugar after water plasticization; (iv) sugar crystallization in mixture systems was composition-dependent and significantly affected by both hydrophilic and hydrophobic components via direct interaction or their presence as physical barriers; (v) the stability of bioactive components was better retained in the amorphous matrices, although small losses of stability were observed for hydrophilic components above glass transition and for hydrophobic components as a function of water activity; (vi) sugar crystallization caused significant loss of hydrophilic bioactive components as a result of the exclusion from the continuous crystalline phase; (vii) loss of hydrophobic bioactive components upon sugar crystallization was a result of dramatic change of emulsion properties and the exclusion of oil particles from the protecting structure. In the present study, the stability of hydrophobic components against sugar crystallization was improved by using double layer formulation during the preparation of emulsions. This indicated the importance of hydrophilic-hydrophobic interface composition in the stability of hydrophobic components in dehydrated systems.

The present study provides information on the physical and chemical stability of sugar-based dehydrated delivery systems, which could be helpful in designing foods and ingredients containing bioactive components with improved storage stability.

TABLE OF CONTENTS

DEDICATION	II
ACKNOWLEDGEMENTS	III
ABSTRACT	V
TABLE OF CONTENTS	VII
LIST OF TABLES	XII
LIST OF FIGURES	XIV
INTRODUCTION	1
CHAPTER 1	5
1.1 INTRODUCTION	5
1.2 ENCAPSULATION BY DEHYDRATION	7
1.2.1 Entrapment	8
1.2.2 Encapsulation	9
1.2.2.1 <i>Oil-in-water emulsion</i>	10
1.2.2.2 <i>Spray-drying</i>	12
1.2.2.3 <i>Freeze-drying</i>	13
1.2.2.4 <i>Microstructure of dehydrated emulsions</i>	15
1.3 GLASS TRANSITION AND CRYSTALLIZATION	17
1.3.1 Instant sugar crystallization	19
1.3.2 Sugar crystallization kinetics.....	20
1.3.3 Sugar crystallization and crystal forms	21
1.4 CHEMICAL STABILITY AND PHYSICAL STATE OF SOLIDS	24
1.4.1 Stability in amorphous phases	25
1.4.2 Stability as affected by structural changes	26

1.4.2.1	Collapse of matrices	26
1.4.2.2	Crystallization of sugars	27
1.5	CONCLUDING REMARKS.....	29
CHAPTER 2	31
2.1	INTRODUCTION	32
2.2	MATERIALS AND METHODS	34
2.2.1	Materials.....	34
2.2.2	Electrophoresis of proteins	35
2.2.3	Frozen state transitions and freeze-drying.....	35
2.2.4	Water sorption isotherms.....	37
2.2.5	Glass transition and crystallization by DSC	38
2.2.6	Prediction of the T_g and the critical water contents	39
2.3	RESULTS AND DISCUSSION	40
2.3.1	Electrophoresis of proteins	40
2.3.2	Frozen state transitions	41
2.3.3	Water sorption behavior	43
2.3.4	Glass transition and crystallization.....	49
2.3.5	The critical a_w values and nutrient delivery.....	53
2.4	CONCLUSIONS	55
CHAPTER 3	57
3.1	INTRODUCTION	58
3.2	MATERIALS AND METHODS	60
3.2.1	Materials.....	60
3.2.2	Water sorption and sorption isotherms	61
3.2.3	Thermal analysis	62
3.2.4	Prediction of the T_g and the critical water contents	63
3.2.5	Determination of vitamin contents	64
3.2.6	Statistics	67

3.3	RESULTS AND DISCUSSION	67
3.3.1	State transitions and stability in frozen systems	67
3.3.2	Water sorption and sorption isotherms	70
3.3.3	Glass transition and crystallization.....	75
3.3.4	Critical water content and water activity	77
3.3.5	Stability of vitamins in freeze-dried systems.....	78
3.3.6	Stabilization of vitamins: process and storage stability	82
3.4	CONCLUSIONS	86
CHAPTER 4	87
4.1	INTRODUCTION	88
4.2	MATERIALS AND METHODS	90
4.2.1	Materials.....	90
4.2.2	Preparation of emulsions and the freeze-dried materials.....	91
4.2.3	Characterization of the non-fat solids.....	92
4.2.3.1	<i>Water sorption and sorption isotherms.....</i>	<i>92</i>
4.2.3.2	<i>Glass transition and crystallization</i>	<i>93</i>
4.2.4	Oil droplet size distribution	94
4.2.5	Spectrophotometry of α -tocopherol.....	94
4.2.6	Storage of freeze-dried materials and stability of α -tocopherol	95
4.2.7	Statistics	96
4.3	RESULTS AND DISCUSSION	97
4.3.1	Water sorption and sorption isotherms	97
4.3.2	Glass transition and instant sugar crystallization.....	101
4.3.3	Oil droplet size distribution	105
4.3.4	Stability of α -tocopherol as affected by water activity	108
4.3.5	Matrices structure and stability of α -tocopherol.....	112
4.4	CONCLUSIONS	114
CHAPTER 5	115

5.1	INTRODUCTION	116
5.2	MATERIALS AND METHODS	119
5.2.1	Materials.....	119
5.2.2	Preparation of emulsions	119
5.2.2.1	Preparation of primary emulsions	119
5.2.2.2	Preparation of layer-by-layer (LBL) emulsions.....	120
5.2.2.3	Preparation of emulsions with sugar.....	121
5.2.3	Characterization of emulsions	121
5.2.4	Frozen state transitions	122
5.2.5	Freezing profiles.....	122
5.2.6	Freezing and freeze-drying of emulsions	123
5.2.7	State transitions of freeze-dried materials	124
5.2.8	Storage of freeze-dried materials and stability of α -tocopherol	124
5.2.9	Statistics	125
5.3	RESULTS AND DISCUSSION	125
5.3.1	Emulsion characteristics	125
5.3.2	Freezing and freeze-drying.....	131
5.3.3	State transitions of freeze-dried systems	136
5.3.4	Stability of α -tocopherol and structural changes during storage	137
5.4	CONCLUSIONS	142
CHAPTER 6	143
6.1	FREEZE-DRYING OF SUGAR-BASED SYSTEMS.....	143
6.2	PHYSICAL PROPERTIES OF FREEZE-DRIED MATERIALS.....	144
6.2.1	Lactose and trehalose	144
6.2.2	Sugars in mixture systems.....	145
6.2.2.1	Water sorption	145
6.2.2.2	Glass transition.....	146
6.2.2.3	Sugar crystallization in mixture systems.....	148
6.3	STABILITY OF BIOACTIVE COMPONENTS	151

6.3.1	Hydrophilic components	151
6.3.1.1	Impact of a_w and T_g	151
6.3.1.2	Impact of sugar crystallization	151
6.3.2	Hydrophobic components.....	152
6.3.2.1	Impact of a_w and T_g	152
6.3.2.2	Impact of sugar crystallization	153
6.3.2.3	Impact of interface composition.....	154
6.4	OVERALL CONCLUSIONS	156
BIBLIOGRAPHY		159
PUBLICATIONS		180
JOURNAL PAPERS		180
CONFERENCE ABSTRACTS.....		180
APPENDIX		182

LIST OF TABLES

Table 1.1	Various microencapsulation techniques and the processes involved in each technique. Adapted and modified from Desai and Park (2005).....	6
Table 2.1	Onset temperatures of glass transition (T_g' , °C) and ice melting (T_m' , °C), and solute concentration (C_g' , %) in maximally freeze-concentrated lactose, trehalose, lactose-CAS (3:1), lactose-SPI (3:1), trehalose-CAS (3:1) and trehalose-SPI (3:1) suspensions with initial solute concentration of 10, 15, and 20% (w/w), respectively.....	42
Table 2.2	Water content (mean values \pm SD, g/100g solid) in freeze-dried lactose, trehalose, lactose-CAS (3:1), lactose-SPI (3:1), trehalose-CAS (3:1) and trehalose-SPI (3:1) systems after equilibration to various water activity (a_w) values for 9 d at room temperature (in general 24 ± 1 °C).....	46
Table 2.3	BET (Brunauer-Emmett-Teller) and GAB (Guggenheim-Anderson-de Boer) constants (K_1 and K_2), monolayer values (m_{m1} and m_{m2} , g/100g solid), and R^2 (R_1^2 and R_2^2) for freeze-dried lactose, trehalose, lactose-CAS (3:1), lactose-SPI (3:1), trehalose-CAS (3:1) and trehalose-SPI (3:1) systems...	47
Table 2.4	Onset, midpoint and endset temperatures of glass transition (T_g , °C) at various water activity (a_w) values for freeze-dried lactose, trehalose, lactose-CAS (3:1), lactose-SPI (3:1), trehalose-CAS (3:1) and trehalose-SPI (3:1) systems.	51
Table 2.5	The instant crystallization temperature (T_{ic} , °C) of freeze-dried lactose, trehalose, lactose-CAS (3:1) and lactose-SPI (3:1) systems at various water activity (a_w) values.	52
Table 2.6	The k constants, critical water contents (g/100g solid) and critical water activity (a_w) values at 24 °C for freeze-dried lactose, trehalose, lactose-CAS (3:1), lactose-SPI (3:1), trehalose-CAS (3:1) and trehalose-SPI (3:1) systems.	54
Table 3.1	Onset temperatures of glass transition (T_g' , °C) and ice melting (T_m' , °C) of maximally freeze-concentrated lactose-vB ₁ , lactose-vC, trehalose-vB ₁ , and trehalose-vC systems.....	67
Table 3.2	Water content (mean values \pm SD) in freeze-dried lactose, trehalose, lactose-vB ₁ , lactose-vC, trehalose-vB ₁ , and trehalose-vC systems after equilibration at various water activities (a_w) for 120 h at room temperature (24 ± 1 °C).....	72
Table 3.3	Molar ratios between components (lactose, L; trehalose, T; water, W; vB ₁ ; vC) in freeze-dried lactose, trehalose, lactose-vB ₁ , lactose-vC, trehalose-vB ₁ ,	

and trehalose-vC systems at high water activities (a_w) after crystallization.	74
Table 3.4 GAB (Guggenheim-Anderson-de Boer) ^a constants (α , β , γ , K , and C), monolayer values (m_m , g/100g solid), and R^2 for freeze-dried lactose-vB ₁ , lactose-vC, trehalose-vB ₁ , and trehalose-vC systems.....	74
Table 3.5 Onset and endset temperatures of glass transition (T_g , °C) at various water activities (a_w) for freeze-dried lactose-vB ₁ , lactose-vC, trehalose-vB ₁ , and trehalose-vC systems.....	75
Table 3.6 Instant crystallization temperature (T_{ic} , °C) of freeze-dried lactose-vB ₁ , lactose-vC, trehalose-vB ₁ , and trehalose-vC systems at various water activities (a_w).....	76
Table 3.7 Critical water content, critical water activity (a_w) at 24 °C, k for Gordon- Taylor equation, and monolayer water activity of freeze-dried lactose-vB ₁ , lactose-vC, trehalose-vB ₁ , and trehalose-vC.....	78
Table 4.1 Water content (mean values \pm SD) in freeze-dried carbohydrate-protein-oil (3:1:2) systems after equilibration at various water activities (a_w) for 5 d at room temperature (24 ± 1 °C).	98
Table 4.2 Onset and endset temperatures of glass transition (T_g , °C) at various water activities (a_w) for freeze-dried lactose-MPI-OO (3:1:2), lactose-SPI-OO (3:1:2), trehalose-MPI-OO (3:1:2), and trehalose-SPI-OO (3:1:2) systems.	102
Table 4.3 The onset temperature of crystallization (T_{ic} , °C) in freeze-dried lactose-MPI- OO (3:1:2) and lactose-SPI-OO (3:1:2) systems.	104
Table 4.4 The volume weighted mean diameter, $D[4,3]$ (mean \pm SD, μm) and 50% volume percentile of droplet size distribution, $D[v, 0.5]$ (median mean diameter \pm SD, μm) of lactose-MPI-OO (3:1:2), lactose-SPI-OO (3:1:2), trehalose-MPI-OO (3:1:2), and trehalose-SPI-OO (3:1:2) systems.....	107
Table 5.1 The zeta-average (Z -average, nm), peak mean diameter (Peak, nm), and zeta- potential (ζ , mV) of ST-LBL, ST-SL, WT-LBL, WT-SL. The emulsion droplet size and charge were measured for fresh emulsions, and emulsions thawed from -20 and -35 °C. Values shown were mean \pm SD of triplicate samples*.....	130
Table 5.2 Freezing properties derived from freezing profiles: super-cooling temperature (T_s , °C) and freezing temperature (T_i , °C) of ST-LBL, ST-SL, WT-LBL, and WT-SL systems frozen at -20 and -35 °C prior to freeze-drying. Values shown were mean \pm SD of triplicate samples*.....	132
Table 5.3 The zeta-average (Z -average, mean \pm SD, nm), peak mean diameter (Peak, mean \pm SD, nm), and zeta-potential (ζ , mean \pm SD, mV) of freeze-dried ST-LBL, ST-SL, WT-LBL, and WT-SL systems.....	135

LIST OF FIGURES

- Figure 1.1 Schematic diagram of a carbohydrate-protein-oil particle formed in spray-drying. The symbols do not represent the real size of the molecules. 15
- Figure 1.2 Schematic diagrams of carbohydrate-protein-oil solids in freeze-drying, showing (A) the formation of glassy carbohydrate-protein matrix occurs during freezing, and (B) the dry structure retained after ice sublimation with pores distributed within the matrices. The symbols do not represent the real size of the molecules. 16
- Figure 1.3 Schematic diagram of freeze-dried carbohydrate-protein-oil solids stored above the glass transition temperature (T_g), showing (A) the collapsed structure above the T_g , and (B) the structure upon sugar crystallization. The symbols do not represent the real size of the molecules. 27
- Figure 2.1 SDS PAGE of the marker, casein, and soy protein isolate: 15% acrylamide gel with marker in lane 1, 8, and 15; casein at reducing condition in lane 2, 3, and 4; casein at non-reducing condition in lane 9, 10, and 11; soy protein isolate at reducing condition in lane 5, 6, and 7; and soy protein isolate at non-reducing condition in lane 12, 13, and 14. 41
- Figure 2.2 Water sorption of freeze-dried lactose, trehalose, lactose-CAS (3:1), lactose-SPI (3:1), trehalose-CAS (3:1) and trehalose-SPI (3:1) systems at 0.33 water activity (a_w) at room temperature (24 ± 1 °C). Vertical bars represent plus and minus (\pm) one standard deviation (SD) of data for triplicate samples. 43
- Figure 2.3 Water sorption of freeze-dried lactose, trehalose, lactose-CAS (3:1), lactose-SPI (3:1), trehalose-CAS (3:1) and trehalose-SPI (3:1) systems at 0.76 water activity (a_w) at room temperature (24 ± 1 °C). The inserted figure shows the whole experimental range of water sorption. Loss of water indicates lactose or trehalose crystallization. Vertical bars represent plus and minus (\pm) one standard deviation (SD) of data for triplicate samples. 45
- Figure 2.4 Water sorption isotherms of (A) freeze-dried lactose (\diamond), lactose-CAS (3:1) (\square), and lactose-SPI (3:1) (Δ), and (B) trehalose (\diamond), trehalose-CAS (3:1) (\square), and trehalose-SPI (3:1) (Δ) systems. Experimental data are at 9 d at room temperature (24 ± 1 °C). The isotherms were modeled using the GAB relationship. 48
- Figure 2.5 Effect of water content and water activity (a_w) on the onset temperature of glass transition (T_g , °C) in freeze-dried lactose, trehalose, lactose-CAS (3:1), lactose-SPI (3:1), trehalose-CAS (3:1) and trehalose-SPI (3:1) systems. 49

- Figure 2.6 The relationships between the glass transition temperatures (T_g , onset), water contents and water activity (a_w) values for freeze-dried lactose, trehalose, lactose-CAS (3:1), lactose-SPI (3:1), trehalose-CAS (3:1), and trehalose-SPI (3:1) systems. The sorption isotherms were predicted with GAB model. The depression of T_g as a result of water plasticization was predicted by Equation 2.1. The critical water contents (g/100g solid) and critical water activity (a_w) values at 24 °C are indicated with arrows..... 53
- Figure 2.7 State diagram for freeze-dried trehalose. The decrease of T_g with increasing water content indicated water plasticization. Maximally freeze-concentrated solutions showed solute concentration in unfrozen phase at C_g' , and constant onset temperature of glass transition (T_g') and onset temperature of ice melting (T_m'). Maximum ice formation occurred at temperature $T_g' < T < T_m'$ 54
- Figure 3.1 Solubility (g/100g water) of lactose (Hunziker and Nissen, 1926) and trehalose (Lammert and Schmidt, 1998) as a function of temperature. 69
- Figure 3.2 Water sorption of freeze-dried lactose (Chapter 2), lactose-vB₁, and lactose-vC systems at (A) 0.23, (B) 0.44, and (C) 0.65 a_w at room temperature (24 ± 1 °C). Loss of water at 0.65 a_w indicates lactose crystallization. Vertical bars represent plus and minus (±) 1 standard deviation (SD) of data for triplicate samples..... 70
- Figure 3.3 Water sorption of freeze-dried trehalose (Chapter 2), trehalose-vB₁, and trehalose-vC systems at (A) 0.23, (B) 0.44, and (C) 0.65 a_w at room temperature (24 ± 1 °C). Loss of water at 0.65 a_w indicates trehalose crystallization. Vertical bars represent plus and minus (±) 1 standard deviation (SD) of data for triplicate samples. 71
- Figure 3.4 Effect of water activity (a_w) on the onset temperature of glass transition (T_g , °C) and instant crystallization (T_{ic} , °C) in freeze-dried lactose-vB₁, lactose-vC, trehalose-vB₁, and trehalose-vC systems. 76
- Figure 3.5 The $\ln(C/C_0)$ of thiamine hydrochloride in lactose-vB₁ and trehalose-vB₁ systems as a function of water content (m, g/100g solid) during 15 d of storage at (A) 0.23 and (B) 0.65 a_w 79
- Figure 3.6 The $\ln(C/C_0)$ of ascorbic acid in lactose-vC and trehalose-vC systems as a function of water content (m, g/100g solid) during 60 d of storage at a_w of (A) 0.11, (B) 0.44, and (C) 0.65..... 80
- Figure 3.7 First-order rate constant ($\times 10^{-2} \text{ day}^{-1}$) of (A) thiamine hydrochloride and (B) ascorbic acid in freeze-dried lactose-vB₁, lactose-vC, trehalose-vB₁ and trehalose-vC systems as a function of water activity (a_w). The a_w corresponding to monolayer water content and critical a_w at 24 °C are indicated with arrows. 81

- Figure 3.8 Diagrams of the model systems frozen at temperatures below T_g' (A) then freeze-dried (D), frozen between T_m' and T_g' (B) then freeze-dried (E), and frozen above T_m' (C) then freeze-dried (F). During storage, the freeze-dried systems could be anhydrous (G), water-plasticized (H), and collapsed (I). Crystallization of sugars may lead to compact lactose crystals (J) or an amorphous sugar-water phase with dispersed vitamins and trehalose crystals (K). The symbols do not represent the real size of components... 83
- Figure 4.1 Water sorption (g/100g solid-non-fat) of freeze-dried lactose (Chapter 2), trehalose (Chapter 2), lactose-SPI (3:1) (Chapter 2), trehalose-SPI (3:1) (Chapter 2), lactose-SPI-OO (3:1:2), and trehalose-SPI-OO (3:1:2) systems at (A and C) 0.33 a_w and at (B and D) 0.65 a_w at room temperature (24 ± 1 °C). Loss of water at 0.65 a_w indicated sugar crystallization..... 97
- Figure 4.2 Water sorption isotherms of freeze-dried lactose (Chapter 2), lactose-SPI (3:1) (Chapter 2), and lactose-SPI-OO (3:1:2) systems. The isotherms were modeled using the GAB relationship with experimental data. 100
- Figure 4.3 The DSC thermographs of lactose-SPI-OO and trehalose-SPI-OO at 0.33 a_w , showing oil melting, glass transition, and sugar crystallization. The thermographs were taken from the 2nd heating scans (heating rate at 5 °C/min)..... 101
- Figure 4.4 Effects of (A) water content (g/100g solid-non-fat) and (B) water activity (a_w) on the onset temperature of glass transition (T_g , °C) in freeze-dried lactose (Chapter 2), lactose-SPI (3:1) (Chapter 2), and lactose-SPI-OO (3:1:2) systems. 103
- Figure 4.5 Emulsion droplet size distribution of (A) lactose-MPI-OO (3:1:2), (B) lactose-SPI-OO (3:1:2), (C) trehalose-MPI-OO (3:1:2), and (D) trehalose-SPI-OO (3:1:2) systems. The emulsion samples for each system were: (a) the fresh emulsions which were measured within 1 h after homogenization, (b) the freeze-dried materials which were reconstituted and measured, and (c) the freeze-dried materials which were stored at 0.76 a_w for 5 d, reconstituted and measured. 105
- Figure 4.6 Retention (%) of α -tocopherol in anhydrous freeze-dried lactose-MPI-OO (3:1:2), lactose-SPI-OO (3:1:2), trehalose-MPI-OO (3:1:2), and trehalose-SPI-OO (3:1:2) systems during 40 d of storage at 60 °C..... 108
- Figure 4.7 Retention (%) of α -tocopherol and water content (g/100g solid-non-fat) for freeze-dried (A) lactose-MPI-OO (3:1:2), (B) lactose-SPI-OO (3:1:2), (C) trehalose-MPI-OO (3:1:2), and (D) trehalose-SPI-OO (3:1:2) systems after storage at various a_w (0.0-0.76) for 5 d. 109
- Figure 4.8 Retention (%) of α -tocopherol for freeze-dried lactose-MPI-OO (3:1:2), lactose-SPI-OO (3:1:2), trehalose-MPI-OO (3:1:2), and trehalose-SPI-OO (3:1:2) systems after storage at 60 °C for 10 d. The materials were

- equilibrated to various a_w (0.0-0.44) for 5 d before transportation to 60 °C. 111
- Figure 4.9 Diagrams of the model systems before (A) and after (B) homogenization, frozen (C), and freeze-dried (D). During storage, water-plasticization (E), and collapse (F) occurred due to water sorption. Crystallization of sugars may lead to exclusion and coalescence of the oil droplets (G). The symbols do not represent the real size of components. 112
- Figure 5.1 The peak mean diameter (nm) (A) and zeta-average (nm) (B) of SPI-primary and WPI-primary emulsions (O/W, 10% oil, 1-5% proteins) at pH 3. 126
- Figure 5.2 Effect of protein content on emulsion particle charge at pH 3. 128
- Figure 5.3 Freezing profiles of ST-LBL, ST-SL, WT-LBL, and WT-SL systems at freezing temperatures of -20 and -35 °C. 131
- Figure 5.4 DSC thermograms of ST-LBL system equilibrated to 0.33 a_w room temperature during storage for 2 d at 55 °C, showing glass transition of amorphous trehalose and melting of trehalose dihydrate crystals. The thermograms are from the second heating scans (heating rate at 5 °C/min). The ST-LBL emulsion was frozen at -20 °C and freeze-dried. 137
- Figure 5.5 Retention (%) of α -tocopherol in freeze-dried ST-LBL and ST-SL systems at $a_w=0$ (Aa) and $a_w=0.33$ (Ab) during storage at 55 °C, and freeze-dried WT-LBL and WT-SL systems at $a_w=0$ (Ba) and $a_w=0.33$ (Bb) during storage at 55 °C. The freeze-dried materials were prefrozen at -20 °C or at -35 °C. The freeze-dried materials were vacuum sealed and packaged hermetically to anhydrous $a_w=0$ or $a_w=0.33$ prior to storage at 55 °C. 139
- Figure 5.6 The zeta-potential (mV) of freeze-dried systems during storage at 55 °C. The systems were ST-LBL at $a_w=0$ (Aa) and $a_w=0.33$ (Ab), ST-SL at $a_w=0$ (Ac) and $a_w=0.33$ (Ad), WT-LBL at $a_w=0$ (Ba) and $a_w=0.33$ (Bb), and WT-SL at $a_w=0$ (Bc) and $a_w=0.33$ (Bd). 140
- Figure 5.7 Schematic diagrams of protein-stabilized oil droplets in amorphous (A) and crystallized (B) trehalose matrices and protein- ι -CAR-stabilized oil droplets in amorphous (C) and crystallized (D) trehalose matrices. The amorphous matrices represent the freeze-dried materials at zero a_w at 55 °C and the matrices with crystallized trehalose represent the freeze-dried materials at $a_w=0.33$ at 55 °C. The inserted diagrams show the visual appearance of amorphous materials (left) and materials with crystallized trehalose (right). 141

INTRODUCTION

Bioactive components are susceptible to degradation due to their labile nature to environmental factors, such as heat, light, oxygen, and water. Entrapment or encapsulation of bioactive components into a dehydrated, protective structure is often applied to separate these components from the surroundings and to improve their stability during processing and storage. Sugars form glassy matrices in freezing and freeze-drying. The stabilizing properties of amorphous glassy sugars in the entrapment of hydrophilic component could be ascribed to (i) the interactions of sugar molecules and the hydrophilic bioactive molecules via hydrogen bonding and (ii) the restricted molecular mobility and kinetics of reactions in the glassy sugar structure (Slade and Levine, 1991; Crowe et al., 1993; Allison et al., 1999; Ubbink and Krüger, 2006; Roos, 2010; Santivarangkna et al., 2011). Oil-in-water emulsion systems are often required in the delivery of hydrophobic bioactive components because of their low solubility in water. The emulsions should be stable prior to and during processing, such as freezing and freeze-drying (Danviriyakul et al., 2002; Cerdeira et al., 2005; McClements et al., 2009). The hydrophobic particles are encapsulated and stabilized in the amorphous glassy structure with the presence of emulsifiers at the hydrophilic-hydrophobic interfaces.

Water content and water activity (a_w) are important determinants of the deteriorative stability of dehydrated food systems. The BET (Brunauer-Emmett-Teller) monolayer water content is often related to the degradation rate, as stability can be maintained around the monolayer water content (Labuza et al., 1970). In food systems containing

amorphous solids, water as a plasticizer also affects the physical state of solids (Roos and Karel, 1991a). The glass transition temperature (T_g) of amorphous solids decreases with increasing water content and a_w as a result of water plasticization. Slade and Levine (1991) and Roos (1993) suggested that, although the diffusion of reactants (e.g. oxygen and water) could be increased above the monolayer water content, the stability could be possibly retained if the solids were in the glassy state. However, the depression of T_g to below the ambient temperature by a critical water content could result in glass transition and loss of stability as a result of significant increase in molecular mobility and diffusion of reactants in the rubbery state. Several authors have emphasized the importance of glass transition of solids as a factor controlling the stability of bioactive components (Cardona et al., 1997; Elizalde et al., 2002; Ramoneda et al., 2011; Harnkarnsujarit et al., 2012). Degradation of bioactive components was found to occur in both glassy (below the glass transition temperature, T_g) and rubbery (above T_g) state of solids. Although degradation of bioactive components was not completely inhibited in the glassy state, the degradation rate was reduced, as was found for milk fat (Grattard et al., 2002) and β -carotene (Elizalde et al., 2002; Ramoneda et al., 2011; Harnkarnsujarit et al., 2012) in dehydrated carbohydrate-based systems. However, it is not always true that the stability of bioactive components is reduced in the rubbery state. Some authors have pointed out that structural collapse above glass transition may improve the chemical stability as a result of the dramatic decrease in the porosity and reduced diffusion of gases in matrix structure, as found for thiamine (Bell and White, 2000) and β -carotene (Prado et al., 2006) in PVP-based systems. In those systems that were formed mainly by sugars, sugar crystallization above the T_g was shown to have significant destabilizing effects on the entrapped/encapsulated bioactive components as

a result of loss of protective action of the solid matrix. Several authors have reported the loss of enzyme activity (Cardona et al., 1997; Mazzobre and Buera, 1999), β -carotene (Elizalde et al., 2002), and lipids (Cerqueira et al., 2005; Drusch et al., 2006) upon sugar crystallization. However, the stabilization and/or destabilization mechanisms of bioactive components may differ significantly depending on food composition and storage conditions.

The objectives of the present study were to investigate the use of amorphous sugars in the entrapment/encapsulation of bioactive components in dehydrated systems and the effects of physical properties of the matrix materials on the stability of bioactive components during storage at various conditions. The specific objectives were:

- (i) to prepare and characterize delivery systems containing hydrophilic (solutions) and hydrophobic bioactive components (oil-in-water emulsions) for freezing and freeze-drying using lactose and trehalose as the glass formers;
- (ii) to characterize water sorption, glass transition, and crystallization behaviour of freeze-dried lactose and trehalose and in mixes with hydrophilic vitamins, proteins, and hydrophobic oil particles;
- (iii) to determine stability of hydrophilic ascorbic acid and thiamine hydrochloride in amorphous lactose and trehalose systems as affected by a_w , glass transition, and sugar crystallization;
- (iv) to evaluate emulsion properties in fresh and dehydrated systems and as affected by interface composition and sugar crystallization;

(v) to investigate stability of hydrophobic α -tocopherol in lactose- and trehalose-based systems as affected by a_w , glass transition, sugar crystallization, and interface composition.

CHAPTER 1

Literature Review

1.1 INTRODUCTION

In the recent two decades, food and nutrition scientists have been investigating food products that not only provide the basic nutritional needs but also deliver components showing health promoting and/or disease preventing effects, which would benefit from adding bioactive components into food and food ingredients. Bioactive food components, including bioactive molecules such as lipids and fatty acids, vitamins, peptides and minerals as well as bioactive living cells such as probiotics, do not remain in the food for long time due to their labile/sensitive nature to surroundings or may react with other food components (McClements et al., 2007; Wilson and Shah, 2007; de Vos et al., 2010). Encapsulation of these sensitive components is therefore of interest and importance to protect them from rapid degradation or inactivation during processing and storage and also to allow controlled release of the bioactive components at specific time during food consumption or in the intestinal gut (McClements et al., 2009; de Vos et al., 2010). Encapsulation is a process by which a solid, liquid or gaseous materials or a mixture of materials in coated with or entrapped within another material or system (Risch, 1995). The material that is coated or entrapped is referred to various terms such as core material, actives, fill or internal phase; the material that forms the coating is often referred to wall material, carrier, membrane, shell or coating (Risch, 1995). The first commercial use of encapsulation dates back in 1954 in the

production of carbonless copy paper (Green and Scheicher, 1955). Encapsulation technology is now well developed in food industries and many encapsulation approaches are available and utilized (Table 1.1), such as spray-drying, extrusion, freeze-drying, fluidized bed coating, spray-chilling/cooling, co-crystallization, liposome entrapment, inclusion complexation, and coacervation (Desai and Park, 2005; Madene et al., 2006; Wilson and Shah, 2007; de Vos et al., 2010).

Table 1.1 Various microencapsulation techniques and the processes involved in each technique. Adapted and modified from Desai and Park (2005).

Encapsulation technique	Major steps in processing
Spray-drying	a. Preparation of the dispersion and homogenization b. Atomization of the infeed dispersion c. Dehydration of the atomized particles
Spray-chilling/cooling	a. Preparation of the dispersion and homogenization b. Atomization of the infeed dispersion
Fluidized-bed coating	a. Preparation of coating solution b. Fluidization of core particles c. Coating of core particles
Extrusion	a. Preparation of core and coating material paste b. Paste pass through extruder under high pressure c. Flash evaporation of water at the die
Freeze-drying	a. Mixing of core in a coating solution b. Freezing of the mixture c. Freeze-drying of the frozen mixture
Coacervation	a. Formation of a three-immiscible chemical phases b. Deposition of the coating c. Solidification of the coating
Cocrystallization	a. Preparation of supersaturated sucrose solution b. Adding of core into supersaturated solution c. Emission of substantial heat after solution reaches the sucrose crystallization temperature
Liposome entrapment	a. Microfluidization b. Ultrasonication c. Reverse-phase evaporation
Inclusion complexation	Preparation of complexes by mixing or grinding or spray-drying

1.2 ENCAPSULATION BY DEHYDRATION

Due to the variation of bioactive components in characteristics, for instance molecular structure, molecular size, solubility, volatility, heat-sensitivity and acid-sensitivity, and the limited availability of food-grade wall materials for each encapsulation technique, there is no method universally applicable for all the bioactive components (Desai and Park, 2005). As water is commonly present in food systems, the dehydration methods, such as spray-drying and freeze-drying, are the most commonly used encapsulation methods in food industries among all the available techniques. In dehydration processes, the rapid removal of water from the liquid containing glass-forming solutes is achieved by evaporation of water as vapour (spray-drying) or the solidification of water into ice crystals followed by ice sublimation (freeze-drying) without allowing the time for the solute to crystallize, as described by Roos and Karel (1991a) and Roos (1995). This often results in the formation of glassy solid structures with entrapped/encapsulated bioactive components, which stabilizes the bioactive components by at least providing a physical barrier against any adverse environmental conditions. However, depending on the nature of the bioactive components, the encapsulation processes can lead to two different results: (i) entrapment, which immobilizes but not necessarily envelops the bioactive components within the matrices; and (ii) encapsulation, which completely covers the bioactive components by the matrix materials and the bioactive components and the matrices are in two separate phases.

1.2.1 Entrapment

The stabilization of volatile compounds, such as flavours, and components that show hydrophilic properties, such as water-soluble vitamins and peptides/proteins, is often considered as entrapment. Back in 1960s and 1970s, researchers have studied the entrapment of volatiles and flavours in dehydrated carbohydrate systems and two mechanisms were proposed to explain the retention of volatile compounds in the solids. Thijssen, Rulkens, and King (Thijssen and Rulkens, 1968 and 1969; Thijssen, 1971; King, 1972) proposed the “selective diffusion” mechanism, which attributed the retention of volatiles to their relatively lower diffusion rate compared with that of water in the solids during spray-drying. The other mechanism was the “microregion entrapment” proposed by Flink and Karel (1970 and 1972), who demonstrated that the volatile compounds were entrapped in localized structure (microregion) by hydrogen-bonding to the molecules of dissolved solids and the microregions were held together in a type of matrix formed by carbohydrates during freezing and freeze-drying. As White and Cakebread (1966) earlier reported that the dehydrated carbohydrates exist in an amorphous glassy state, the “selective diffusion” or “microregion” concepts can be considered as interpretations in macro- or micro-scale of the same general phenomenon that the diffusion of gaseous molecules within the glassy solids are low and the glassy solids are able to entrap components within their structure via hydrogen bonding. It was also proved that the formation of an amorphous glassy solid during dehydration and the interactions between the biomaterials with the glass-forming materials, particularly some disaccharides, via hydrogen bonding are responsible for the stabilization of living organisms and other bioactive components (such as proteins and enzymes) in

pharmaceutical industries (Slade and Levine, 1991; Crowe et al., 1993; Taylor and Zografi, 1998; Allison et al., 1999). For instance, trehalose has been employed as a stabilizing agent for bioactive molecules during drying and later storage in pharmaceutical industries. The stabilizing properties of trehalose can be ascribed to both specific and kinetic effects. At a specific level, trehalose interacts with the bioactive molecules via hydrogen bonding and stabilizes them during drying. When water is removed, hydrogen bonds between bioactive molecules and trehalose replace essential water molecules to maintain the structure of bioactive molecules (Crowe et al., 1993; Allison et al., 1999). At the kinetic level, trehalose forms an amorphous glassy structure and influences the kinetics of reactions responsible for deterioration during storage (Slade and Levine, 1991). The importance of the formation of glassy solids in relation to the entrapment of bioactive components has also been emphasized by recent studies (Ubbink and Krüger, 2006; Santivarangkna et al., 2011).

1.2.2 Encapsulation

Stabilization of bioactive components, mostly hydrophobic vegetable/fruit oils (Fäldt and Bergenståhl, 1996a and 1996b; Beristain et al., 2002; Grattard et al., 2002; Kaushik and Roos, 2007), milk fat (Danviriyakul et al., 2002; Cerdeira et al., 2005; Vega et al., 2007), and β -carotene (Prado et al., 2006; Ramoneda et al., 2011; Elizalde et al., 2002), is considered as encapsulation. In dehydration encapsulation processes, the dispersion of the bioactive components in the solution/suspension of the protecting materials is necessary. As the hydrophobic bioactive components have a low solubility in water, one

of the challenges associated with their encapsulation is to incorporate these hydrophobic compounds into an aqueous-based systems with stability for a reasonable period of time for further processing or storage (Danviriyakul et al., 2002; Cerdeira et al., 2005; McClements et al., 2009).

1.2.2.1 Oil-in-water emulsion

The distribution of oil particles (as a bioactive component itself or with dissolved hydrophobic bioactive components) in the water phase of an emulsion system may significantly affect their distribution within the amorphous matrices after dehydration (the microstructure of the dehydration systems) (Danviriyakul et al., 2002; Cerdeira et al., 2005).

The development of emulsion technology provides a wide variety of techniques for the encapsulation of hydrophobic bioactive components (McClements et al., 2007). Conventional oil-in-water emulsions are the most widely used delivery systems, which consist of oil particles dispersed in an aqueous continuous phase, with the oil particles (typically between 0.1-100 μm in size) being surrounded by a thin interface layer consisting of emulsifier molecules (Dickinson, 1992; McClements, 2005). The oil phase is homogenized with the aqueous phase in the presence of a water-soluble emulsifier, which can be done using several techniques such as high shear mixers, high-pressure homogenizers, colloid mills, ultrasonic homogenizers, and membrane homogenizers (McClements, 2005; McClements et al., 2007). Carbohydrates and/or other solids (for example, proteins) are often needed in the aqueous phase as the glass-forming materials for later dehydration purposes, typically at 10-40% solid concentration (Fäldt and

Bergensstahl, 1996a; Danviriyakul et al., 2002; Elizalde et al., 2002; Vega et al., 2007). Proteins also play a role as emulsifiers when no other emulsifiers are present (McClements, 2004). The characteristics of the materials being homogenized, for example the viscosity generated in the aqueous phase by dissolving/suspending the solids at various concentrations, may limit the use of some particular homogenization methods (McClements et al., 2007). With a suitable homogenization technique, the final properties of the emulsions, such as oil particle size, can be controlled by the processing parameters of homogenization (Kaushik and Roos, 2007) as well as other parameters like oil load and the interface composition (Danviriyakul et al., 2002; Cornacchia and Roos, 2011a). The oil particle size and distribution in emulsions is one of the most concerned characteristics affecting the encapsulation and microstructure of the dehydrated systems. Danviriyakul et al. (2002) found that in spray-dried emulsion systems, the level of surface fat (unencapsulated fat) of dried particles increased significantly with increasing oil particle size in the emulsions and the instability of emulsions with larger oil particle size led to poor encapsulation efficiency. The encapsulation efficiency is the percentage of encapsulated/unextracted oil based on the total oil in the systems, but strongly affected by the solvent used for the extraction of surface/unencapsulated oil. However, Vega et al. (2007) implied that the encapsulation efficiency was only partially dependent on the emulsion properties and the composition of the glass-forming materials also contributed to the encapsulation of the oil particles in spray-dried carbohydrate-based systems. It was also reported that the emulsion properties were significantly changed after spray-drying, as indicated by the increased oil particle size and shifted distribution in the reconstituted emulsions, which could be a result of the changed interface activity under stresses during atomization and drying

(McClements, 2004). These changes were found to be smaller when the interface component has a more flexible structure (caseinate, compared with micellar casein, in Vega et al, 2005) or in the presence of small sugars as glass-forming material that interacted and stabilized the interface (maltodextrin DE 36, compared with DE 10, in Danviriyakul et al., 2002). The encapsulation efficiency of freeze-dried systems was also improved by the better emulsion stability; however the most stable emulsion not giving the highest encapsulation efficiency suggested the matrix composition plays another key role (Cerqueira et al., 2005). Moreover, freeze-dried systems on reconstitution showed similar oil particle size and distribution to the fresh emulsions (Cerqueira et al., 2005), which compared with the spray-dried systems, suggested that the dehydration procedures may also contribute to the microstructures of the dehydrated systems.

1.2.2.2 Spray-drying

Spray-drying is the most economical and widely applied technique in the encapsulation of bioactive components in food industries. Spray-drying involves both particle formation and drying. The feed liquid is atomized into droplets and then dried by spraying it continuously into hot drying air. Water evaporation during drying proceeds until the desired water level in the product is reached. The drying is controlled by means of the product and air input conditions, such as the flow rate and inlet temperature. During drying, glass formation of the solids occurs as water is removed and the drying particles should be free-flowing towards the completion of dehydration (Roos, 1995; Bhandari et al., 1997). The properties of the dried particles and the retention and encapsulation efficiency of the bioactive components are significantly

affected by the composition of the wall materials and the ratio of the core to wall components (Fäldt and Bergenståhl, 1996a and 1996b; Vega et al., 2007). The use of low-molecular weight sugars, such as sucrose, lactose, and maltodextrins with high DE values, in spray-drying makes the process difficult because of the low glass transition temperature of the sugars and the consequent stickiness problems during drying (Roos and Karel, 1991b; Bhandari et al., 1997; Bhandari and Howes, 1999). The stickiness problems can be avoided by adding high-molecular weight polysaccharide and proteins (Silalai and Roos, 2010 and 2011). Several studies have also demonstrated the use of proteins together with glass-forming sugars in the entrapment of volatiles and encapsulation of oil, which may enhance the retention of the bioactive components (Fäldt and Bergenståhl, 1996a; Vega et al., 2007). The application of spray-drying in entrapment/encapsulation requires the dispersion of the sensitive components into the solution/suspension of the matrix materials before atomization and drying (Dziezak, 1988; Desai and Park, 2005).

1.2.2.3 Freeze-drying

Freeze-drying requires the pre-freezing of water in the solution/suspension of wall materials with dispersed core materials and subsequent removal of ice through sublimation. The freezing process significantly affects the freeze-dried structure. First, the number and size of ice crystals formed during freezing are determined mainly by the freezing temperature (or the freezing rate). For instance, freezing at high temperature results in smaller number of larger ice crystals surrounded by thicker membranes/walls; freezing at low temperature results in larger number of smaller ice crystals surrounded by thinner membranes/walls (Flink and Karel, 1970; Petersen et al., 1973;

Harnkarnsujarit et al., 2012). Second, the amount of water transformed into ice crystals is determined by the annealing temperature (isothermal holding temperature). For a frozen system, at temperatures below the glass transition temperature of the maximally freeze-concentrated solute, T_g' , ice formation ceases due to the high viscosity of the freeze-concentrated unfrozen phase (Roos and Karel, 1991c). Therefore, the formation of a maximally freeze-concentrated system could be obtained by annealing the system above the T_g' but below the ice melting temperature, T_m' (Roos and Karel, 1991c). Third, in the case of bioactive delivery systems, the ice crystals and the bioactive components are dispersed or encapsulated in the unfrozen continuous solute phase. The drying process retains the solid state of the unfrozen solute phase that approaches an anhydrous, glassy solid state at the end of the drying process, with the bioactive components and the pores left after ice sublimation encapsulated or dispersed within the continuous matrix structure. Successfully freeze-dried materials can be produced only at drying conditions at which the ice temperature is kept lower than the T_m' . This can be achieved by the control of dehydration pressure, which determines the ice sublimation temperature. At temperatures above the T_m' during freeze-drying, collapse of the matrix structure occurs as a result of water plasticization. On the other hand, maximally freeze-concentration of the systems is also important since it ensures the maximal amount of water transformed into ice crystals and the unfrozen phase is able to support its own weight and resist flow (collapse) during sublimation of ice (Roos, 2010).

1.2.2.4 Microstructure of dehydrated emulsions

The microstructure of dehydrated systems is highly dependent on the emulsion properties (often oil particle size and oil load) (Fäldt and Bergenståhl, 1996b), the composition of solids (Fäldt and Bergenståhl, 1996a), dehydration methods and processing parameters (Danviriyakul et al., 2002; Haque and Roos, 2006; Harnkarnsujarit et al., 2012). The structures of a carbohydrate-protein-oil system formed in dehydration were illustrated and are shown in Figure 1.1 for spray-dried particles and Figure 1.2 for freeze-dried solids.

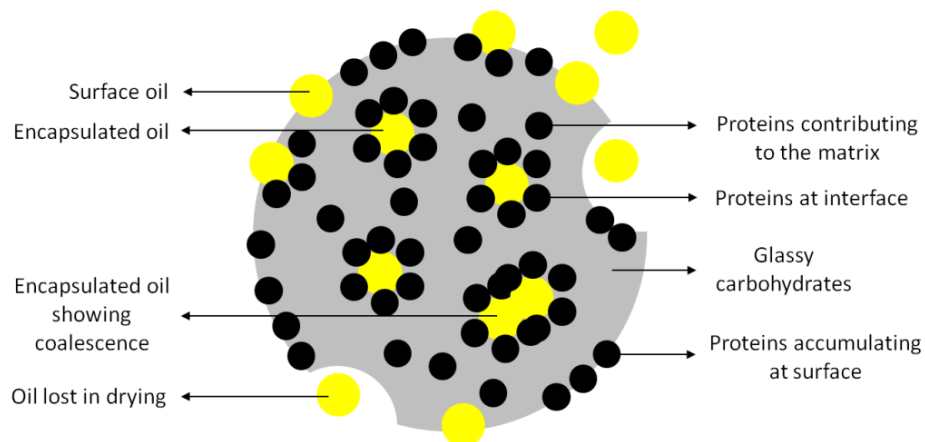


Figure 1.1 Schematic diagram of a carbohydrate-protein-oil particle formed in spray-drying. The symbols do not represent the real size of the molecules.

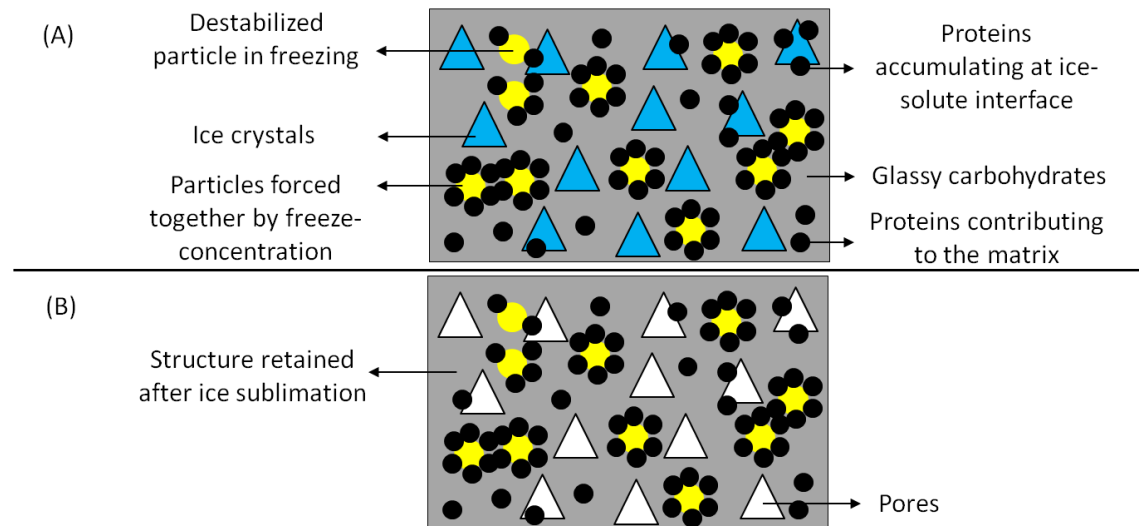


Figure 1.2 Schematic diagrams of carbohydrate-protein-oil solids in freeze-drying, showing (A) the formation of glassy carbohydrate-protein matrix occurs during freezing, and (B) the dry structure retained after ice sublimation with pores distributed within the matrices. The symbols do not represent the real size of the molecules.

As discussed earlier, glassy carbohydrate matrices are formed as a result of the rapid evaporation/solidification of water during dehydration processes. Major components other than carbohydrates may contribute to the glassy matrices but phase separation is possible and depends on their miscibility with carbohydrates (Kelichevski and Blanshard, 1993; Silalai and Roos, 2010 and 2011). For example, proteins may be found to accumulate at the surfaces of spray-dried particles (Fäldt and Bergenståhl, 1996a) or at the ice-solute interfaces of a frozen system (Millqvist-Fureby et al., 1999), and also exist in the continuous matrix phase (Fäldt and Bergenståhl, 1996a; Haque and Roos, 2006). Proteins used as emulsifiers are at hydrophilic-hydrophobic interfaces (McClements, 2004). The oil particles may be encapsulated in the amorphous matrices, exposed to powder surfaces, or lost in drying and changes in oil particle size and

distribution after drying could be a result of coalescence of oil particles during spray-drying (Danviriyakul et al., 2002; Vega et al., 2007). During freezing, the protein-stabilized oil particles are forced together as a result of freeze-concentration (Vanapalli et al., 2002). Mechanical deformation caused by ice formation may lead to destabilization of protein-stabilized oil particles (possibly detachment of proteins from interface), which may show coalescence if the oil particles gain mobility, for example on thawing (Cornacchia and Roos, 2011b). The structure formed during freezing is retained after ice sublimation, resulting in a highly porous matrix (Roos, 1995); the porosity is determined by the number and size of ice crystals formed during freezing, which are dependent on the freezing rate (Tsourouflis et al., 1976; Harnkarnsujarit et al., 2012). However, the integrity of the microstructures retained from dehydration could be lost when the glassy matrices undergo glass transition (Cerdeira et al., 2005; Vega et al., 2007) and the stability of the bioactive components could be changed consequently.

1.3 GLASS TRANSITION AND CRYSTALLIZATION

Sugars and carbohydrates are commonly present in food systems and form amorphous glassy solids with hygroscopic and thermoplastic properties in dehydration. Commonly used glass-forming materials for stabilization purpose include lactose, trehalose, sucrose, corn syrup solids, maltodextrins, several gums and proteins alone or in mixtures of them (Fäldt and Bergenståhl, 1996a and 1996b; Beristain et al., 2002; Danviriyakul et al., 2002; Elizalde et al., 2002; Grattard et al., 2002; Cerdeira et al.,

2005; Kaushik and Roos, 2007; Vega et al., 2007). The dehydrated sugar matrices exist in their glassy state, showing disordered molecular structure and solid-like characteristics; glass transition of these solids occurs when the molecules gain translational mobility, for example on heating, and results in a viscous liquid-like material (White and Cakebread, 1966; Roos, 1995). The temperature, at which a material undergoes the transition from the solid-like glassy state to the liquid-like rubbery state, can be referred to the glass transition temperature, T_g . Glass transition can also be observed when water is absorbed by the glasses, since water as a plasticizer strongly interacts with the solids via hydrogen bonding (Flink and Karel, 1972; Slade and Levine, 1991; Roos and Karel, 1991b). The T_g of solids shows water content dependence and decreases with increasing water contents, which could be predicted by the Gordon-Taylor equation as suggested by Roos and Karel (1991d). A critical water content with its corresponding a_w , at which condition the T_g of the materials is decreased to the ambient temperature, can be predicted by fitting the Gordon-Taylor equation together with the GAB (Guggenheim-Anderson-de Boer) relationship to glass transition, water plasticization, and water sorption data (Roos, 1993). Glass transition occurs when the dehydrated systems are stored above their critical values, and several time-dependent physical changes, such as stickiness and caking of spray-dried particles and collapse of freeze-dried structures, and sugar crystallization may occur above the T_g (Roos and Karel, 1991a).

1.3.1 Instant sugar crystallization

The instant sugar crystallization temperature, T_{ic} , is often taken as the onset temperature of the exothermal peak above glass transition from a dynamic heating scan. The T_{ic} was found to be about 50 ± 10 °C higher than the T_g and to decrease with increasing a_w as a result of water plasticization, as reported for pure lactose (Roos and Karel, 1990; Cardona et al., 1997; Haque and Roos, 2004a) and pure sucrose (Roos and Karel, 1990; Cardona et al., 1997), and the presence of proteins and starch increased the T_{ic} more than the increase of T_g at corresponding a_w conditions in the mixture systems. In the presence of several salts, the T_g of lactose was found to be lower than that of pure lactose as a result of slightly higher amount of sorbed water in lactose-salt systems at various a_w conditions; however, the T_{ic} in lactose-salt systems was higher than that of pure lactose (Omar and Roos, 2007). These results suggested that the increased T_{ic} in the presence of other components was not always attributed to their effect on the T_g of the sugar. In lactose-trehalose mixture systems, the T_g of the systems was not affected by increasing the component trehalose up to 40% (w/w) as a result of the similar glass transition behavior between lactose and trehalose; however, the T_{ic} of lactose increased significantly with increasing amount of trehalose (Mazzobre et al., 2001). These results indicated that the delayed sugar crystallization in mixture systems was also a result of the interference effects from other components in the process of sugar crystallization. In the case of trehalose, its instant crystallization was significantly affected by water. Most of the authors (Cardona et al., 1997; Mazzobre et al., 2001) could not find the T_{ic} for trehalose in anhydrous systems in the temperature range of measurements (up to 200 °C), indicating that trehalose does not crystallize in the absence of water.

1.3.2 Sugar crystallization kinetics

In the glassy state, most structural changes occur very slowly as a result of the high viscosity and restricted molecular mobility and crystallization of the amorphous sugar is kinetically delayed. Crystallization of sugars from the non-equilibrium amorphous state towards the equilibrium crystalline state occurs when the molecules gain translational mobility above the glass transition. During isothermal storage at room temperature, sugar crystallization is often observed as a result of water sorption, which consequently decreases the T_g to below the room temperature. Roos and Karel (1990) fitted the WLF (William-Landel-Ferry) equation to lactose crystallization data obtained with the isothermal DSC measurements and found the time to crystallization was a function of $T-T_g$ and water-plasticized lactose crystallized slightly faster at equal $T-T_g$ than anhydrous lactose. The well fit of WLF equation suggested that the rate of sugar crystallization was related to viscosity and relaxation times of mechanical properties above the T_g of solids. However, due to the limited available data (data obtained in a fairly narrow temperature range), other equations, such as Arrhenius equation and VTF (Vogel-Tamman-Fulcher) equation (Roos and Karel, 1990; Mazzobre et al., 2001), were also found to fit sugar crystallization data. Besides the above equations used to model the temperature dependence of sugar crystallization, the Avrami equation was also found to fit the crystallization data (Mazzobre et al., 2001; Haque and Roos, 2005a; Miao and Roos, 2005a).

1.3.3 Sugar crystallization and crystal forms

With the purpose of stabilizing bioactive components, sugar crystallization from the amorphous matrices causes phase separation between the entrapped/encapsulated components and the protecting materials. Thus, crystallization of sugars used as glass-forming materials during storage could be detrimental for the stability of bioactive components. Lactose is one of the most intensively studied sugars and commonly present in dairy products, such as milk powders. During isothermal storage (at room temperature) at various a_w conditions, the crystallization behavior of sugars can be observed from the loss of water content, which indicates the formation of sugar crystals (Jouppila and Roos, 1994a). Lactose alone showed crystallization at 0.44 a_w within 24 h and the time to lactose crystallization decreased with increasing a_w and delayed lactose crystallization was found at $\geq 0.54 a_w$ in milk powders (Jouppila and Roos, 1994a) and in the presence other components, such as proteins (Haque and Roos, 2004b), salts (Barham et al., 2006a), and other sugars (Miao and Roos, 2005a). The final water contents after crystallization may suggest the type of crystals formed during crystallization; for instance the water content for pure lactose after crystallization at $\geq 0.54 a_w$ was $< 5\%$ (water content in lactose monohydrate), indicating a mixture of lactose anhydrate and monohydrate was formed. However, the presence of other components, particularly proteins, often resulted in water contents $> 5\%$ after lactose crystallization, which was attributed to the residual water retained in proteins or the hindered movement of lactose molecules by proteins hence incomplete lactose crystallization (Lai and Schmidt, 1990; Jouppila and Roos, 1994a; Haque and Roos, 2004b). The use of X-ray diffraction gives more precise results on the type of crystals

formed after crystallization. Spray-dried pure lactose crystallized into three phases: the stable α -lactose monohydrate and anhydrous β -lactose phases and the unstable phase of anhydrous α - and β -lactose mixtures at $\geq 0.54 a_w$ at room temperatures (22-23 °C), and the transformation of the unstable anhydrous form of α -lactose into the more stable α -lactose monohydrate and anhydrous β -lactose may take place during storage (Haque and Roos, 2005a; Barham et al., 2006a). Although freeze-dried lactose crystallized after spray-dried lactose during storage at room temperature at corresponding a_w conditions, the types of crystals formed were the same in lactose prepared from both methods (Haque and Roos, 2005a). However, the crystal forms and the ratios between these forms were found different in the presence of various proteins. The anhydrous β -lactose was found only in pure lactose and not in any of the measured lactose-protein (3:1, w/w) systems, including WPI, sodium caseinate, albumin, and gelatin, and the ratios between the crystal forms in the presence of different proteins varied as reported by Barham et al. (2006a).

In contrast, sugars that form hydrated crystals may retain higher amounts of water without crystallization, since they need not only the molecular mobility from water plasticization, but they also need to have enough water to form the hydrated crystals. For instance, trehalose was found to crystallize earlier than lactose at corresponding conditions above $0.54 a_w$ at room temperature and the final water content of 10.5% indicated the formation of trehalose dihydrate. However, crystallization was not observed at $0.44 a_w$ for trehalose for up to 220 h but for lactose within 24 h of storage (Miao and Roos, 2005a). Although most authors (Cardona et al., 1997; Iglesias et al., 1997) reported the formation of only trehalose dihydrate at $\geq 0.54 a_w$, trehalose

anhydrate was also found by Miao and Roos (2005a) in pure trehalose and trehalose-lactose mixture systems after crystallization at $\geq 0.54 a_w$. It should also be noted that in a mixture system, trehalose crystallized independently into its characteristic crystals, although the intensities of crystal peaks were lower, indicating the lower extent of crystallization of trehalose in the presence of other sugars (Miao and Roos, 2005a).

The types of crystals formed during sugar crystallization become significant when sugar crystallization occurs in a sealed package. For instance, the formation of anhydrous crystals is often accompanied by water release from the crystalline phase, which plasticizes the remaining amorphous phase and causes a decrease in the T_g hence increased $T-T_g$, as found for lactose (Roos and Karel, 1992). Therefore, the rate of lactose crystallization could become accelerated in a closed system, leading to more rapid structural changes. However, sugar crystallization may be beneficial. It was suggested that the crystallization of trehalose into hydrate forms may provide partial desiccation by removing water from the amorphous phase, thereby increasing the T_g of the remaining amorphous phase (Aldous et al., 1995; Schebor et al., 2010). The formation of hydrated crystalline forms by some sugars, and the amount of extracted water from the amorphous phase into the hydrated crystal structure would therefore seem to be vital in relation to the stability of the entrapped/encapsulated bioactive components.

1.4 CHEMICAL STABILITY AND PHYSICAL STATE OF SOLIDS

Several mechanisms may lead to the degradation of bioactive components. For bioactive compounds possessing antioxidant activity, such as hydrophobic tocopherols and hydrophilic ascorbic acid, their loss could result from both their degradation as affected by the exposure to oxygen, transitional metals, light, and high temperature, as well as their consumption as antioxidant reactants in the presence of free radicals in the lipid or aqueous phase (Fennema, 1977; Widicus et al., 1980; Widicus and Kirk, 1981; Burton and Ingold, 1986; Davies et al., 1991; Uddin et al., 2002; Valenzuela et al., 2002; Zingg and Azzi, 2004). The rate of degradation is dependent on the diffusion of the reactive species towards the bioactive components. Water content and a_w are important to the deteriorative stability of dehydrated food systems (Labuza et al., 1970). In dehydrated food systems, the diffusion of oxygen increases with increasing water content. The relative rate of degradation is related to the BET monolayer value, below which the stability can be maintained (Labuza et al., 1970). Water as a plasticizer also affects the physical state of food components (Roos and Karel, 1991a, 1991c and 1991d). The glass transition temperature of the food materials decreases with increasing water content as a result of water plasticization. The depression of T_g to below the ambient temperature by a critical water content caused glass transition hence loss of stability, which suggested that although the diffusion of reactants (e.g., oxygen) could be increased above the monolayer water content, the stability could be probably maintained in the glassy state (Slade and Levine, 1991; Roos, 1993). In bioactive component delivery systems, the physical state of the protecting matrices under various conditions has been reported to affect not only the properties of the matrices but also

the stability of the bioactive components within the structure (Bell and White, 2000; Elizalde et al., 2002; Grattard et al., 2002; Beristain et al., 2002; Ramoneda et al., 2011).

1.4.1 Stability in amorphous phases

The hydrophilic bioactive components, such as water-soluble vitamins, often exist as part of the hydrophilic phase. Degradation of thiamin occurred both below and above the T_g in amorphous Polyvinylpyrrolidone (PVP) matrices and the degradation rates increased with increasing a_w . Bioactive peptides or proteins in amorphous carbohydrate matrices were stabilized via hydrogen bonding between protein and carbohydrate molecules (Allison et al., 1999). However, the stability of the peptides or proteins is more complex since these molecules may undergo many changes such as aggregation and non-enzymatic browning, oxidation.

Lipid oxidation in amorphous matrices was found to be significantly affected by the diffusion of oxygen and not strictly controlled by the glass transition of the matrix, however, relatively slow lipid oxidation was observed above the T_g in the rubbery state of the matrices. (Beristain et al., 2002; Grattard et al., 2002). Several studies were published to investigate the degradation of β -carotene in dehydrated systems as affected by the state of the protecting matrices. The degradation of β -carotene was not inhibited in the glassy state of the carbohydrate-based matrices (below the T_g), although the degradation rate was slower or the infinite retention after storage was higher than in the rubbery state (above the T_g) (Elizalde et al., 2002; Ramoneda et al., 2011). This was

because diffusion of oxygen in glassy matrices was possible, as also observed for other small molecules (Tromp et al., 1997; Schoonman et al., 2002; Goubet et al., 2002). Above the T_g , the degradation of β -carotene was found to increase with increasing matrix mobility, which was indicated by the decreasing of structural relaxation time with increasing $T-T_g$ (Harnkarnsujarit et al., 2012).

1.4.2 Stability as affected by structural changes

A compromise between collapse (favourable for retention of encapsulated compounds) and matrix crystallinity (promoting the release of encapsulated compounds) was always observed in relation to the stability of bioactive components.

1.4.2.1 *Collapse of matrices*

In non-crystalline sugar systems, the stability of encapsulated lipids may be increased upon collapse of the samples above the T_g . Prado et al. (2006) reported a relatively smaller degradation above the T_g than below the T_g in amorphous PVP systems, which was found to correlate with the structural changes above the T_g . They suggested that the high porosity of the matrices in glassy state allowed higher oxygen diffusion hence fast β -carotene degradation. When the systems were plasticized and collapse occurred, lower degradation rates were observed as a result of the disappearance or a dramatic decrease in the number of micropores in the matrices above T_g (Figure 1.3A). The enhanced stability of β -carotene by decreased porosity and collapsed structure was also reported by Harnkarnsujarit et al. (2012) for freeze-dried carbohydrate-agar based

systems. Reduced rates of degradation of hydrophilic thiamine in PVP matrices were also observed when collapse of structure was observed above the T_g (Bell and White, 2000). However, rapid lipid oxidation was found upon collapse of the matrices, which caused a rejection of the encapsulated oil to the surroundings (Figure 1.3A) (Grattard et al., 2002) or significant loss of volatile oil due to dissolution of the structure at high a_w (Beristain et al., 2002).

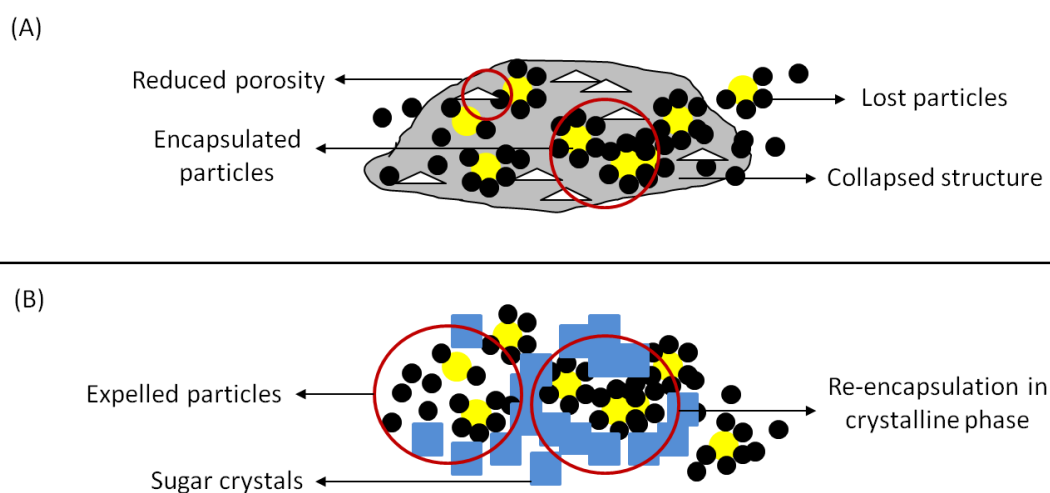


Figure 1.3 Schematic diagram of freeze-dried carbohydrate-protein-oil solids stored above the glass transition temperature (T_g), showing (A) the collapsed structure above the T_g , and (B) the structure upon sugar crystallization. The symbols do not represent the real size of the molecules.

1.4.2.2 Crystallization of sugars

In those matrices formed mainly by sugars, crystallization has a direct impact on quality loss. In systems containing encapsulated components, the protective action of the solid matrix is lost when crystallization occurs, as reported for loss of invertase activity (Cardona et al., 1997) and lactase activity (Mazzobre and Buera, 1999), the degradation

of β -carotene (Elizalde et al., 2002), and oxidation of fish oil (Drusch et al., 2006) upon trehalose crystallization. It should be noted that trehalose crystallization requires sufficient amount of water (10.5%) to form the trehalose dihydrate. However, trehalose crystallization could be delayed in the presence of salt (5:1 molar ratio of trehalose:salt) resulting in incomplete crystallization within experimental time, although the water content was sufficient to form trehalose dihydrate. Because the T_g of trehalose was not affected by that amount of salt, the smaller loss of lactase activity in trehalose-salt systems compared with trehalose alone could be attributed to the delayed/incomplete trehalose crystallization (Mazzobre and Buera, 1999). However, trehalose crystallization was not delayed by salts when hydrophobic components (β -carotene) were incorporated into the systems, indicating the hydrophilic and hydrophobic interactions affected trehalose crystallization. The rate of loss of β -carotene in trehalose and trehalose-salt systems was mainly affected by the excess amount of water above that needed to form trehalose dihydrate. That means at a_w that lead to similar degree of crystallization but with different amount of excess water present, the degradation of β -carotene was significantly affected by the excess water, which was involved in the remaining noncrystalline matrix and liberate the encapsulated oil to higher exposure to oxidation (Figure 1.3B) (Elizalde et al., 2002). However, it was assumed that re-encapsulation of the bioactive components in the crystalline structures was also possible, as suggested by Buera et al., (2005). Sugar crystallization in food materials is expected to be naturally delayed in the presence of other food components. However, once sugar crystallization occurs, dramatic loss of stability would take place. Since there are not many studies focusing on the effects of sugar crystallization on the

stability of bioactive components, much research is required to investigate the effects of sugar (not limited to trehalose) crystallization on the stability of bioactive components.

1.5 CONCLUDING REMARKS

Encapsulation and stabilization of sensitive compounds in dehydrated structures can be achieved by controlling the physical state of the solids during processing and storage. Dehydration results in amorphous glassy structures. Bioactive components are entrapped/encapsulated as a result of fast evaporation/solidification of water and glass formation in dehydration. The dehydrated glassy matrices contribute to the stability of bioactive components mainly because of the high viscosity and restricted molecular mobility in the glasses. However, water sorption plasticizes the glasses and the dehydrated materials may show changes of physical state. The measurement of glass transition of the dehydrated matrices provided meaningful information in understanding the stability of encapsulated bioactive components. The structural changes above glass transition, particularly sugar crystallization, could cause more severe loss of both physical and chemical stability of the systems. Understanding the characteristics of encapsulating materials and their properties during processing would benefit the development of functional foods with bioactive components. The stability of bioactive components in relation to the physical state of encapsulating structures and structural changes during storage at various conditions is important and needs to be studied to improve the quality of functional foods and ingredients. Moreover, factors other than physical properties of the matrices, such as the nature of the bioactive component, a_w ,

temperature, system composition, are also important and affect the stability of the bioactive components in dehydrated delivery systems. Investigation of the physical properties of the matrices in their glassy or rubbery state and the effects of structural changes above the T_g of the matrices are helpful in both predicting the stability of bioactive components as well as designing more appropriate and stable delivery systems.

CHAPTER 2

Characterization of carbohydrate-protein matrices for nutrient delivery

Published in *Journal of Food Science*, Zhou and Roos, 2011, 76(4):E368-376

ABSTRACT

Amorphous carbohydrates may show glass transition and crystallization as a result of thermal or water plasticization. Proteins often affect the state transitions of carbohydrates in carbohydrate-protein systems. Water sorption behavior and effects of water on glass transition and crystallization in freeze-dried lactose, trehalose, lactose-casein (3:1), lactose-soy protein isolate (3:1), trehalose-casein (3:1), and trehalose-soy protein isolate (3:1) systems were studied. Water sorption was determined gravimetrically as a function of time, and BET (Brunauer-Emmett-Teller) and GAB (Guggenheim-Anderson-deBoer) models were fitted to the experimental data. Glass transition temperature (T_g) and instant crystallization temperature (T_{ic}) in anhydrous and water plasticized systems were measured using Differential Scanning Calorimetry (DSC). The Gordon-Taylor equation was used to model water content dependence of the T_g values. The critical water content and water activity (a_w) at 24 °C were calculated and crystallization of lactose and trehalose in the systems was followed at and above 0.54 a_w . Carbohydrate-protein systems showed higher amounts of sorbed water and less

rapid sugar crystallization than pure sugars. A greater sugar crystallization delay was found in carbohydrate-casein systems than in carbohydrate-soy protein isolate systems. The T_g and T_{ic} values decreased with increasing water content and a_w . However, higher T_{ic} values for lactose-protein systems were found than for lactose at the same a_w . Trehalose showed lower T_{ic} value than lactose at 0.44 a_w but no instant crystallization was measured below 0.44 a_w . State diagrams for each system are useful in selecting processing parameters and storage conditions in nutrient delivery applications.

Keywords: lactose, trehalose, freeze-drying, water sorption, state transition

2.1 INTRODUCTION

Amorphous carbohydrates exist as noncrystalline solids (glass) at temperatures below their glass transition (Roos and Karel, 1990). Water sorption by amorphous carbohydrates results in an increase in molecular mobility and decrease of viscosity, associated with a decrease of the glass transition temperature, T_g , and plasticization (softening) of the material (Roos and Karel, 1990). Storage of dehydrated foods at humid conditions may increase water activity (a_w) as a result of water sorption and the glass transition of the materials may decrease to below ambient temperature. The difference between storage temperature and the glass transition ($T-T_g$) often controls the rate of time-dependent changes, for example, stickiness and caking of powders and sugar crystallization (Chuy and Labuza, 1994; Bhandari et al., 1997; Silalai and Roos,

2010). Such changes of physical state may cause rapid quality losses of foods with amorphous components (Slade and Levine, 1991; Roos, 1993 and 2010).

In dehydrated foods, the retention of flavors, volatiles, and nutrients is often enhanced by their low diffusivity or the sensitive components may be protected as a result of entrapment or encapsulation within a continuous amorphous, glassy solids phase (Roos, 1995). At temperatures above the glass transition temperatures of such food solids, collapse of the matrices and crystallization of the components may lead to the release of entrapped volatiles and the exposure of encapsulated particles to surroundings. Most foods contain carbohydrates and proteins as the main nonfat solids. Proteins are also used as emulsifiers and required as hydrophilic-hydrophobic interface components in delivery of hydrophobic nutrients (McClements et al., 2007). The glass transition behavior of various carbohydrates is well-known, but a higher T_g may be found for carbohydrate-protein mixtures than for carbohydrates alone (Haque and Roos, 2004a). Depending on the miscibility of proteins and carbohydrates, the component proteins may restrict molecular movements and increase the T_g of carbohydrate-protein mixes (Kalichevsky and Blanshard, 1993; Jouppila and Roos, 1994a). The higher T_g of a carbohydrate-protein system may enhance physical stability in dehydrated materials. In formulated food systems, a higher T_g can be assumed to improve protection and stability of entrapped or encapsulated sensitive compounds.

Lactose is a typical amorphous component of food and pharmaceutical materials. As a milk component, it significantly affects the physical characteristics of dairy powders (Jouppila and Roos, 1994b; Özkan et al., 2002; Silalai and Roos, 2010). Trehalose is a disaccharide that has a fairly similar glass transition behavior to that of lactose (Roos,

1995; Miao and Roos, 2005b). However, the crystallization properties of lactose and trehalose are quite different (Miao and Roos, 2005a). The purpose of the present study was to characterize the water sorption and state transition behavior of freeze-dried lactose and trehalose and when mixed with proteins. The relationship between the T_g , water sorption as well as the critical values of water content and a_w (Roos, 2003) of these materials contribute to a scientific basis for nutrient stabilization and delivery using these carbohydrate-protein formulations.

2.2 MATERIALS AND METHODS

2.2.1 Materials

α -Lactose monohydrate (Sigma-Aldrich, U.S.A.), trehalose dihydrate (Cargill, Ireland), casein (CAS, Kerry ingredients, Ireland), and soy protein isolate (SPI, PRO-FAM891, Archer Daniels Midland, U.S.A.) were used. Lactose, trehalose, lactose-CAS (3:1), lactose-SPI (3:1), trehalose-CAS (3:1), and trehalose-SPI (3:1) suspensions were prepared (10, 15, and 20%, w/w) in distilled water. All materials were kept under stirring at 45 °C up to 3 h, with the assumption of proper protein hydration when carbohydrate-CAS systems became clear but carbohydrate-SPI systems remained cloudy. The suspensions were cooled to room temperature, in general 24 ± 1 °C, and reweighed to adjust water content by adding the amount of water lost by evaporation.

2.2.2 Electrophoresis of proteins

Casein and soy protein isolate proteins were separated on a 15% acrylamide gel according to the method of Laemmli (1970). The gels were stained with Coomassie brilliant blue (G-250) and digitalized at 300 dpi by a GS-620 densitometer (Bio-Rad, Hercules, CA). Standard molecular weight markers were supplied by Sigma-Aldrich (SigmaMarker Wide Range, Steinheim, Germany). Molecular weights of the standard markers used for protein profile study ranged from 6.5 to 200 kDa (Sigma-Aldrich). A sample of approximately 10 mg of each powder was weighted and transferred to a 1.5 ml Eppendorf tube (Sarstedt, Germany). Each sample was subsequently suspended in 1 ml of sodium dodecyl sulfate (SDS) buffer under reducing (with mercaptoethanol) and non-reducing (without mercaptoethanol) conditions. Suspensions of marker (10 μ l) and samples (5 μ l) were injected into SDS PAGE gels which were pre-run at 200 V for 30 min. Suspensions were run at 200 V through the gel until the tracking dye front was close to the bottom of the gel slab.

2.2.3 Frozen state transitions and freeze-drying

Frozen state transitions of the materials were analyzed using differential scanning calorimetry (DSC, Mettler Toledo 821e with liquid N₂ cooling, Switzerland). To analyze the onset temperature of glass transition of the maximally freeze-concentrated solutes, T_g' , and the onset temperature of ice melting of the maximally freeze-concentrated systems, T_m' , 20-25 mg of the suspensions (10, 15, and 20%, w/w) were transferred into 40 μ l preweighed DSC aluminum pans (Mettler Toledo, Switzerland).

Filled pans were hermetically sealed and weighed (Mettler Toledo AG245 balance). A sealed empty pan was used as a reference in all measurements. As reported by Roos and Karel (1991b), frozen systems could be maximally freeze concentrated by annealing at a temperature slightly below T_m' . To locate the T_m' , two runs were applied for each system: (1) samples were cooled from 25 °C to -100 °C at a rate of 10 °C/min and heated from -100 °C to 25 °C at a rate of 5 °C/min, and the onset temperature of ice melting, T_m , was analyzed from the heating scan; (2) with the knowledge of T_m value of each system, samples were cooled from 25 °C to -100 °C at a rate of 10 °C/min, heated to a temperature < 1 °C below the onset T_m value at a rate of 5 °C/min and held at this temperature for 15 min to allow maximum freeze-concentration, followed by cooling to -100 °C at a rate of 10 °C/min and final heating to 25 °C at a rate of 5 °C/min. The final heating scans confirmed that the onset T_m was T_m' , and the scans were analyzed for the T_g' and T_m' values of the maximally freeze-concentrated systems, using STAR thermal analysis software, version 6.0 (Mettler Toledo, Switzerland). All measurements were carried out in triplicate.

Suspensions (20%, w/w) of the carbohydrate and carbohydrate-protein systems were freeze-dried to obtain anhydrous materials. For water sorption study, the suspensions were transferred using an adjustable-volume pipette (Pipetman P5000, Gilson Inc., U.S.A.) into glass vials (Clear glass ND18, 10 ml, VWR, U.K.) (5 ml per vial), frozen at -35 °C ($T_g' < T < T_m'$) for 24 h, and subsequently transferred to a -80 °C freezer for 5 h. Samples at -80 °C were transferred to a freeze-dryer to delay temperature increase and avoid ice melting during sample transfer to the freeze-dryer and establishment of appropriate freeze-drying conditions. The freeze-dryer (Lyovac GT2, STERIS, Hürth,

Germany) was pre-run for 2 h for precooling of condenser prior to sample loading and dehydration at a chamber pressure of < 0.1 mbar corresponding to sublimation temperature < -40 °C. Samples in glass vials with semi-closed rubber septa were freeze-dried for ≥ 72 h. All vials were hermetically closed in the freeze-dryer using the rubber septa prior to breaking the vacuum with ambient air. For state transitions study, the suspensions were frozen and freeze-dried on petri dishes (92×16 mm, Sarstedt AG & Co, Nümbrecht, Germany). Freeze-dried materials for the state transitions study were ground into fine powder using a mortar and pestle, and stored over P_2O_5 in evacuated desiccators for 5 d to maintain the dehydrated state and to avoid water sorption.

2.2.4 Water sorption isotherms

The materials prepared in the glass vials were used in the water sorption study. Triplicate samples of each material in opened vials were equilibrated to reach constant water contents (up to 9 d) at room temperature (in general 24 ± 1 °C) in evacuated desiccators over various saturated salt solutions (LiCl, CH_3COOK , $MgCl_2$, and K_2CO_3), which at experimental conditions gave water activity (a_w) values of 0.11, 0.23, 0.33, and 0.44, respectively, at equilibrium (Labuza et al., 1985). Desiccators were vacuumized for about 1 min until onset of boiling of water to establish desired vapor pressure conditions. The samples in vials were weighed at 0, 3, 6, 9, 12, and 24 h, and then at 24-h intervals. Time-dependent lactose or trehalose crystallization was monitored during storage of samples in vials over saturated salt solutions of $Mg(NO_3)_2$, $NaNO_2$, and NaCl, which at experimental conditions gave a_w values of 0.54, 0.65, and

0.76, respectively, at equilibrium (Labuza et al., 1985). The vials with samples were weighed every hour up to 6 h, at 8, 10, 12, and 24 h, and at 24-h intervals thereafter. The a_w values of the saturated salt solutions were confirmed with an a_w meter (Aqua Lab CX-2, Decagon Devices, Inc. Pullman, Washington, U.S.A.). The initial sample weights and the weights after storage were used to derive water contents. The mean water content \pm standard deviation (SD) of triplicate samples for each material was plotted against time (Berlin et al., 1968) to assess water sorption kinetics and crystallization.

The BET (Brunauer-Emmett-Teller) and GAB (Guggenheim-Anderson-de Boer) equations were used to model water sorption (Roos, 1993). The BET and GAB isotherm parameters, m_m (monolayer value) and K , were obtained by plotting $a_w/(1-a_w)m$ against a_w (Labuza, 1968) and a_w/m against a_w (Bizot, 1983), respectively. Linear regression for BET and second order polynomial regression for GAB were applied for a_w values of 0.11 to 0.44, as crystallization of sugars was occurring during experiments at higher a_w values.

2.2.5 Glass transition and crystallization by DSC

The onset, T_g (onset), midpoint, T_g (midpoint), and endset, T_g (endset), temperatures of the glass transition of anhydrous systems and those equilibrated to various a_w values, and the instant crystallization temperature (the onset temperature of crystallization), T_{ic} , were measured using DSC. To determine the T_g and T_{ic} , 10-15 mg of the powdered freeze-dried materials were prepared in open DSC pans and equilibrated over P_2O_5 and

saturated salt solutions to a_w values of 0 to 0.44 at room temperature. After equilibration, the pans were hermetically sealed and samples analyzed (Table 2.4). The T_g and T_{ic} were taken from the 2nd heating scans. In glass transition study, the 2nd heating scan was used to reduce differences in interpretation and variations in thermal history resulting from equilibration at varying a_w conditions. We have used the onset T_g which agreed with the onset temperatures of the first heating scans. This interpretation was in line with the use of T_g onset as described by Angell (2002). Anhydrous samples were analyzed using punctured pans; the 1st heating scan evaporated the water sorbed during sample preparation, and ‘anhydrous’ state of the samples during the 2nd heating scan was expected. All DSC pans with humidified samples were weighed before and after measurements to ensure the pans were hermetically sealed and no water was lost from the samples during the 1st heating scan. All measurements were carried out in triplicate.

2.2.6 Prediction of the T_g and the critical water contents

The Gordon-Taylor (Gordon and Taylor, 1952) equation (Equation 2.1) was used to model water plasticization.

$$T_g = \frac{w_1 T_{g1} + k w_2 T_{g2}}{w_1 + k w_2} \quad (2.1)$$

where w_1 and w_2 are the respective weight fractions of the solid and water, T_{g1} is the T_g of the anhydrous solids, T_{g2} is the T_g of amorphous water (-135 °C was used, Johari et al., 1987), and k is a constant. The constant k was derived from the experimental T_g

data. The critical water content and critical a_w values at 24 °C were obtained using Equation 2.1 and the GAB water sorption isotherms (Jouppila and Roos, 1994a). The solute concentration of maximally freeze-concentrated systems, C_g' , was calculated using Equation 2.1 with the experimental T_g' , and state diagrams (Roos, 1995) for each system were established.

2.3 RESULTS AND DISCUSSION

2.3.1 Electrophoresis of proteins

The 15% SDS PAGE of casein and soy protein isolate was carried out under both reducing and non-reducing conditions to determine the molecular weight profile of the proteins. The principal intrinsic proteins in SPI were 11S and 7S with molecular weights (MW) in the range of 370 and 140 kDa, respectively (Thanh and Shibasaki, 1978; Arrese et al., 1991). SPI at reducing conditions showed bands from 14.2 to 97 kDa (Figure 2.1), indicating the subunits of soy proteins. The non-reduced conditions for SPI showed molecular weights of 55 kDa and above. There was also SPI retained at the top of the gel, indicating aggregation of the subunits. Casein at reducing conditions showed molecular weights to range from 14.2 to 36 kDa. The non-reducing conditions for casein showed absence of some bands with smaller MW from 14.2 to 24 kDa. These smaller molecules may be formed as a result of the breakdown of disulphide bonds in κ -casein at reducing conditions (Woychik, 1965). Our results suggested that the casein contained β -casein and α -casein, and a small amount of κ -casein was present.

Compositional and molecular factors often affect the glass transitions of food materials (Roos and Karel, 1991b). Depending on the miscibility of the components, proteins may increase the average effective MW in carbohydrate-protein systems. Therefore, the electrophoresis of proteins was important to see whether the size of proteins affected glass transition and crystallization properties of component sugars.

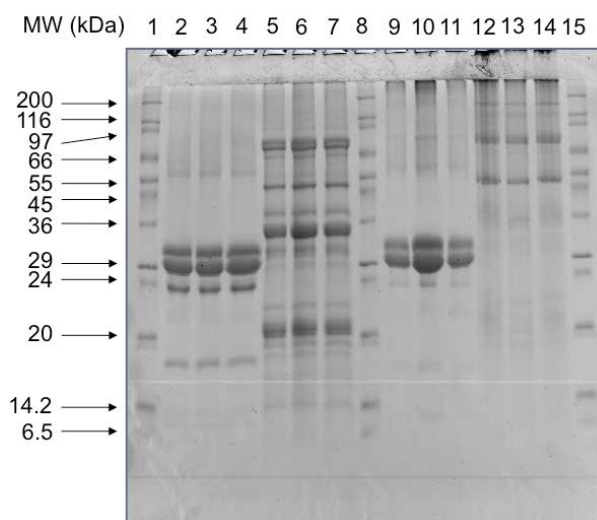


Figure 2.1 SDS PAGE of the marker, casein, and soy protein isolate: 15% acrylamide gel with marker in lane 1, 8, and 15; casein at reducing condition in lane 2, 3, and 4; casein at non-reducing condition in lane 9, 10, and 11; soy protein isolate at reducing condition in lane 5, 6, and 7; and soy protein isolate at non-reducing condition in lane 12, 13, and 14.

2.3.2 Frozen state transitions

The onset temperatures of glass transition and ice melting in maximally freeze-concentrated systems (T_g' and T_m') and the solute concentration of maximally freeze-concentrated systems (C_g') are given in Table 2.1. Both pure carbohydrate and carbohydrate-protein suspensions showed initial concentration-independent T_g' and T_m' values (Roos, 1995). Lactose and trehalose showed similar T_g' and T_m' values. Singh and Roos (2006 and 2007) reported higher T_m' and lower T_g' values for frozen

carbohydrate-protein systems than for pure carbohydrates. In the present study, the component proteins were not found to affect the ice melting in carbohydrate-protein systems as compared to pure carbohydrates.

Table 2.1 Onset temperatures of glass transition (T_g' , °C) and ice melting (T_m' , °C), and solute concentration (C_g' , %) in maximally freeze-concentrated lactose, trehalose, lactose-CAS (3:1), lactose-SPI (3:1), trehalose-CAS (3:1) and trehalose-SPI (3:1) suspensions with initial solute concentration of 10, 15, and 20% (w/w), respectively.

Systems	10% (w/w)		15% (w/w)		20% (w/w)		Average	
	T_g'	T_m'	T_g'	T_m'	T_g'	T_m'	$(T_m' - T_g')$ ^a	C_g' ^b
Lactose	-42 ± 1	-30 ± 1	-42 ± 1	-30 ± 1	-42 ± 1	-30 ± 1	12	84
Trehalose	-43 ± 1	-32 ± 1	-42 ± 1	-32 ± 1	-42 ± 1	-32 ± 1	10	83
Lactose-CAS	-47 ± 1	-30 ± 1	-47 ± 1	-30 ± 1	-47 ± 1	-30 ± 1	17	77
Lactose-SPI	-47 ± 1	-32 ± 1	-47 ± 1	-32 ± 1	-47 ± 1	-32 ± 1	15	78
Trehalose-CAS	-47 ± 1	-32 ± 1	-47 ± 1	-32 ± 1	-47 ± 1	-32 ± 1	15	76
Trehalose-SPI	-46 ± 1	-33 ± 1	-46 ± 1	-34 ± 1	-46 ± 1	-33 ± 1	13	78

^a $(T_m' - T_g')$ showed the broadness of maximum freeze concentration zone

^b C_g' was calculated using Equation 2.1 with the experimental T_g' .

There was, however, a lower T_g' value suggesting that the carbohydrate-protein systems contained a higher quantity of unfrozen water in the maximally freeze-concentrated state than the component carbohydrates alone. That could be possibly because proteins increased the viscosity of the systems and increased the unfrozen water by hydrogen bonding to water molecules linked to carbohydrates. Therefore, a broader temperature difference between T_g' and T_m' values was observed for carbohydrate-protein systems than pure carbohydrates (Table 2.1). The protein type and MW did not affect the frozen state transitions. In nutrient delivery, freezing temperatures may determine the structure of the freeze-dried materials and the success of entrapment or encapsulation of nutrients.

2.3.3 Water sorption behavior

Water sorption of freeze-dried lactose, trehalose, lactose-CAS, lactose-SPI, trehalose-CAS, and trehalose-SPI systems over various a_w values as a function of time was plotted, as shown in Figures 2.2 and 2.3, respectively. All systems showed rapid water sorption within the first 12 h. At a_w values of 0.11 to 0.44, lactose and trehalose showed similar water sorption although slightly less water was sorbed by lactose. Carbohydrate-protein systems showed more rapid initial water sorption and higher amounts of sorbed water than pure carbohydrates (Figure 2.2), which was a result of the high water sorption of proteins. All systems reached steady state water contents within 48 h. The water sorption data for lactose were in agreement but slightly higher than those found by Roos and Karel (1990).

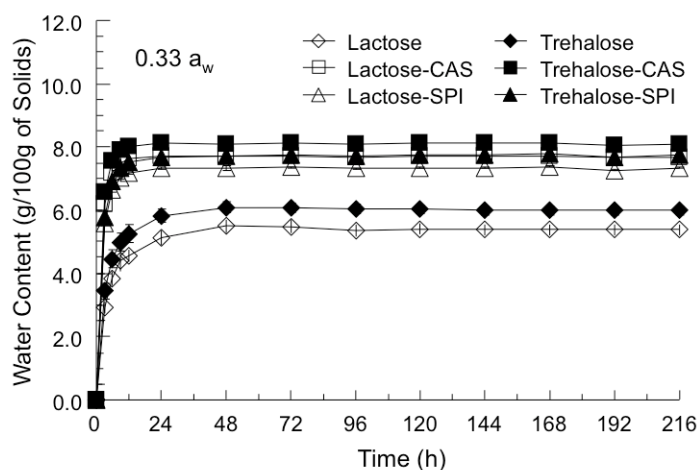


Figure 2.2 Water sorption of freeze-dried lactose, trehalose, lactose-CAS (3:1), lactose-SPI (3:1), trehalose-CAS (3:1) and trehalose-SPI (3:1) systems at 0.33 water activity (a_w) at room temperature (24 ± 1 °C). Vertical bars represent plus and minus (\pm) one standard deviation (SD) of data for triplicate samples.

Lactose, trehalose and lactose with soy protein isolate showed reduced water contents indicating sugar crystallization after 24 h, 12 h, and 96 h respectively at 0.54 a_w . Other

carbohydrate-protein systems did not show significant sugar crystallization during 9 d of storage. There is intermolecular hydrogen bonding between the carbohydrate molecules (Carpenter and Crowe, 1989), but the bonding can be diminished and replaced by carbohydrate-protein bonding in the presence of proteins (Allison et al., 1999; Souillac et al, 2002). The delayed sugar crystallization in various carbohydrate-protein systems also suggested interactions between carbohydrates and proteins. At 0.65 a_w , sugar crystallization occurred after 6 h and 4 h storage, and constant water contents were reached within 18 h and 2 h for lactose and trehalose, respectively. The sugar crystallization, especially trehalose crystallization, was retarded by the component proteins in carbohydrate-protein systems. In the presence of SPI, both lactose and trehalose showed crystallization after 12 h storage. Constant water contents, however, were reached within 12 h and 36 h for lactose and trehalose, respectively. In the presence of CAS, lactose crystallized after 12 h and trehalose 36 h and the time required to reach constant water contents was 36 h and 48 h for lactose and trehalose, respectively. At 0.76 a_w , all systems showed sugar crystallization within 12 h (Figure 2.3). Trehalose showed the shortest time to crystallization (3 h), followed by lactose (4 h), lactose-SPI (6 h), trehalose-SPI (8 h), lactose-CAS (8 h), and trehalose-CAS (10 h). Different times were found to reach the final water contents, which were the most rapid for trehalose (2 h), followed by trehalose-SPI (4 h), lactose-SPI (6 h), lactose (8 h), trehalose-CAS (14 h) and lactose-CAS (16 h) (Figure 2.3).

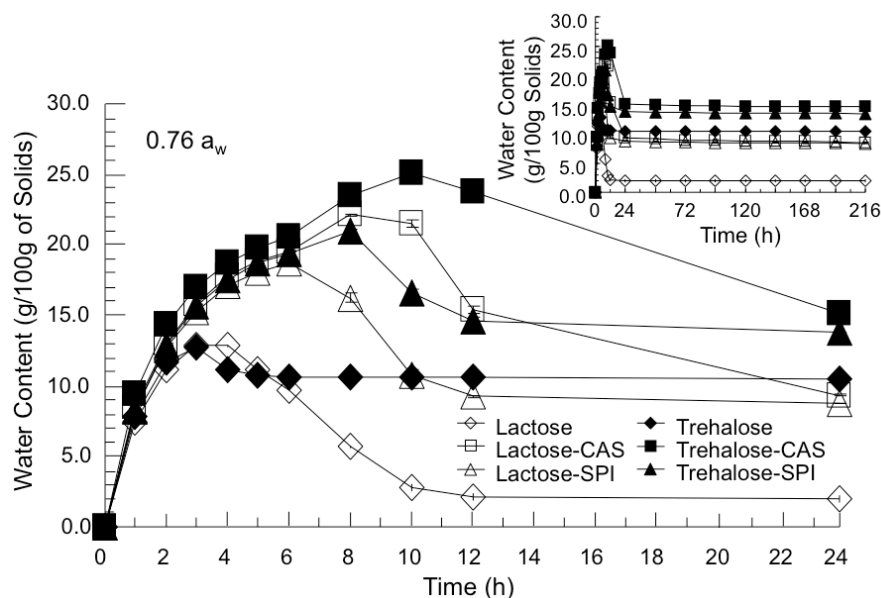


Figure 2.3 Water sorption of freeze-dried lactose, trehalose, lactose-CAS (3:1), lactose-SPI (3:1), trehalose-CAS (3:1) and trehalose-SPI (3:1) systems at 0.76 water activity (a_w) at room temperature (24 ± 1 °C). The inserted figure shows the whole experimental range of water sorption. Loss of water indicates lactose or trehalose crystallization. Vertical bars represent plus and minus (\pm) one standard deviation (SD) of data for triplicate samples.

The final water contents after crystallization are given in Table 2.2, which showed that a mixture of crystalline monohydrate and anhydrate was formed by lactose (Haque and Roos, 2005b) but crystalline dihydrate and possibly some anhydrate by trehalose (Miao and Roos, 2005a). The longer time to trehalose crystallization than to lactose crystallization in carbohydrate-protein systems may have resulted from (i) the higher amount of water required to form crystalline trehalose dihydrate than to form crystalline lactose monohydrate or anhydrate at limited sorbed water contents; and (ii) the higher solubility and lower number of available crystalline forms of trehalose. More delayed sugar crystallization by CAS than by SPI (Figure 2.3) indicated that the molecular movement of sugars was more restricted in the presence of CAS than SPI.

Table 2.2 Water content (mean values \pm SD, g/100g solid) in freeze-dried lactose, trehalose, lactose-CAS (3:1), lactose-SPI (3:1), trehalose-CAS (3:1) and trehalose-SPI (3:1) systems after equilibration to various water activity (a_w) values for 9 d at room temperature (in general 24 ± 1 °C).

Systems	Water content (g/100g of solids)							
	0.00 a_w	0.11 a_w	0.23 a_w	0.33 a_w	0.44 a_w	0.54 a_w	0.65 a_w	0.76 a_w
Lactose	0 \pm 0.0	2.5 \pm 0.1	4.5 \pm 0.1	5.4 \pm 0.2	8.4 \pm 0.3	3.4 \pm 0.1	2.4 \pm 0.2	2.0 \pm 0.3
Trehalose	0 \pm 0.0	2.8 \pm 0.1	4.8 \pm 0.2	6.0 \pm 0.1	9.2 \pm 0.2	9.6 \pm 0.7	10.5 \pm 0.0	10.4 \pm 0.2
Lactose-CAS	0 \pm 0.0	4.0 \pm 0.0	6.1 \pm 0.0	7.7 \pm 0.0	9.9 \pm 0.1	13.4 \pm 0.1	7.5 \pm 0.0	8.7 \pm 0.1
Lactose-SPI	0 \pm 0.0	3.7 \pm 0.0	5.8 \pm 0.0	7.3 \pm 0.0	9.5 \pm 0.0	11.9 \pm 0.1	6.8 \pm 0.0	8.4 \pm 0.0
Trehalose-CAS	0 \pm 0.0	4.1 \pm 0.0	6.4 \pm 0.0	8.1 \pm 0.0	10.4 \pm 0.0	14.2 \pm 0.1	13.5 \pm 0.0	14.7 \pm 0.0
Trehalose-SPI	0 \pm 0.0	3.9 \pm 0.0	6.1 \pm 0.0	7.8 \pm 0.0	10.0 \pm 0.0	13.5 \pm 0.0	12.8 \pm 0.0	13.5 \pm 0.0

The BET (Brunauer-Emmett-Teller) and GAB (Guggenheim-Anderson-de Boer) relationships were fitted to the water sorption data. Values for K , m_m , and R^2 found for BET (K_1 , m_{m1} , and R_1^2 , respectively) and GAB (K_2 , m_{m2} and R_2^2 , respectively) models are given in Table 2.3.

Table 2.3 BET (Brunauer-Emmett-Teller) and GAB (Guggenheim-Anderson-de Boer) constants (K_1 and K_2), monolayer values (m_{m1} and m_{m2} , g/100g solid), and R^2 (R_1^2 and R_2^2) for freeze-dried lactose, trehalose, lactose-CAS (3:1), lactose-SPI (3:1), trehalose-CAS (3:1) and trehalose-SPI (3:1) systems.

Systems	BET ^a			GAB ^a		
	K_1 ^d	m_{m1} ^d	R_1^2 ^b	K_2 ^e	m_{m2} ^e	R_2^2 ^c
Lactose	4.75	5.65	0.9136	1.27	4.01	0.7009
Trehalose	4.73	6.20	0.9365	1.33	4.08	0.8668
Lactose-CAS	10.35	6.19	0.9997	1.00	6.21	0.9987
Lactose-SPI	9.39	6.02	0.9995	1.03	5.79	0.9987
Trehalose-CAS	9.83	6.56	0.9998	1.01	6.50	0.9993
Trehalose-SPI	9.49	6.31	0.9998	1.03	6.11	0.9998

^a Experimental sorption data at a_w values from 0.11 to 0.44 were used to fit equations

^b R_1^2 for the linear regression $a_w/m(1-a_w)=ba_w+c$

^c R_2^2 for quadratic regression $a_w/m=\alpha a_w^2+\beta a_w+\gamma$

^d K_1 and m_{m1} derived from constants b and c , which was shown in materials and methods

^e K_2 and m_{m2} derived from constants α , β and γ , which was shown in materials and methods

Trehalose showed similar sorption isotherms but slightly higher m_m values than lactose. Carbohydrate-protein systems showed higher m_m values than pure carbohydrates. The sorption isotherms (Figure 2.4) for all systems followed the Type II isotherm (Brunauer et al., 1938; Roos, 1995). Lactose and trehalose showed less sigmoid shape sorption isotherms than carbohydrate-protein systems due to their fairly low initial sorption of water. The higher m_m values of carbohydrate-protein systems were possibly a result of the water sorption by proteins, which were found to accumulate on the surface of carbohydrate-protein particles (Millqvist-Fureby et al., 1999; Nasirpour et al., 2007). Different m_m values but similar corresponding a_w values were obtained for all systems. The corresponding a_w values for the GAB m_m values were 0.22, 0.20, 0.24, 0.23, 0.24,

and 0.24 for lactose, trehalose, lactose-CAS, lactose-SPI, trehalose-CAS, and trehalose-SPI systems, respectively. The a_w corresponding to the m_m values are often used in predicting the stability of low-moisture foods. Systems at these a_w conditions were found to have fairly low rates of chemical reactions (Dennison et al., 1977) and the lowest rate of lipid oxidation (Nelson and Labuza, 1992). However, in amorphous glassy systems, the glass transition behavior may also affect rates of chemical reactions, especially those of diffusion-controlled reactions (Roos, 1995).

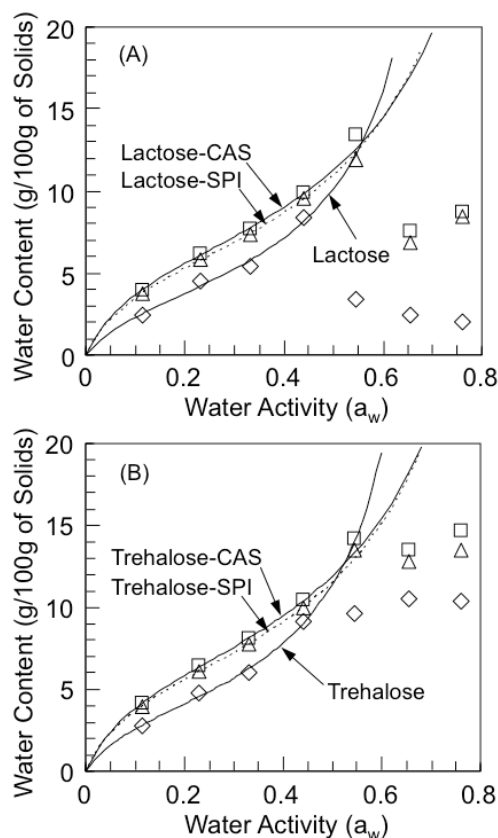


Figure 2.4 Water sorption isotherms of (A) freeze-dried lactose (\diamond), lactose-CAS (3:1) (\square), and lactose-SPI (3:1) (\triangle), and (B) trehalose (\diamond), trehalose-CAS (3:1) (\square), and trehalose-SPI (3:1) (\triangle) systems. Experimental data are at 9 d at room temperature (24 ± 1 °C). The isotherms were modeled using the GAB relationship.

2.3.4 Glass transition and crystallization

The glass transition temperatures for anhydrous and water plasticized lactose, trehalose, lactose-CAS, lactose-SPI, trehalose-CAS, and trehalose-SPI systems are given in Table 2.4. Anhydrous carbohydrate-protein systems, especially carbohydrate-SPI systems, showed higher T_g (onset) values than pure carbohydrates, suggesting that the molecular movement of carbohydrates was restricted more strongly by the high MW protein molecules. The decrease of T_g with increasing a_w indicated water plasticization (Roos and Karel, 1990). The decrease was most pronounced at 0.11 a_w . The T_g (onset) as a function of water content (g/100g solid) and a_w are shown in Figure 2.5.

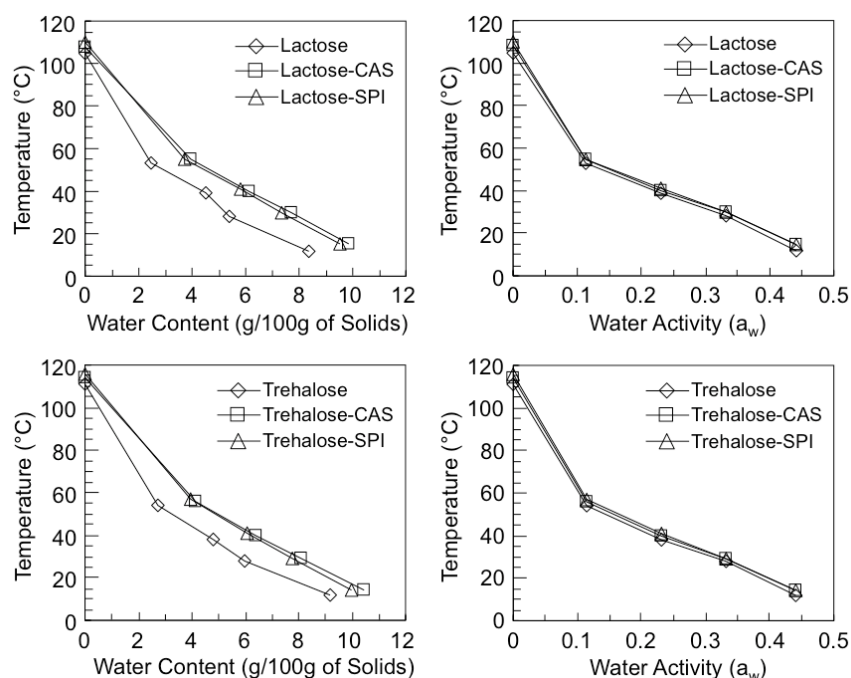


Figure 2.5 Effect of water content and water activity (a_w) on the onset temperature of glass transition (T_g , °C) in freeze-dried lactose, trehalose, lactose-CAS (3:1), lactose-SPI (3:1), trehalose-CAS (3:1) and trehalose-SPI (3:1) systems.

Corresponding T_g (onset) values at the same a_w were found for the water plasticized systems with the same carbohydrates (lactose or trehalose) showing that the T_g values were dependent on the carbohydrate component. The protein type and MW did not significantly affect the glass transition of water plasticized systems, since the plasticizing effect of water diminished the effect of proteins as the water content increased (Kalichevsky and Blanshard, 1993). One single glass transition for carbohydrate-protein systems was observed, but less broad glass transition zones and lower T_g (endset) values were found for carbohydrate-protein systems than for pure carbohydrates (Table 2.4). Enthalpy relaxations of the pure carbohydrate systems broadened their glass transition temperature range at all a_w values, but no relaxations were present in the second heating scans of the carbohydrate-protein systems.

Crystallization of amorphous lactose was found in humidified materials and also in the anhydrous systems (Table 2.5). Below 0.44 a_w , no instant crystallization was found for trehalose. This was possibly because of the low water content, which was not sufficient for trehalose to crystallize as a dihydrate. At 0.44 a_w , the T_{ic} for trehalose was lower than that for lactose, which supported the shorter time to crystallization of trehalose (Figure 2.3) above the critical a_w value. This was opposite to the results of Cardona et al. (1997) and Surana et al. (2004), who found trehalose crystallization at 0.22 a_w at about 95 °C and as anhydrous crystals at about 189 °C, respectively, using DSC. Plasticized lactose-protein systems showed higher T_{ic} values than pure lactose (Table 2.5), indicating delayed lactose crystallization in the presence of proteins.

Table 2.4 Onset, midpoint and endset temperatures of glass transition (T_g , °C) at various water activity (a_w) values for freeze-dried lactose, trehalose, lactose-CAS (3:1), lactose-SPI (3:1), trehalose-CAS (3:1) and trehalose-SPI (3:1) systems.

Systems		Glass transition temperature (T_g , °C)				
		0.00 a_w ^a	0.11 a_w ^b	0.23 a_w ^c	0.33 a_w ^d	0.44 a_w ^e
Lactose	T_g (onset)	105 ± 1	53 ± 1	39 ± 1	28 ± 1	12 ± 1
	T_g (midpoint)	113 ± 1	61 ± 1	45 ± 1	35 ± 1	19 ± 1
	T_g (endset)	123 ± 1	71 ± 1	56 ± 1	45 ± 1	28 ± 1
Trehalose	T_g (onset)	111 ± 1	54 ± 1	38 ± 1	28 ± 1	12 ± 1
	T_g (midpoint)	117 ± 1	60 ± 1	45 ± 1	35 ± 1	18 ± 1
	T_g (endset)	125 ± 1	70 ± 1	55 ± 1	44 ± 1	28 ± 1
Lactose-CAS	T_g (onset)	108 ± 1	55 ± 1	40 ± 1	30 ± 1	15 ± 1
	T_g (midpoint)	113 ± 1	61 ± 1	46 ± 1	35 ± 1	21 ± 1
	T_g (endset)	119 ± 1	66 ± 1	51 ± 1	41 ± 1	26 ± 1
Lactose-SPI	T_g (onset)	110 ± 1	55 ± 1	41 ± 1	30 ± 1	15 ± 1
	T_g (midpoint)	116 ± 1	63 ± 1	47 ± 1	36 ± 1	22 ± 1
	T_g (endset)	121 ± 1	67 ± 1	52 ± 1	41 ± 1	27 ± 1
Trehalose-CAS	T_g (onset)	114 ± 1	56 ± 1	40 ± 1	29 ± 1	14 ± 1
	T_g (midpoint)	119 ± 1	63 ± 1	46 ± 1	35 ± 1	20 ± 1
	T_g (endset)	125 ± 1	68 ± 1	51 ± 1	40 ± 1	26 ± 1
Trehalose-SPI	T_g (onset)	116 ± 1	57 ± 1	41 ± 1	29 ± 1	14 ± 1
	T_g (midpoint)	121 ± 1	64 ± 1	47 ± 1	36 ± 1	21 ± 1
	T_g (endset)	124 ± 1	68 ± 1	52 ± 1	40 ± 1	26 ± 1

^a DSC method: (i) 25 °C to 150 °C at 5 °C/min, (ii) 150 °C to 25 °C at 10 °C/min, and (iii) 25 °C to 200 °C at 5 °C/min.

^b DSC method: (i) 25 °C to 90 °C at 5 °C/min, (ii) 90 °C to 25 °C at 10 °C/min, and (iii) 25 °C to 150 °C at 5 °C/min.

^c DSC method: (i) 10 °C to 70 °C at 5 °C/min, (ii) 70 °C to 10 °C at 10 °C/min, and (iii) 10 °C to 140 °C at 5 °C/min.

^d DSC method: (i) 0 °C to 60 °C at 5 °C/min, (ii) 60 °C to 0 °C at 10 °C/min, and (iii) 0 °C to 130 °C at 5 °C/min.

^e DSC method: (i) -10 °C to 50 °C at 5 °C/min, (ii) 50 °C to -10 °C at 10 °C/min, and (iii) -10 °C to 120 °C at 5 °C/min.

The higher T_{ic} values of lactose-CAS agreed with the results of water sorption showing that lactose crystallization was more delayed in the lactose-CAS than in the lactose-SPI systems. The higher T_{ic} values showed that the mobility of lactose required for crystallization was decreased. Although trehalose-protein mixtures sorbed higher amounts of water than pure trehalose (Table 2.2), no instant crystallization was found at

or below 0.44 a_w . The T_{ic} decreased with increasing water content and a_w . However, the T_{ic} was more dependent on composition, especially the component proteins, than the T_g values.

Table 2.5 The instant crystallization temperature (T_{ic} , °C) of freeze-dried lactose, trehalose, lactose-CAS (3:1) and lactose-SPI (3:1) systems at various water activity (a_w) values.

Systems	Instant crystallization temperature (T_{ic} , °C)				
	0.00 a_w	0.11 a_w	0.23 a_w	0.33 a_w	0.44 a_w
Lactose	174 ± 1	115 ± 1	97 ± 1	88 ± 1	65 ± 1
Trehalose	N/O ^a	N/O ^a	N/O ^a	N/O ^a	48 ± 1
Lactose-CAS	N/O ^a	N/O ^a	121 ± 1	112 ± 1	87 ± 1
Lactose-SPI	N/O ^a	125 ± 1	108 ± 1	97 ± 1	80 ± 1

^a N/O=not observed

Proteins affected the glass transition by decreasing the free volume available to the carbohydrates, therefore, restricting the molecular mobility (Kalichevsky and Blanshard, 1993). The MW of CAS was lower than that of SPI (Figure 2.1). SPI proteins had quaternary structures, which were composed of various subunits (Kinsella, 1979). Those subunits were associated via disulphide and perhaps hydrogen bonding, which made the SPI difficult to unfold and interact with the carbohydrate molecules. The components with the higher MW (SPI) possibly decreased more free volume than those with lower MW (CAS). Sugar crystallization caused structural changes of the matrices which in nutrient delivery applications could lead to the release of entrapped volatiles or exposure of the encapsulated compounds to surroundings. The water released during sugar crystallization may also cause further destabilization of the structure as well as deteriorate sensitive components.

2.3.5 The critical a_w values and nutrient delivery

The T_g (onset) values as a function of water contents (g/100g solid) were predicted using Equation 1 (Gordon and Taylor, 1952). The k constants, critical water contents (g/100g solid) and critical a_w values at 24 °C for lactose, trehalose, lactose-CAS, lactose-SPI, trehalose-CAS, and trehalose-SPI are given in Table 2.6. Examples of the relationships between water plasticization and the critical water content and the corresponding critical a_w value at 24 °C are shown in Figure 2.6. State diagrams were plotted for all systems, as shown for trehalose in Figure 2.7.

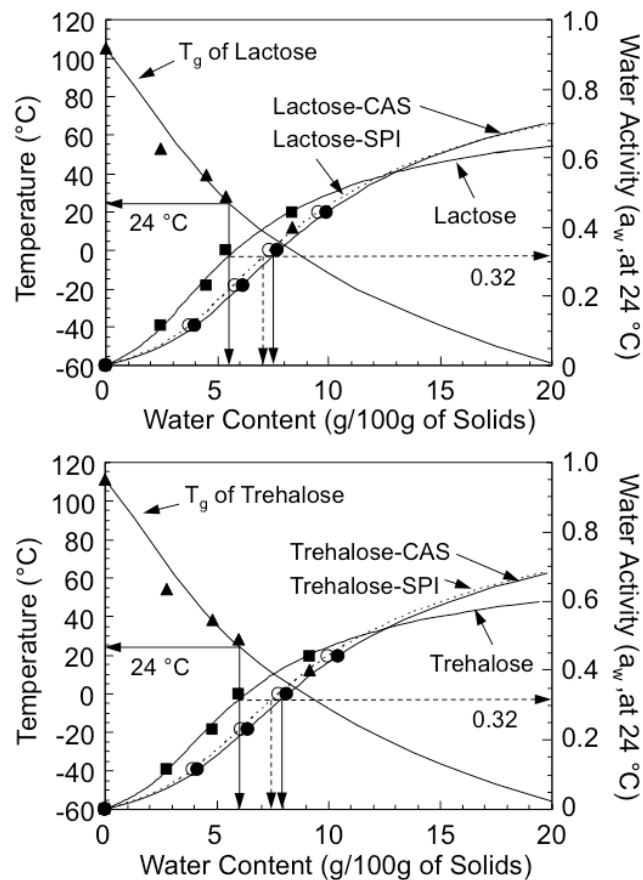


Figure 2.6 The relationships between the glass transition temperatures (T_g , onset), water contents and water activity (a_w) values for freeze-dried lactose, trehalose, lactose-CAS (3:1), lactose-SPI (3:1), trehalose-CAS (3:1), and trehalose-SPI (3:1) systems. The sorption isotherms were predicted with GAB model. The depression of T_g as a result of water plasticization was predicted by Equation 2.1. The critical water contents (g/100g solid) and critical water activity (a_w) values at 24 °C are indicated with arrows.

Table 2.6 The k constants, critical water contents (g/100g solid) and critical water activity (a_w) values at 24 °C for freeze-dried lactose, trehalose, lactose-CAS (3:1), lactose-SPI (3:1), trehalose-CAS (3:1) and trehalose-SPI (3:1) systems.

Systems	k^a	Critical water content (g/100g solid)	Critical a_w
Lactose	8.3 ± 1.4	5.6	0.32
Trehalose	8.3 ± 1.6	6.1	0.32
Lactose-CAS	5.9 ± 0.5	8.1	0.35
Lactose-SPI	6.4 ± 0.7	7.7	0.34
Trehalose-CAS	6.1 ± 0.4	8.3	0.35
Trehalose-SPI	6.5 ± 0.6	8.1	0.35

^a k constants were derived from Equation 2.1

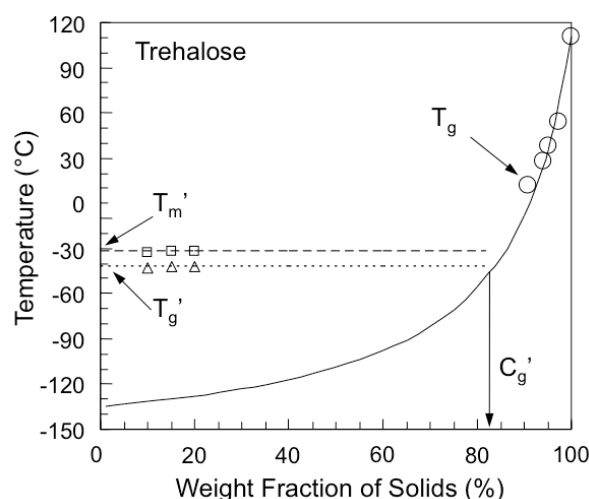


Figure 2.7 State diagram for freeze-dried trehalose. The decrease of T_g with increasing water content indicated water plasticization. Maximally freeze-concentrated solutions showed solute concentration in unfrozen phase at C_g' , and constant onset temperature of glass transition (T_g') and onset temperature of ice melting (T_m'). Maximum ice formation occurred at temperature $T_g' < T < T_m'$.

The critical water contents and a_w values were higher than the m_m values and the corresponding a_w values, respectively. Based on previous studies, we expect that the m_m value is important as a reference to a water content above which reaction rates may increase because of the increasing capability of water to act as a reaction medium (Labuza, 1980). Although higher a_w values may cause the degradation of encapsulated

particles (Widicus et al., 1980), reactions may still exhibit low rates due to the low diffusion of reactants in the glassy matrices (Miao and Roos, 2004). The critical water content as well as the corresponding a_w is important for the stability of low-moisture foods (Slade and Levine, 1991) when changes are controlled by the glass transition of the solids. Above the critical a_w values, the matrices exist in the rubbery state with increased diffusion of reactants, leading to increased reaction rates (Miao and Roos, 2004). Carbohydrate-protein matrices in the present study showed delayed sugar crystallization and higher critical water contents and critical a_w values than were found for the component carbohydrates. Therefore, we expect that carbohydrate-protein systems when designed for nutrient may provide better stability for the nutrients than simple glass forming sugars. Also the role of proteins as emulsifiers supports their use in nutrient delivery formulations together with the glass-forming carbohydrates. The state diagrams as well as the relationships between water plasticization and critical water contents and a_w values provided information on the selection of processing parameters and storage conditions for nutrient delivery applications using lactose and trehalose.

2.4 CONCLUSIONS

The present study compared the water sorption, glass transition, and crystallization behavior of lactose and trehalose with and without the presence of proteins. The results showed that lactose and trehalose had similar water sorption but different crystallization properties. We found that trehalose crystallized earlier than lactose at all a_w conditions

as a pure carbohydrate. In the presence of proteins, the crystallization of carbohydrates, especially trehalose crystallization, was delayed. It should be noted that the water content was more important for trehalose crystallization than for lactose crystallization. Trehalose did not show instant crystallization without the presence of sufficient amount of water for the formation of dihydrate crystals. The freeze-dried carbohydrate-protein materials showed improved stability against component sugar crystallization and, therefore, better stabilization through entrapment or encapsulation of nutrients. Further studies are required to determine the stability of nutrients in carbohydrate-protein systems as possibly affected by formulation and a_w conditions.

CHAPTER 3

Stability and plasticizing and crystallization effects of vitamins in amorphous sugar systems

Published in *Journal of Agricultural and Food Chemistry*, Zhou and Roos, 2012, 60(4):1075-1083

ABSTRACT

Increased molecular mobility and structural changes resulting from water plasticization of glassy solids may lead to loss of the entrapped compounds from encapsulant systems. In the present study, stability of water soluble vitamins, vitamin B₁ (vB₁, thiamine hydrochloride) and vitamin C (vC, ascorbic acid) in freeze-dried lactose and trehalose at various water activities (a_w) was studied. Water sorption of lactose-vB₁, lactose-vC, trehalose-vB₁ and trehalose-vC systems was determined gravimetrically. Glass transition and crystallization of anhydrous and plasticized sugar-vitamin systems were determined using thermal analysis. Critical water activity was calculated using water sorption and glass transition data. The retention of the vitamins was measured spectrophotometrically. The results showed that the amorphous structure protected the entrapped vitamins at low a_w . Crystallization of lactose accelerated vitamin degradation while trehalose retained much higher amounts of the vitamins. Glass transition and

critical water activity of solids and crystallization of component sugars should be considered in stabilization of sensitive components.

Keywords: ascorbic acid, crystallization, glass transition, lactose, thiamine, trehalose, water activity

3.1 INTRODUCTION

Ascorbic acid retention correlates well with retention of other nutrients in foods. Its retention is often used as an index for nutrient quality in processed and stored foods (Fennema, 1977; Uddin et al., 2002). Thiamine is one of the least heat stable vitamins (Labuza and Kamman, 1982) and it is sensitive to pH (Pachapurkar and Bell, 2005), oxygen (Dennison and Kirk, 1978), and trace metals (Dennison and Kirk, 1982) similarly to other water soluble vitamins. Their stability is also dependent on water content and water activity (a_w) in low water systems (Lee and Labuza, 1975; Dennison and Kirk, 1978; Laing et al., 1978; Labuza, 1980). The degradation of sensitive compounds increased with increasing water activity (a_w), which decreased viscosity and increased the level of dissolved oxygen (Labuza et al., 1970).

Carbohydrates often exist as amorphous solids (glasses), which makes them potential food components for nutrient entrapment and use as encapsulant materials in nutrient stabilization. The amorphous encapsulants are well-known to provide rapid release of active substances in pharmaceuticals and they are desirable in therapeutic uses (Hancock and Zografi, 1997). However, the amorphous glasses are non-equilibrium

materials. When plasticized by temperature or water they may transform to the supercooled liquid state, i.e., the glass transition takes place leading to physical changes and loss of shelf life (Levine and Slade, 1988; Slade and Levine, 1991). The glass transition also affects the stability of food ingredients, which may show collapse and crystallization of components (Roos and Karel, 1990; Chuy and Labuza, 1994; Bhandari et al., 1997; Chapter 2). Chen et al. (1999) and Bell et al. (2000) reported that the stability of tyrosinase and thiamine in model systems was more correlated to the glass transition than water activity. The glass transition of the matrices increased the molecular mobility of the encapsulants and also the entrapped particles, resulting in an increased rate of diffusion-controlled chemical reactions (Chen et al., 1999; Bell and White, 2000; Miao and Roos, 2005b). Therefore the glass transition behaviour of the solids should be considered in addition to water activity in the stabilization of sensitive components.

Lactose and trehalose are glass-forming disaccharides that are commonly used in the food industry. They have similar hygroscopic and glass transition properties, but very different solubilities in water and crystallization behavior (Miao and Roos, 2005a; Chapter 2). Numerous studies have addressed the amorphous state and crystallization behavior of common encapsulant sugars, but the effects of water and sugar crystallization on the retention of sensitive components, such as vitamins, have not been intensively studied. The purpose of the present study was to entrap and stabilize model water soluble vitamins (B₁ and C) in amorphous lactose and trehalose matrices by freezing and freeze-drying. The water sorption and glass transition properties of the systems in the presence of the vitamins were analyzed, and the stability of the vitamins

in frozen and freeze-dried lactose and trehalose systems, as affected by composition, process, storage conditions (temperature and a_w), and physical changes (glass transition and sugar crystallization), was determined.

3.2 MATERIALS AND METHODS

3.2.1 Materials

α -Lactose monohydrate (Sigma-Aldrich, St. Louis, Mo., U.S.A.), trehalose dihydrate (Cargill Inc., Minneapolis, Minn., U.S.A.), L-ascorbic acid (vC, Sigma-Aldrich, St. Louis, MO, U.S.A.), and thiamine hydrochloride (vB₁, Sigma-Aldrich, St. Louis, MO, U.S.A.) were purchased to prepare lactose-vB₁, lactose-vC, trehalose-vB₁, and trehalose-vC (250 ml; 20% sugar, w/v; 0.5% vitamin, w/v) systems. Sugars were dissolved in distilled water at 45 °C on a hot plate to obtain clear solutions and then cooled to room temperature (24 ± 1 °C). The vitamins were firstly dissolved in water then added to sugar solutions and the volume was adjusted to 250 ml in a volumetric flask.

Aliquots of the lactose-vB₁, lactose-vC, trehalose-vB₁, and trehalose-vC solutions (5 ml) at pH 3.0 ± 0.1 were transferred using a volumetric pipette (Pipetman P5000, Gilson Inc., Middleton, WI, U.S.A.) into glass vials (Clear glass ND18, 10 ml, VWR, U.K.). The samples in the vials were frozen at -35 °C ($T_g' < T < T_m'$ (Levine and Slade, 1988; Slade and Levine, 1991)) for 24 h, and subsequently transferred to a -80 °C freezer for 5 h to lower the sample temperature to avoid ice melting during transfer to a

freeze-dryer (Lyovac GT2, STERIS, Hürth, Germany), which was pre-run for 2 h for pre-cooling of condenser prior to sample loading. Frozen samples in glass vials with semi-closed rubber septa were freeze-dried at < 0.1 mbar ($T < -40$ °C) for ≥ 72 h. All vials were hermetically closed in the freeze-dryer using the rubber septa prior to breaking the vacuum with ambient air. The freeze-dried materials theoretically contained 2.44% (w/w) of either ascorbic acid (vitamin C) or thiamine hydrochloride (vitamin B₁).

3.2.2 Water sorption and sorption isotherms

Triplicate samples of lactose-vB₁, lactose-vC, trehalose-vB₁ and trehalose-vC in opened vials were equilibrated to reach constant water contents (up to 120 h) at room temperature (24 ± 1 °C) in evacuated desiccators over saturated salt solutions (LiCl, CH₃COOK, MgCl₂, and K₂CO₃), which at experimental conditions gave water activities (a_w) of 0.11, 0.23, 0.33, and 0.44, respectively, at equilibrium (Labuza et al., 1985). Desiccators were evacuated (approx. 1 min) until the onset of boiling of water to establish desired water vapor pressure conditions. The samples in vials were weighed at 0, 3, 6, 9, 12, 24, 48, 72, 96 and 120 h. Time-dependent sugar crystallization was monitored during storage of samples in vials over saturated salt solutions of Mg(NO₃)₂, NaNO₂, and NaCl, which at experimental conditions gave a_w of 0.54, 0.65, and 0.76, respectively, at equilibrium (Labuza et al., 1985). The vials with samples were weighed every hour up to 6 h, and then at 8, 10, 12, 24, 48, 72, 96 and 120 h. The a_w of the saturated salt solutions was confirmed with an a_w meter (Aqua Lab 4TE, Decagon

Devices, Inc. Pullman, Washington, U.S.A.). The initial sample weights and the weights after storage were used to derive water contents. The mean water content \pm standard deviation (SD) of triplicate samples for each material and a_w was plotted against time to assess water sorption kinetics and crystallization.

The GAB (Guggenheim-Anderson-de Boer) relationship was used to model water sorption as suggested by Roos (1993). The GAB isotherm parameters were obtained by plotting a_w/m against a_w (Bizot, 1983; Roos, 1993). The constants α , β , and γ were calculated by applying the second order polynomial regression for GAB over the a_w range of 0.11 to 0.44, as higher a_w values could not be used because of the crystallization of the sugars (steady state water contents for fully amorphous solids could not be obtained). The m_m (monolayer value), K , and C were derived from α , β , and γ (Bizot, 1983).

3.2.3 Thermal analysis

Thermal behaviour of water and solids was determined using differential scanning calorimetry (DSC, Mettler Toledo 821e with liquid N_2 cooling, Schwerzenbach, Switzerland). The DSC was calibrated as described by Haque and Roos (Haque and Roos, 2004a). The thermograms were analyzed using STAR thermal analysis software, version 6.0 (Mettler Toledo, Schwerzenbach, Switzerland).

For frozen state transitions, freshly prepared solutions of lactose-vB₁, lactose-vC, trehalose-vB₁, and trehalose-vC (15-25 mg) were transferred using a volumetric pipette (Pipetman P200, Gilson Inc., Middleton, WI, U.S.A.) into pre-weighed DSC aluminium

pans (40 μ L, Mettler Toledo, Schwerzenbach, Switzerland), and the pans with samples were hermetically sealed and weighed (Mettler Toledo AG245 balance). A sealed empty pan was used as a reference in all measurements. Measurements were carried out according to Chapter 2 for the onset temperature of glass transition of the maximally freeze-concentrated solutes, T_g' , and the onset temperature of ice melting in the maximally freeze-concentrated systems, T_m' .

For transitions in low-water systems, the onset, T_g (onset), and endset, T_g (endset), temperatures of the glass transition of anhydrous lactose-vB₁, lactose-vC, trehalose-vB₁, and trehalose-vC and those equilibrated to various water activities (a_w), and the instant crystallization temperature (the onset temperature of crystallization), T_{ic} , were measured using DSC. To determine the T_g and T_{ic} , 10-15 mg of the powdered freeze dried materials were prepared in pre-weighed DSC aluminium pans and equilibrated over P₂O₅ or saturated salt solutions for 72 h to a_w of 0 to 0.44 at room temperature (24 ± 1 °C). After equilibration, the pans were hermetically sealed and weighed. A sealed empty pan was used as a reference in all measurements. The T_g and T_{ic} were taken from the second heating scans and anhydrous samples were analyzed using punctured pans (Chapter 2). All measurements were carried out in triplicate. The mean values of triplicate samples were used in modeling water plasticization.

3.2.4 Prediction of the T_g and the critical water contents

The Gordon-Taylor (Gordon and Taylor, 1952) equation (Equation 3.1) was used to model water plasticization.

$$T_g = \frac{w_1 T_{g1} + k w_2 T_{g2}}{w_1 + k w_2} \quad (3.1)$$

where w_1 and w_2 are the respective weight fractions of the solid and water, T_{g1} is the T_g of the anhydrous solids, T_{g2} is the T_g of amorphous water (-135 °C was used, Johari et al., 1987), and k is a constant. The constant k was derived from the experimental T_g data. The critical water content and the corresponding critical a_w at 24 °C were obtained using Equation 3.1 and the GAB water sorption isotherms (Jouppila and Roos, 1994a). Diagrams of the relationships between water plasticization and the critical water content and the corresponding critical a_w at 24 °C were plotted.

3.2.5 Determination of vitamin contents

The retention of vitamins were measured spectrophotometrically (Varian Cary 300, Bio UV-Visible Spectrophotometer, Agilent Technologies, Santa Clara, CA. U.S.A.). To determine the retention of thiamine hydrochloride, the anhydrous and humidified lactose- vB_1 and trehalose- vB_1 were reconstituted to the original weight and diluted using 0.1 M hydrochloric acid (1/400). The absorbance was measured at 246 nm using a spectrophotometer (Dinç et al., 2000) and no effect of sugars on the absorbance was observed. This wavelength was found to correspond to the maximum absorbance of thiamine hydrochloride in 0.1 M hydrochloric acid over the spectrum of wavelengths from 200 to 300 nm. The standard curve was obtained by measuring the absorbance of thiamine hydrochloride at various concentrations (0-25 $\mu\text{g/ml}$) in 0.1 M hydrochloric acid. A blank sample of 0.1 M hydrochloric acid was used in the double beam

spectrophotometer along with the samples as reference. A pair of Quartz cuvettes (CEL1600, Hellma Cuvette UV Quartz, Scientific Laboratory Supplies LTD, Nottingham, U.K.) was used in this study. The sample cuvette was washed using 0.1 M hydrochloric acid after each measurement and pre-rinsed with sample solutions before each measurement.

To determine the retention of ascorbic acid, the anhydrous and humidified lactose-vC and trehalose-vC were reconstituted to the original weight and diluted using corresponding sugar solutions (20%, w/v). The diluted solution (4 ml) was mixed with 0.2M Folin-Ciocalteu reagent (FCR, 0.8 ml, 1/10 dilution from 2M, Sigma-Aldrich, St. Louis, MO, U.S.A.) vigorously and left at room temperature for 30 min before the colour was measured at 760 nm (Proot et al., 1994) using a spectrophotometer. The standard curve was obtained by measuring the absorbance of the color intensity produced by reaction between the FCR and ascorbic acid at various concentrations (0-100 µg/ml) in corresponding sugar solutions. A blank sample of the FCR with corresponding sugar solutions was used in the spectrophotometer along with the samples as reference.

The stability of thiamine hydrochloride in lactose and trehalose during freezing was studied at various temperatures (-10, -20, -35, and -80 °C) for 60 d. The retention of thiamine hydrochloride was measured every 5 d up to 30 d of storage then every 10 d up to 60 d of storage. Triplicate samples were removed from the freezers and thawed at room temperature for 1 h in dark. The retention of thiamine hydrochloride was diluted using 0.1 M hydrochloric acid and measured as described above.

The retention of thiamine hydrochloride in freshly freeze-dried systems was measured and the resultant amount of thiamine hydrochloride was considered as 100% during the storage study. The freeze-dried lactose-vB₁ and trehalose-vB₁ in open glass vials were stored over P₂O₅ and various saturated salt solutions giving a_w of 0, 0.23, 0.44, and 0.65 in evacuated desiccators at room temperature (24 ± 1 °C). The retention of thiamine hydrochloride was measured at day 0, 1, 3, 6, 9, and 15 of storage. Triplicate samples were taken out at each time point and the salt solutions were stirred using a glass rod to avoid the formation of film on the surface of salt solutions and dehydration of samples. The weight of each sample was recorded before and after storage to monitor water sorption during storage.

The retention of ascorbic acid in freshly freeze-dried systems was measured and the resultant amount of ascorbic acid was considered as 100% during the storage study. The freeze-dried lactose-vC and trehalose-vC in open glass vials were stored over P₂O₅ and various saturated salt solutions giving a_w of 0, 0.11, 0.23, 0.33, 0.44, and 0.65 in evacuated desiccators at room temperature (24 ± 1 °C). The retention of ascorbic acid was measured at day 0, 1, 5, 10, 15, 20, 30, and 60 of storage. Triplicate samples were taken out at each time point and the salt solutions were stirred using a glass rod. The weight of each sample was recorded before and after storage to monitor water sorption during storage.

3.2.6 Statistics

All measurements were carried out in triplicate. The water sorption data, transition temperatures and the retention of vitamins are reported as mean values \pm one standard deviation. All the predictions were based on the triplicate data and the mean values.

3.3 RESULTS AND DISCUSSION

3.3.1 State transitions and stability in frozen systems

The onset temperatures of glass transition and ice melting in maximally freeze-concentrated lactose-vB₁, lactose-vC, trehalose-vB₁, and trehalose-vC systems (T_g' and T_m') are given in Table 3.1. Lactose-vitamin and trehalose-vitamin systems showed corresponding transition temperatures to those of pure lactose and trehalose systems, respectively (Chapter 2), showing that at the level of 0.5% (w/v) addition of vitamins, differences in ice melting or glass transition properties could not be found using differential scanning calorimetry.

Table 3.1 Onset temperatures of glass transition (T_g' , °C) and ice melting (T_m' , °C) of maximally freeze-concentrated lactose-vB₁, lactose-vC, trehalose-vB₁, and trehalose-vC systems.

Systems	T_g' (°C)	T_m' (°C)
Lactose- vB ₁	-41 \pm 1	-31 \pm 1
Lactose-vC	-42 \pm 1	-31 \pm 1
Trehalose- vB ₁	-42 \pm 1	-32 \pm 1
Trehalose-vC	-42 \pm 1	-32 \pm 1

The cryostabilization technology proposed by Levine and Slade (1988) assumed frozen food stability during storage at temperatures below the T_g' . Above the T_g' , the glass transition of the freeze-concentrated solute matrix may control the rates of deteriorative changes in frozen foods (Roos, 1995). In the present study, more than 95% and about 100% of thiamine hydrochloride were retained in lactose-vB₁ and trehalose-vB₁ systems, respectively, after 60 d of storage at -80 °C. This high retention was possibly a result of (i) the low rate of chemical reactions at low temperatures; and (ii) the low diffusion rates in the viscous glassy structures of the freeze-concentrated solutes (Levine and Slade, 1988; Roos, 1995).

At -35 °C, which was above T_g' but below T_m' , the temperature dependence of rates of diffusion and viscosity-related changes in frozen foods may follow the Williams-Landel-Ferry (WLF) relationship using $T-T_g'$ as the temperature difference to the T_g' (Levine and Slade, 1988; Roos, 1995). The $T-T_g' = 7$ °C applied to the present study during storage at -35°C. Such a small $T-T_g'$ in the storage of frozen systems is within the glass transition temperature range. It may result in a decrease of the viscosity from 10^{12} to 10^{10} Pa s, but coupled with the low temperature the rates of deteriorative changes of thiamine, such as nonenzymatic browning, may not be affected. The results showed that in storage below T_m' , thiamine hydrochloride stability was temperature independent, and retention of thiamine hydrochloride was similar at -35 and -80°C. A thin layer of sediments was observed in the thawed lactose-vB₁ system after 5 d of storage and onwards, indicating crystallization of lactose during thawing of the system. No trehalose crystallization was found in thawing of the trehalose-vB₁ system.

Storage at $-20\text{ }^{\circ}\text{C}$ and $-10\text{ }^{\circ}\text{C}$ increased substantially the $T-T_g$ for storage, and the $T-T_g$ values were affected by the melting of ice above the T_m ' (Roos, 1995). Degradation of thiamine hydrochloride was, however, less than 5% in both lactose- vB_1 and trehalose- vB_1 systems at $-20\text{ }^{\circ}\text{C}$ and $-10\text{ }^{\circ}\text{C}$. Sedimentation was pronounced in the thawed lactose- vB_1 system, suggesting an increased extent of lactose crystallization above T_m ', because of dilution and decreased viscosity of the supersaturated unfrozen solute phase (Roos, 1995). Clear solutions were obtained after thawing of trehalose- vB_1 , because trehalose had a higher solubility than lactose and it was less likely to crystallize from the freeze-concentrated solute phase (Figure 3.1).

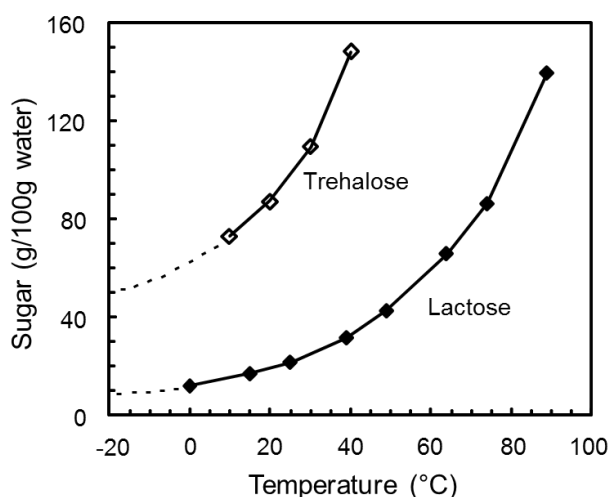


Figure 3.1 Solubility (g/100g water) of lactose (Hunziker and Nissen, 1926) and trehalose (Lammert and Schmidt, 1998) as a function of temperature.

The solubility of lactose was significantly influenced by the α/β form of lactose. The $\alpha:\beta$ ratio of lactose changes depending on the temperature. At the low temperature, the solubility of lactose is mainly controlled by the α form. Due to the high amount of α form, lactose showed very low solubility at $-20\text{ }^{\circ}\text{C}$ and $-10\text{ }^{\circ}\text{C}$. It should be remembered that rates of deteriorative changes, such as nonenzymatic browning, are significantly

decreased at low temperatures (Roos and Himberg, 1994), which may aid to retain the thiamine hydrochloride in frozen systems. The stability of thiamine hydrochloride in the unfrozen phase was possibly also promoted by the low pH (Pachapurkar and Bell, 2005).

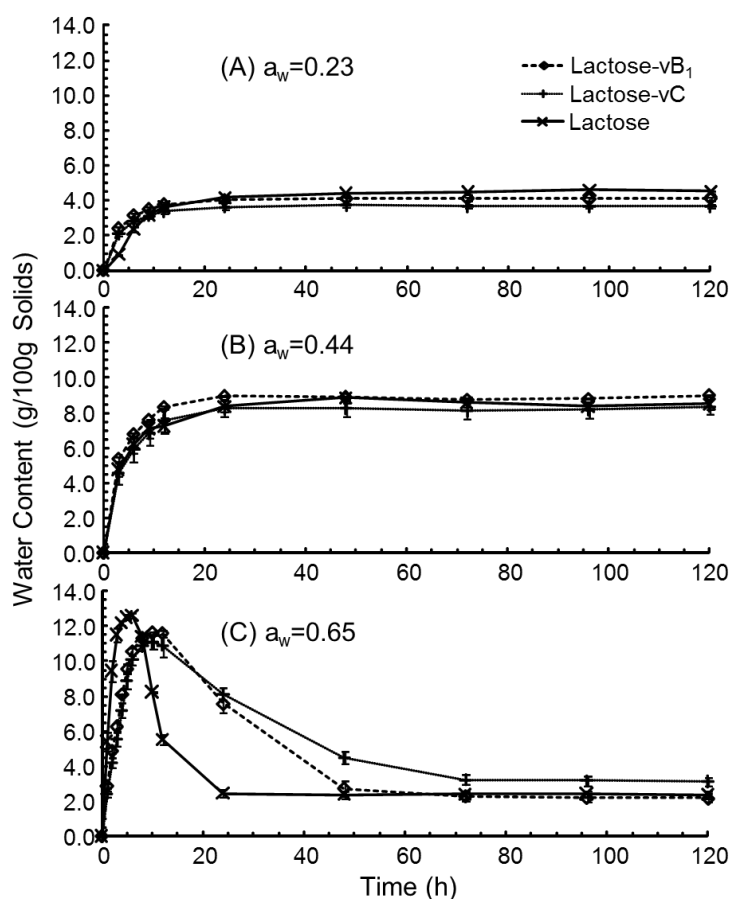


Figure 3.2 Water sorption of freeze-dried lactose (Chapter 2), lactose-vB₁, and lactose-vC systems at (A) 0.23, (B) 0.44, and (C) 0.65 a_w at room temperature (24 ± 1 °C). Loss of water at 0.65 a_w indicates lactose crystallization. Vertical bars represent plus and minus (\pm) 1 standard deviation (SD) of data for triplicate samples.

3.3.2 Water sorption and sorption isotherms

Water sorption of freeze-dried lactose-vB₁, lactose-vC, trehalose-vB₁, and trehalose-vC systems over various water activities as a function of time was plotted, as shown in Figures 3.2 and 3.3, respectively. The final water contents are given in Table 3.2.

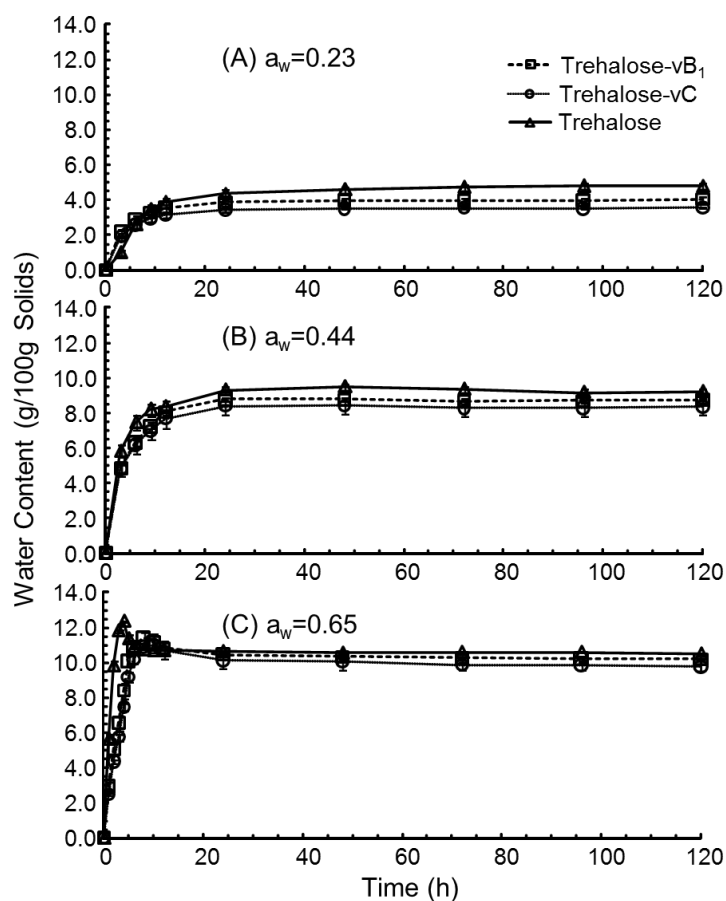


Figure 3.3 Water sorption of freeze-dried trehalose (Chapter 2), trehalose-vB₁, and trehalose-vC systems at (A) 0.23, (B) 0.44, and (C) 0.65 a_w at room temperature (24 ± 1 °C). Loss of water at 0.65 a_w indicates trehalose crystallization. Vertical bars represent plus and minus (\pm) 1 standard deviation (SD) of data for triplicate samples.

At a_w of 0.11 to 0.44, all systems showed rapid water sorption initially and reached constant water contents. At low a_w , lactose-vB₁ and lactose-vC, and trehalose-vB₁ and trehalose-vC showed more rapid water sorption but reached lower final water contents than pure lactose and trehalose, respectively (Figures 3.2A and 3.3A). The final water contents were found to be higher in lactose-vB₁ and trehalose-vB₁ systems than in lactose-vC and trehalose-vC systems, respectively (Table 3.2).

Table 3.2 Water content (mean values \pm SD) in freeze-dried lactose, trehalose, lactose- vB₁, lactose-vC, trehalose- vB₁, and trehalose-vC systems after equilibration at various water activities (a_w) for 120 h at room temperature (24 \pm 1 °C).

Systems	Water content (g/100g of Solids)							
	0.00 a _w	0.11 a _w	0.23 a _w	0.33 a _w	0.44 a _w	0.54 a _w	0.65 a _w	0.76 a _w
Lactose ^a	0 \pm 0.0	2.5 \pm 0.1	4.5 \pm 0.1	5.4 \pm 0.2	8.4 \pm 0.3	3.4 \pm 0.1	2.4 \pm 0.2	2.0 \pm 0.3
Trehalose ^a	0 \pm 0.0	2.8 \pm 0.1	4.8 \pm 0.2	6.0 \pm 0.1	9.2 \pm 0.2	9.6 \pm 0.7	10.5 \pm 0.0	10.4 \pm 0.2
Lactose- vB ₁	0 \pm 0.0	2.3 \pm 0.1	4.1 \pm 0.1	5.5 \pm 0.3	9.0 \pm 0.1	2.5 \pm 0.3	2.2 \pm 0.3	2.9 \pm 0.1
Lactose-vC	0 \pm 0.0	2.0 \pm 0.1	3.7 \pm 0.1	5.0 \pm 0.3	8.4 \pm 0.4	3.5 \pm 0.2	3.1 \pm 0.3	3.3 \pm 0.6
Trehalose- vB ₁	0 \pm 0.0	2.3 \pm 0.0	4.0 \pm 0.2	5.7 \pm 0.1	8.7 \pm 0.1	10.0 \pm 0.2	10.2 \pm 0.2	9.8 \pm 0.1
Trehalose- vC	0 \pm 0.0	2.0 \pm 0.1	3.6 \pm 0.1	5.4 \pm 0.1	8.4 \pm 0.5	9.7 \pm 0.1	9.8 \pm 0.3	9.9 \pm 0.2

^aData from Chapter 2

At 0.44 a_w , a minor loss of sorbed water was observed for pure lactose and trehalose systems after 72 h of storage; however, loss of water was not found for vB₁-containing and vC-containing systems. Loss of water was pronounced at 0.54 a_w and above; all systems showed time-dependent loss of sorbed water, indicating component sugar crystallization during storage. Sugar crystallization was delayed by the component vitamins. At 0.65 a_w , different rates of water sorption and crystallization were found for lactose and trehalose in the presence of component vitamins. Lactose-vB₁ and trehalose-vB₁ showed slightly more rapid and higher water sorption than lactose-vC and trehalose-vC systems, respectively; however, the water sorption of the above systems was less rapid compared to the corresponding pure sugar systems. A delayed lactose crystallization was observed during storage for lactose-vB₁ and lactose-vC systems (after 12 h) than for lactose system (after 6 h), which is shown in Figure 3.2C. The desorption of water from the systems indicated the rate of lactose crystallization. The rate was the most rapid for lactose, followed by lactose-vB₁; and lactose-vC showed the most delayed lactose crystallization. Similar effects of crystallization delay by the vitamins were found for trehalose-containing systems. Trehalose crystallization was observed after 4 h and 12 h of storage for trehalose and trehalose-vitamin systems, respectively (Figure 3.3C). All systems reached constant but different final water contents after crystallization (Table 3.2). However, the molar ratio of the sugar:water indicated similar crystalline forms for lactose and trehalose at different a_w in the absence/presence of vitamins, which were a mixture of anhydrate and monohydrate for lactose and dihydrate for trehalose (Table 3.3). Regarding the rate of sugar crystallization, the molar ratio of sugar:vB₁ and sugar:vC were considered. The molar ratio was approximately 40:1 for lactose:vB₁ and trehalose:vB₁ and 20:1 for lactose:vC

and trehalose:vC. That means there were twice as many ascorbic acid molecules in comparison to thiamine hydrochloride molecules per a mole of sugar. This explained the more delayed sugar crystallization in the presence of ascorbic acid than thiamine hydrochloride.

Table 3.3 Molar ratios between components (lactose, L; trehalose, T; water, W; vB₁; vC) in freeze-dried lactose, trehalose, lactose-vB₁, lactose-vC, trehalose-vB₁, and trehalose-vC systems at high water activities (a_w) after crystallization.

Systems	Components	Molar ratio		
		0.54 a _w	0.65 a _w	0.76 a _w
Lactose	L : W	5 : 1	2 : 1	3 : 1
Trehalose	T : W	1 : 2	1 : 2	1 : 2
Lactose-vB ₁	L : W : vB ₁	39 : 20 : 1	39 : 17 : 1	39 : 20 : 1
Lactose-vC	L : W : vC	21 : 14 : 1	21 : 13 : 1	21 : 13 : 1
Trehalose-vB ₁	T : W : vB ₁	39 : 77 : 1	39 : 77 : 1	39 : 75 : 1
Trehalose-vC	T : W : vC	21 : 40 : 1	21 : 40 : 1	21 : 40 : 1

The GAB model was fitted to the water sorption data. Different m_m values were obtained for all systems. Lactose-vB₁ and trehalose-vB₁ systems showed higher m_m values than lactose-vC and trehalose-vC systems, respectively (Table 3.4). The monolayer value is important since above that value there would be water which could be available for chemical reactions (Labuza, 1980).

Table 3.4 GAB (Guggenheim-Anderson-de Boer)^a constants (α, β, γ, K, and C), monolayer values (m_m, g/100g solid), and R² for freeze-dried lactose-vB₁, lactose-vC, trehalose-vB₁, and trehalose-vC systems.

Systems	α	β	γ	K	C	m _m	R ^{2b}
Lactose-vB ₁	-0.3484	0.1943	0.0318	1.45	6.22	3.49	0.8872
Lactose-vC	-0.4081	0.2194	0.0361	1.49	6.07	3.06	0.9051
Trehalose-vB ₁	-0.3176	0.1793	0.0335	1.40	5.81	3.66	0.9788
Trehalose-vC	-0.3615	0.1883	0.0398	1.47	5.23	3.28	0.9898

^a Experimental sorption data at a_w from 0.11 to 0.44 were used to fit equations

^b R² for quadratic regression $a_w/m = \alpha a_w^2 + \beta a_w + \gamma$

3.3.3 Glass transition and crystallization

The glass transition temperatures for anhydrous and water plasticized lactose- vB_1 , lactose- vC , trehalose- vB_1 , and trehalose- vC systems are given in Table 3.5.

Table 3.5 Onset and endset temperatures of glass transition (T_g , °C) at various water activities (a_w) for freeze-dried lactose- vB_1 , lactose- vC , trehalose- vB_1 , and trehalose- vC systems.

Systems		Glass transition temperature (T_g °C)				
		0.00 a_w	0.11 a_w	0.23 a_w	0.33 a_w	0.44 a_w
Lactose- vB_1	T_g (onset)	99 ± 1	50 ± 1	39 ± 1	29 ± 1	13 ± 1
	T_g (endset)	117 ± 1	69 ± 1	54 ± 1	44 ± 1	27 ± 1
Lactose- vC	T_g (onset)	101 ± 1	47 ± 1	39 ± 1	29 ± 1	12 ± 1
	T_g (endset)	117 ± 1	62 ± 1	53 ± 1	43 ± 1	26 ± 1
Trehalose- vB_1	T_g (onset)	103 ± 1	51 ± 1	39 ± 1	28 ± 1	13 ± 1
	T_g (endset)	119 ± 1	68 ± 1	53 ± 1	43 ± 1	27 ± 1
Trehalose- vC	T_g (onset)	106 ± 1	49 ± 1	38 ± 1	27 ± 1	13 ± 1
	T_g (endset)	117 ± 1	63 ± 1	53 ± 1	42 ± 1	26 ± 1

Anhydrous lactose and trehalose systems with ascorbic acid and thiamine hydrochloride showed lower T_g (onset) values than those for pure lactose (105 °C) and trehalose (111 °C), respectively (Chapter 2). The anhydrous systems contained about 2.44% of either ascorbic acid or thiamine hydrochloride (molar ratios 1:20 and 1:40, respectively, Table 3.3), at which level, the component vitamins showed plasticizing effects on the component sugars. At increasing a_w , the T_g of all systems decreased (Figure 3.4). The water plasticized systems showed similar T_g to those of the pure sugars. This was probably because the plasticizing effect of water as a small molecular weight plasticizer was substantially stronger (Slade and Levine, 1991) than that of the vitamins. Crystallization of lactose and trehalose in the DSC measurements was found only for the humidified systems (Table 3.6). Pure lactose showed T_{ic} at 174 °C (Chapter 2). The T_{ic} of anhydrous lactose- vB_1 and lactose- vC systems were not found in DSC

thermograms in scans up to 200 °C. It is hypothesized that, though the vitamins did appear to show plasticizing effect on the systems, diffusion of lactose molecules to nucleation and crystal growth sites was restricted due to the interactions between lactose and other molecules. The T_{ic} of lactose-vB₁ and lactose-vC decreased with increasing a_w as a result of water plasticization (Figure 3.4).

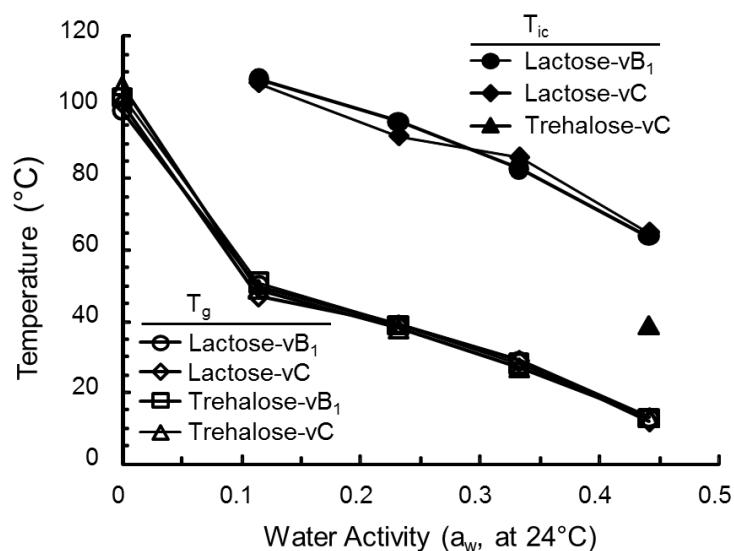


Figure 3.4 Effect of water activity (a_w) on the onset temperature of glass transition (T_g , °C) and instant crystallization (T_{ic} , °C) in freeze-dried lactose-vB₁, lactose-vC, trehalose-vB₁, and trehalose-vC systems.

Table 3.6 Instant crystallization temperature (T_{ic} , °C) of freeze-dried lactose-vB₁, lactose-vC, trehalose-vB₁, and trehalose-vC systems at various water activities (a_w).

Systems	Instant crystallization temperature (T_{ic} , °C)				
	0.00 a_w	0.11 a_w	0.23 a_w	0.33 a_w	0.44 a_w
Lactose-vB ₁	N/O ^a	108 ± 1	96 ± 1	83 ± 1	64 ± 1
Lactose-vC	N/O ^a	107 ± 1	92 ± 1	86 ± 1	65 ± 1
Trehalose-vB ₁	N/O ^a	N/O ^a	N/O ^a	N/O ^a	N/O ^a
Trehalose-vC	N/O ^a	N/O ^a	N/O ^a	N/O ^a	39 ± 1

^a N/O=not observed

Lactose showed crystallization in lactose-vB₁ and lactose-vC systems in the presence of water which was possibly due to (i) the increased molecular mobility in the water-plasticized solids; (ii) the interaction between lactose and vitamins was diminished by the interaction between lactose and water; and (iii) the predominant plasticizing effects of water than that of vitamins at increasing a_w . No instant crystallization was found for trehalose in anhydrous and also in humidified trehalose-vB₁ and trehalose-vC systems with a_w lower than 0.44, possibly due to the insufficient amount of water for trehalose to crystallize as dihydrate during a dynamic measurement.

3.3.4 Critical water content and water activity

The T_g (onset) curves as a function of water content (g/100g solid) were predicted using Equation 3.1 (Gordon and Taylor, 1952). The k constants, critical water contents (g/100g solid) and critical a_w at 24 °C for lactose-vB₁, lactose-vC, trehalose-vB₁, and trehalose-vC were calculated using Equation 3.1 and the GAB water sorption isotherms and are given in Table 3.7. Lactose-vB₁ and trehalose-vB₁ systems showed slightly higher critical water contents than lactose-vC and trehalose-vC systems, respectively, but corresponding critical a_w were observed for all systems. The critical water content as well as the corresponding a_w is important for the stability of low-moisture foods (Slade and Levine, 1991; Chapter 2) when changes are controlled by the glass transition of the solids.

Table 3.7 Critical water content, critical water activity (a_w) at 24 °C, k for Gordon-Taylor equation, and monolayer water activity of freeze-dried lactose-vB₁, lactose-vC, trehalose-vB₁, and trehalose-vC.

Systems	Critical Water Content (g/100g solid)	Critical a_w	k	Monolayer a_w^a
Lactose-vB ₁	5.5	0.32	8.1 ± 2.3	0.20
Lactose-vC	4.8	0.31	9.7 ± 3.3	0.20
Trehalose-vB ₁	5.4	0.32	8.7 ± 2.4	0.21
Trehalose-vC	4.8	0.31	10.3 ± 3.5	0.21

^a a_w corresponding to the monolayer water content as predicted from GAB model.

3.3.5 Stability of vitamins in freeze-dried systems

About 100% of thiamine hydrochloride was retained in both lactose and trehalose systems after freeze-drying. This was in good agreement with the high retention of the compounds in frozen storage below T_m . The retention of thiamine hydrochloride in freeze-dried lactose and trehalose systems during 15 d of storage at various a_w was plotted against time (Figure 3.5). The first-order kinetics was applied to the degradation data. At zero and 0.23 a_w (Figure 3.5A), the rate constants for thiamine hydrochloride loss were very small ($< 0.001 \text{ day}^{-1}$) and the correlation coefficient was less than 0.60. Other kinetic functions were also applied to the degradation data, but none of them revealed a better fit. Therefore, thiamine hydrochloride was considered stable at zero and 0.23 a_w in lactose-vB₁ and trehalose-vB₁ systems during 15 d of storage. At 0.44 and 0.65 a_w (Figure 3.5B), thiamine hydrochloride degraded slowly. Sugar crystallization, as indicated by loss of water, caused simultaneous loss of thiamine hydrochloride (about 30%) in the lactose-vB₁ system; while in trehalose-vB₁ systems, no significant loss of thiamine hydrochloride was observed.

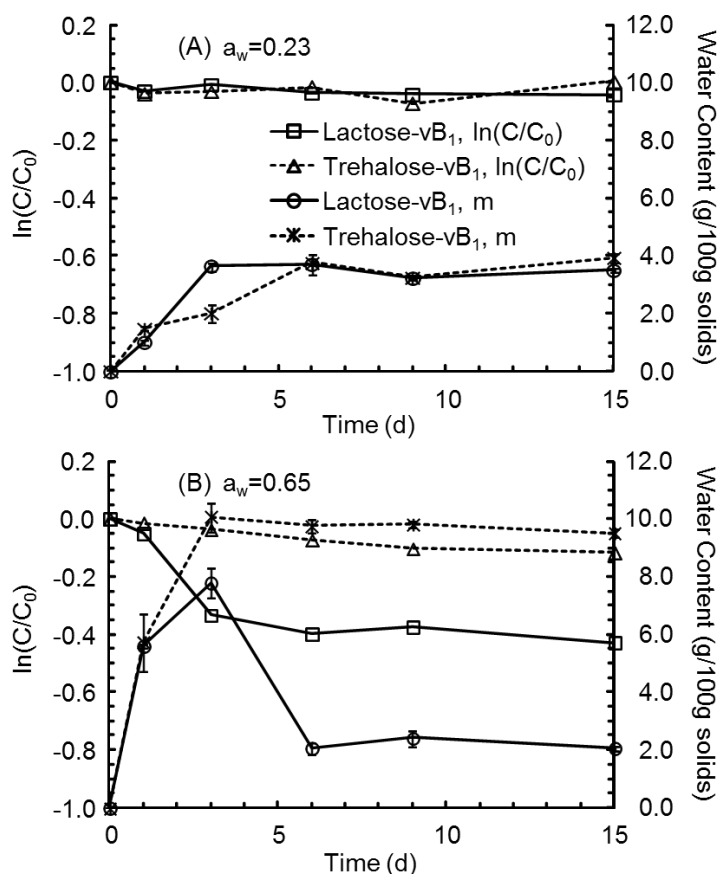


Figure 3.5 The $\ln(C/C_0)$ of thiamine hydrochloride in lactose- vB_1 and trehalose- vB_1 systems as a function of water content (m, g/100g solid) during 15 d of storage at (A) 0.23 and (B) 0.65 a_w .

About 95% and 100% of ascorbic acid were retained in lactose- vC and trehalose- vC systems, respectively, after freeze-drying. The resultant amount of ascorbic acid was considered as 100% retention in the storage study. The retention of ascorbic acid in freeze-dried lactose and trehalose systems at various a_w was plotted against time as shown in Figure 3.6. At zero a_w , degradation of ascorbic acid was very slow and followed first-order kinetics. Rate constants 0.0012 day^{-1} ($R^2=0.9439$) and 0.0007 day^{-1} ($R^2=0.9724$) were determined for lactose- vC and trehalose- vC , respectively. At low a_w , loss of ascorbic acid was observed in lactose- vC system within one day of storage but

the degradation was still very slow (Figure 3.6A). At 0.44 a_w , concomitant loss of ascorbic acid (about 30%) and loss of water from lactose crystallization were observed at day 15 (Figure 3.6B).

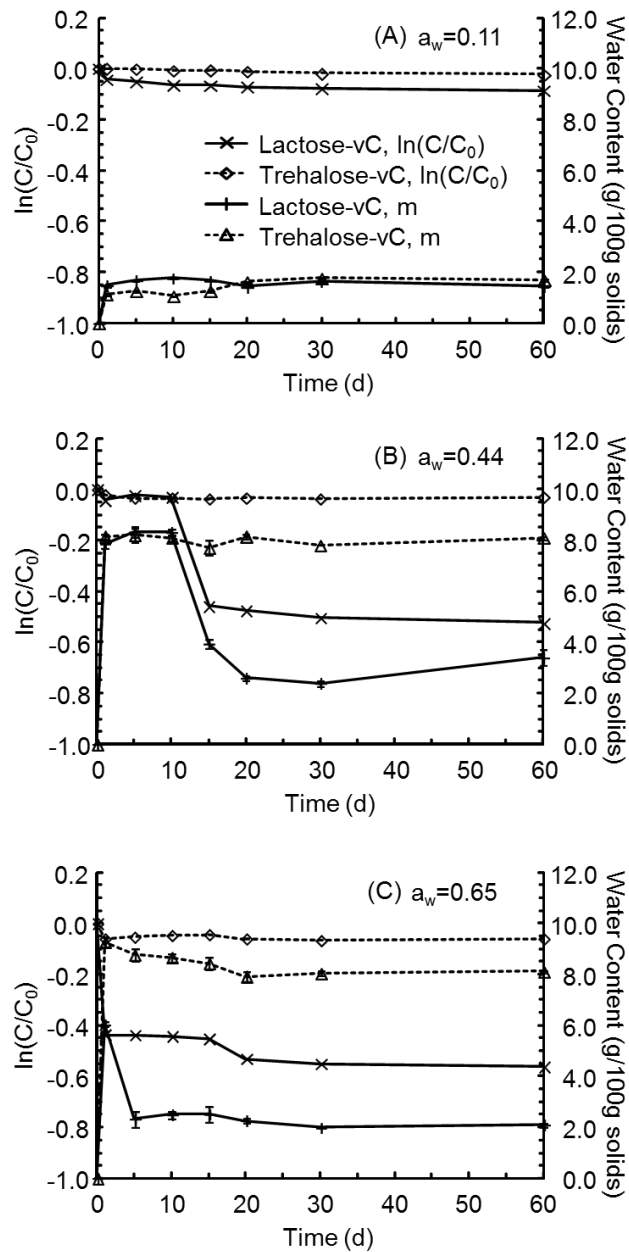


Figure 3.6 The $\ln(C/C_0)$ of ascorbic acid in lactose-vC and trehalose-vC systems as a function of water content (m, g/100g solid) during 60 d of storage at a_w of (A) 0.11, (B) 0.44, and (C) 0.65.

Trehalose crystallization did not cause this sharp loss of ascorbic acid in trehalose-vC system. The effect of lactose crystallization on loss of ascorbic acid was confirmed in lactose-vC system after 1 day of storage at 0.65 a_w (Figure 3.6C).

The degradation k constants were plotted as a function of a_w , as shown in Figure 3.7. Thiamine hydrochloride (Figure 3.7A) and ascorbic acid (Figure 3.7B) showed very low degradation rates in lactose-vB₁, lactose-vC, trehalose-vB₁, and trehalose-vC systems at a_w up to 0.44 ($< 0.004 \text{ day}^{-1}$ and $< 0.006 \text{ day}^{-1}$ for thiamine hydrochloride and ascorbic acid, respectively).

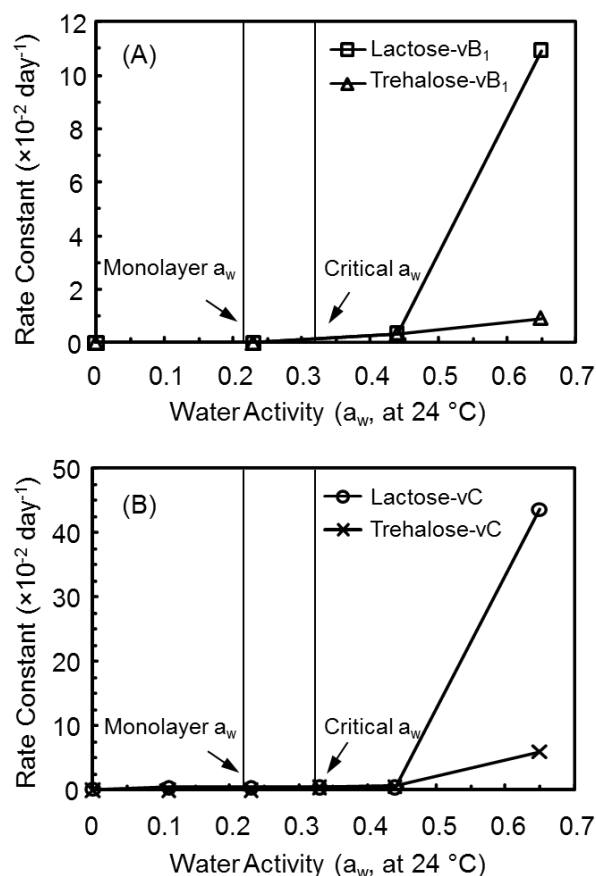


Figure 3.7 First-order rate constant ($\times 10^{-2} \text{ day}^{-1}$) of (A) thiamine hydrochloride and (B) ascorbic acid in freeze-dried lactose-vB₁, lactose-vC, trehalose-vB₁ and trehalose-vC systems as a function of water activity (a_w). The a_w corresponding to monolayer water content and critical a_w at 24 °C are indicated with arrows.

Greatest stability of thiamine hydrochloride and ascorbic acid was observed for anhydrous systems, showing that the degradation of thiamine hydrochloride and ascorbic acid in lactose and trehalose systems was strongly influenced by water (Lee and Labuza, 1975; Dennison and Kirk, 1978; Laing et al., 1978). Thiamine hydrochloride exhibited less sensitivity to water as compared with ascorbic acid. At 0.54 a_w and above, increase of the k constants for thiamine hydrochloride and ascorbic acid in lactose and trehalose was observed. This was corresponding to the phenomenon of lactose and trehalose crystallization. The effect of lactose crystallization was more severe than that of trehalose crystallization on the stability of the vitamins.

3.3.6 Stabilization of vitamins: process and storage stability

Diagrams of the structure formation during freezing and freeze-drying, as well as the structural changes during storage for model systems are shown in Figure 3.8. Sugar-vitamin solutions which were frozen and held at different temperatures had different structures (Levine and Slade, 1988). At -80 °C, a large amount of small ice crystals were formed as a result of fast freezing. The solute sugar was freeze-concentrated due to the crystallization of water, and a continuous amorphous glass was formed. The vitamin molecules were entrapped as dispersed particles in the structure (Figure 3.8A). At -35 °C, which was above T_g' but below T_m' , the ice crystals were expected to be larger than at -80 °C due to the slower freezing rate and less rapid nucleation (Figure 3.8B). At -20 °C and -10 °C, which were above the T_m' , the systems may have a large amount of unfrozen water, slow nucleation and large ice crystals (Figure 3.8C). In the

unfrozen sugar solutions, lactose may crystallize out due to its low solubility (Figure 3.1). Freezing is important for the structure of the freeze-dried systems. Pores were left after sublimation of ice crystals and the size of ice crystals determined the porosity of the freeze-dried matrices. The vitamins were either well entrapped in the thick glassy membranes or partially exposed to the pores (Figure 8D, 8E, 8F).

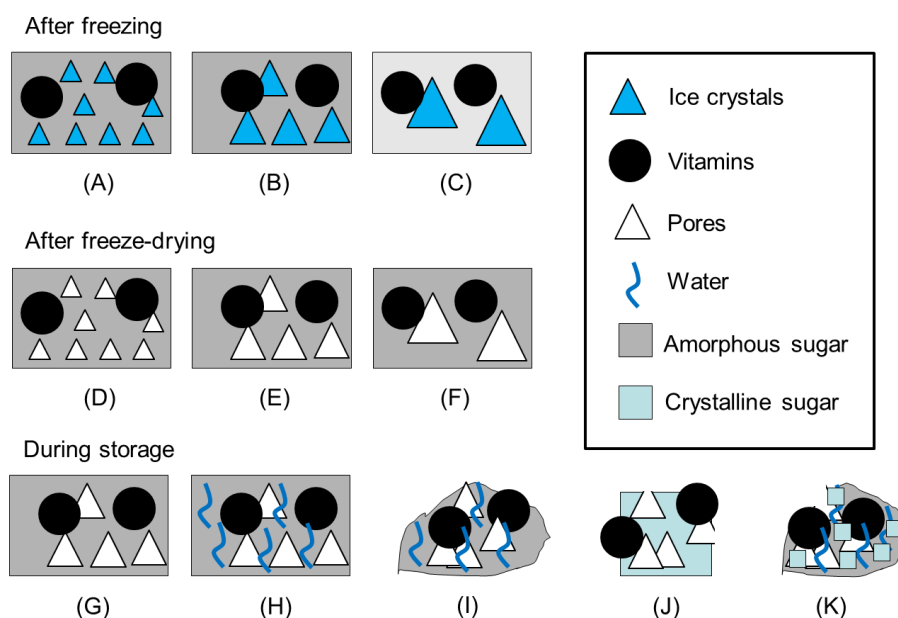


Figure 3.8 Diagrams of the model systems frozen at temperatures below T_g' (A) then freeze-dried (D), frozen between T_m' and T_g' (B) then freeze-dried (E), and frozen above T_m' (C) then freeze-dried (F). During storage, the freeze-dried systems could be anhydrous (G), water-plasticized (H), and collapsed (I). Crystallization of sugars may lead to compact lactose crystals (J) or an amorphous sugar-water phase with dispersed vitamins and trehalose crystals (K). The symbols do not represent the real size of components.

In the present study, the solutions were frozen at $-35\text{ }^\circ\text{C}$ and freeze-dried. The anhydrous glasses were very hygroscopic due to the high surface areas and porosity (Figure 3.8G). Water was sorbed when the materials were exposed to the humidity. Both the sugar and the vitamin sites may be hydrogen-bonded to water molecules till the monolayer water content was reached (Figure 3.8H). The corresponding a_w for

monolayer water content was about 0.2 (Table 3.7). At this a_w , the systems showed T_g around 40 °C, which was higher than room temperature, indicating the systems were in the glassy state during storage. No significant change of k constants was observed at 0.23 a_w . The stability of vitamins was possibly retained due to the low molecular mobility in the viscous solids (Roos, 1995), though above that monolayer value, water became increasingly available for chemical reactions (Labuza, 1980). Therefore, thiamine hydrochloride and ascorbic acid were generally considered stable in glassy lactose and trehalose matrices. However, further water plasticization caused the depression of the glass transition temperature to the room temperature (storage temperature in the present study, 24 ± 1 °C) and the materials could undergo glass transition. The molecular mobility may be increased significantly above the T_g (Slade and Levine, 1991; Roos, 1995). A slight increase of k constants was found in lactose-vB₁, lactose-vC, trehalose-vB₁, and trehalose-vC systems at 0.33 and 0.44 a_w , which were higher than the critical a_w (Table 3.5). Therefore, the critical a_w had a larger correlation to the degradation of thiamine hydrochloride and ascorbic acid compared with the a_w corresponding to the monolayer water content, and the glass transition properties should be considered in the stabilization of water soluble active components (Slade and Levine, 1991), in agreement with Chen et al. (1999) for tyrosinase and with Bell and White (2000) for thiamine.

The effects of glass transition on the stability of the entrapped sensitive compounds were pronounced when time-dependent physical changes occurred above the T_g . The materials may no longer retain the structure and collapse may happen during storage due to the softening (Figure 3.8I). When surface saturation of water sorption was

reached, as well as the increased molecular mobility, the sugar molecules gained translational mobility and approached other sugar molecules and formed sugar crystals. The presence of vitamin molecules disturbed the sugar-sugar interactions and delayed the lactose and trehalose crystallization. Water sorption-induced sugar crystallization occurred in all the systems, as shown in Figures 3.5B, 3.6B, and 3.6C. Sharp increase of rate constants was found for lactose-vB₁ (Figure 3.7A) and lactose-vC (Figure 3.7B) systems, while much smaller changes of rate constants were found for trehalose-vB₁ (Figure 3.7A) and trehalose-vC (Figure 3.7B) systems. The vitamins may be excluded from the continuous phase and exposed to the environment (Figure 3.8J), which could be the main cause of the loss of vitamins. However, trehalose-containing systems still retained most of the vitamins after crystallization. This could possibly result from their protection by the viscous trehalose syrup (Figure 3.8K), since trehalose crystals showed higher solubility and the extent of trehalose crystallization was less than that of lactose (Figure 3.1).

In addition to the physical changes above the T_g, other factors dependent on the T_g may also affect the stability of vitamins. For example, the rate of non-enzymatic browning was extremely low below the T_g and increased sharply above the T_g due to the increased diffusion (Roos and Himberg, 1994; Miao and Roos, 2005b). Browning was visually observed in lactose-vB₁ and lactose-vC systems at 0.65 a_w during storage, but not in trehalose- vB₁ and trehalose-vC systems, suggesting that reactions between thiamine hydrochloride or ascorbic acid and reducing sugar occurred (Hodge, 1953; Brownley and Lachman, 1964; Doyib and Smyrl, 1983). This could be responsible for the higher loss of vitamins in lactose-containing systems.

3.4 CONCLUSIONS

Storage stability of thiamine hydrochloride below the melting temperature of the maximally-freeze-concentrated lactose-vB₁ and trehalose-vB₁ systems (T_m') was retained, possibly due to the low rate of chemical reactions at low temperatures and the low diffusion rates in the viscous, freeze-concentrated solutes. The stability of thiamine hydrochloride in the systems stored above T_m' may be enhanced by the low pH. Thiamine hydrochloride and ascorbic acid showed good stability in freeze-dried lactose-vB₁, lactose-vC, trehalose-vB₁, and trehalose-vC systems at 0.44 a_w and below, especially at zero a_w . The critical a_w had a larger effect on the degradation of thiamine hydrochloride and ascorbic acid compared with the a_w corresponding to the monolayer water content. The critical a_w related the glass transition temperature, T_g , to the a_w of the systems; it interpreted the T_g of a water-plasticized solid at room temperature (24 °C) in terms of the extent of water plasticization (at which a_w the systems were equilibrated). Above the critical a_w (i.e., the room temperature was higher than the T_g), the molecular mobility in the solids was increased; time-dependent changes, particularly component sugar crystallization, caused the loss of the water-soluble vitamins. Therefore, the T_g should be considered in the stability assessment of vitamins. Vitamins appeared to show plasticizing effects on the sugars, especially in the anhydrous state, and appeared to delay sugar crystallization, which was more dependent on the molar ratio of sugar:vitamin than their weight ratios. Depending on the crystallization properties of the sugars, different protecting effects of the sugars on the stability of water-soluble vitamins would be expected. Trehalose, because of its higher solubility, showed better stabilizing properties on the water-soluble vitamins than lactose, even when trehalose crystallization occurred.

CHAPTER 4

Stability of α -tocopherol in freeze-dried sugar-protein-oil emulsion solids as affected by water plasticization and sugar crystallization

Published in Journal of Agricultural and Food Chemistry, Zhou and Roos, 2012, 60(30):7497-7505

ABSTRACT

Water plasticization of sugar-protein encapsulants may cause structural changes and decrease the stability of encapsulated compounds during storage. The retention of α -tocopherol in freeze-dried lactose-milk protein-oil, lactose-soy protein-oil, trehalose-milk protein-oil, and trehalose-soy protein-oil systems at various water activities (a_w) and in the presence of sugar crystallization was studied. Water sorption was determined gravimetrically. Glass transition and sugar crystallization were studied using differential scanning calorimetry and the retention of α -tocopherol spectrophotometrically. The loss of α -tocopherol followed lipid oxidation but the greatest stability was found at zero a_w presumably because of α -tocopherol immobilization at interfaces and consequent reduction in antioxidant activity. Considerable loss of α -tocopherol coincided with sugar crystallization. The results showed that glassy matrices may protect encapsulated α -tocopherol; however, its role as antioxidant at increasing a_w accelerated its loss. Sugar

crystallization excluded the oil containing α -tocopherol from the protecting matrices and exposed it to surroundings, which decreased the stability of α -tocopherol.

Keywords: encapsulation, α -tocopherol, carbohydrate-protein, water activity, crystallization

4.1 INTRODUCTION

Vitamin E contributes to many biological functions, including enzymatic activities, gene expression activity, neurological function, and antioxidant activity (Zingg and Azzi, 2004). α -Tocopherol is the main vitamin E compound with antioxidant activity that inhibits the formation and decomposition of hydroperoxides (Lea and Ward, 1959), although it may become pro-oxidative at elevated concentrations (Riejtens et al., 2002; Valenzuela et al., 2002). Losses of α -tocopherol in food systems could result from (i) degradation, which was affected by exposures to oxygen, light, and high temperatures (Kanner et al., 1979; Widicus et al., 1980) as well as from (ii) its consumption as an antioxidant reactant in the presence of lipids, i.e., accelerated degradation during lipid oxidation (Labuza, 1980; Widicus and Kirk, 1981; Kamal-Eldin et al., 2002). Freeze-drying entraps and encapsulates sensitive compounds into a dry wall material, which may also enhance stability of bioactive components (Roos, 1995; Slade and Levine, 1991). Encapsulation of the hydrophobic α -tocopherol requires (i) breakdown of the lipid phase into small droplets by emulsification and dispersion of these droplets into the continuous aqueous phase; (ii) freezing to immobilize and encapsulate the lipid

droplets in freeze-concentrated solutes; and (iii) stabilization of the system by sublimation of the ice (Roos, 1995; Kaushik and Roos, 2008). Sugars are effective encapsulating agents since they form amorphous glassy solids that restrict the movement of entrapped and encapsulated compounds (Roos, 1995; Slade and Levine, 1991; Flink, 1972; Roos and Karel, 1991e; Goubet et al., 1998; Grattard et al., 2002; Farias et al., 2007). The glass formation occurs in freezing and the stability of freeze-dried solid structures is accounted for their glassy state. Plasticization resulting in glass transition of freeze-dried materials affects numerous changes in storage of dried solids, e.g., crystallization of sugars (Roos, 1995; Slade and Levine, 1991; Roudaut et al., 2004). Dehydrated sugar-protein mixtures showed delayed crystallization of component sugars (Chapter 2), and showed reduced changes in solid structures. This suggested carbohydrate-protein systems as potential encapsulants. Proteins may also act as emulsifiers (McClements et al., 2007), and the emulsification properties of proteins are important in stabilization of hydrophobic nutrient delivery systems.

Widicus et al. (1980) reported first order kinetics of degradation of α -tocopherol in freeze-dried model systems containing no fat. The degradation rate of α -tocopherol increased with increasing water activity (a_w) and it was diffusion-dependent. Widicus and Kirk (1981) found that in freeze-dried model systems containing fat, α -tocopherol degraded more rapidly than in systems containing no fat and followed the progression of lipid oxidation. In fat-containing systems, water affected the stability of α -tocopherol through protecting lipids against oxidation by (i) hydrogen bonding to the hydroperoxides; and (ii) hydration of metal catalysts which made them less effective as a result of changes in their coordination sphere (Labuza et al., 1972) up to 0.5 a_w . At

higher a_w , the rate of lipid oxidation increased with increasing a_w , due to the mobilization of catalytes and exposure of lipids to increased number of catalytes (especially in swelling systems). However, the effects of physical changes, e.g., glass transition and crystallization of matrices, as a result of water sorption on the stability of α -tocopherol have not been studied intensively. Especially at zero a_w , when lipid oxidation is rapid, the consumption of antioxidants may be assumed to be the most rapid. However, due to the polar paradox that hydrophobic antioxidants, e.g., α -tocopherol, are more active in emulsions than in oils (Porter et al., 1989; Frankel et al., 1994), we would expect α -tocopherol to show less antioxidant activity in anhydrous systems, i.e. systems containing no water (similar as bulk oil systems).

The objectives of the present study were to encapsulate and stabilize emulsified oil droplets containing α -tocopherol in amorphous carbohydrate-protein matrices by freezing and freeze-drying. The physicochemical properties (water sorption, glass transition, and crystallization) of the matrices, and the stability of α -tocopherol in these matrices, as affected by water activity and physical changes, were determined.

4.2 MATERIALS AND METHODS

4.2.1 Materials

α -Lactose monohydrate (Sigma-Aldrich, St. Louis, Mo., U.S.A.), trehalose dihydrate (Cargill Inc., Minneapolis, MN, U.S.A.), milk protein isolate (MPI, Kerry Ingredients, Listowel, Co. Kerry, Ireland), and soy protein isolate (SPI, PRO-FAM891, Archer

Daniels Midland, Decatur, IL, U.S.A.) were used as encapsulating matrices. Olive oil (OO, Extra Virgin Olive Oil, Don Carlos, Hacienda Don Carlos, purchased from the local market) was used as a lipid carrier for the hydrophobic α -tocopherol (Sigma-Aldrich, St. Louis, MO, U.S.A.). Reagents used for extraction of α -tocopherol, including ascorbic acid, potassium hydroxide (KOH), methanol, butylated hydroxytoluene (BHT), n-hexane and anhydrous sodium sulfate (Na_2SO_4), were all purchased from Sigma-Aldrich (Sigma-Aldrich, St. Louis, MO, U.S.A.). Ethanol (ETHANOL 100), which was also used for extraction of α -tocopherol was purchased from Carbon Group (Carbon Group, Ringaskiddy, Co. Cork, Ireland).

4.2.2 Preparation of emulsions and the freeze-dried materials

Lactose-MPI (3:1), lactose-SPI (3:1), trehalose-MPI (3:1), and trehalose-SPI (3:1) suspensions were prepared (250g, 20% w/w of solids) using distilled water. All materials were allowed to hydrate at 45 °C for at least 3 h, with an assumption of sufficient hydration of materials. The suspensions were reweighed, and the amount of water equivalent to the amount of evaporated water was added. The suspensions were left to cool to room temperature (24 ± 1 °C). α -Tocopherol (5%, w/w) was mixed with olive oil, which naturally contains a smaller amount of α -tocopherol than other oils (Contreras-Guzmán and Strong III, 1982), under stirring at room temperature. The olive oil with α -tocopherol (25g) was mixed into the carbohydrate-protein suspensions (250g), pre-homogenized using Ultra-Turrax (T25 Digital, Staufen, Germany) at 10,000 rpm for 30 s, and immediately homogenized at room temperature (APV-1000 High-

Pressure homogenizer, Wilmington, MA, U.S.A.) at 24 MPa (two stages, 20 and 4 MPa) for three cycles.

Freshly prepared emulsions (275g, 9.1% oil phase, w/w) were transferred using an adjustable-volume pipette (Pipetman P5000, Gilson Inc., Middleton, WI, U.S.A.) into glass vials (clear glass ND18, 10 ml, VWR, U.K.) (5 ml per vial), frozen at $-35\text{ }^{\circ}\text{C}$ ($T_g' < T < T_m'$, Chapter 2) for 24 h, and subsequently transferred to a $-80\text{ }^{\circ}\text{C}$ freezer for 5 h to avoid ice melting during transfer to a freeze-dryer (Lyovac GT2, STERIS, Hürth, Germany). Samples in glass vials with semi-closed rubber septa were freeze-dried for ≥ 72 h at < 0.1 mbar ($T < -40\text{ }^{\circ}\text{C}$). All vials at completion of freeze-drying were hermetically closed inside the freeze-dryer using the rubber septa prior to breaking the vacuum with ambient air. The freeze-dried lactose-MPI-OO (3:1:2), lactose-SPI-OO (3:1:2), trehalose-MPI-OO (3:1:2), and trehalose-SPI-OO (3:1:2) systems were theoretically composed of two parts of non-fat solids and one part of lipid and the α -tocopherol accounted for 1.67% (w/w) of the total solids.

4.2.3 Characterization of the non-fat solids

4.2.3.1 *Water sorption and sorption isotherms*

Triplicate samples of each freeze-dried emulsion in open vials were equilibrated up to 5 d at room temperature (in general, $24 \pm 1\text{ }^{\circ}\text{C}$) in evacuated desiccators over various saturated salt solutions, LiCl, CH_3COOK , MgCl_2 , K_2CO_3 , giving respective water activities (a_w) of 0.11, 0.23, 0.33, and 0.44 at equilibrium (Labuza et al, 1985). The samples were weighed at 0, 3, 6, 9, 12, 24, 48, 72, 96, and 120 h. Gradual decrease of

sorbed water indicated time-dependent lactose or trehalose crystallization. This was monitored during storage over saturated solutions of $\text{Mg}(\text{NO}_3)_2$, NaNO_2 , and NaCl , giving respective a_w of 0.54, 0.65, and 0.76 at equilibrium (Labuza et al., 1985). The vials with samples were weighed every hour up to 6 h, at 8, 10, 12, 24, 48, 72, 96, and 120 h. The a_w of the saturated salt solutions was confirmed using an Aqua Lab 4TE instrument (Decagon Devices, Inc. Pullman, WA, U.S.A.). Water content of each material was measured gravimetrically as a function of time and the mean weight of triplicate samples was calculated (Berlin et al., 1968).

The GAB (Guggenheim-Anderson-de Boer) equation was used to model water sorption (Roos, 1993). The GAB isotherm parameters, m_m (monolayer value) and K , were obtained by plotting a_w against a_w/m and from a second order polynomial regression over the a_w range from 0.11 to 0.44.

4.2.3.2 *Glass transition and crystallization*

The onset, T_g (onset), and endset, T_g (endset), temperatures of glass transition and the instant crystallization temperature, T_{ic} , were measured using differential scanning calorimetry (DSC, Mettler Toledo 821e with liquid N_2 cooling, Switzerland). The thermograms were analyzed using STAR thermal analysis software, version 6.0 (Mettler Toledo, Switzerland), as reported by Roos and Karel (1990). The freeze-dried materials were powdered using a spatula in glass vials. To determine the T_g (onset) and T_{ic} , 10-15 mg of the powdered freeze-dried materials were prepared in open DSC pans and equilibrated over P_2O_5 and saturated salt solutions to a_w of 0-0.44 at room temperature. After equilibration, the pans were hermitically sealed and the samples

were analyzed (Table 4.2) according to Chapter 2. Triplicate samples were analyzed for each material.

4.2.4 Oil droplet size distribution

The droplet size distribution of emulsions was analyzed by laser diffraction (Malvern Mastersizer S, Malvern Instruments Ltd. Malvern, U.K.) according to O'Regan and Mulvihill (2010). Fresh emulsions were analyzed within 1 h after preparation. Frozen emulsions after 24 h storage at -35 °C were thawed (room temperature, 1 h) and analyzed. Freeze-dried materials were reconstituted to the original weight, gently mixed, and analyzed. The droplet size (μm) was reported as the volume-weight mean diameter, $D[4,3]$, and the volume median diameter, $D[v, 0.5]$.

4.2.5 Spectrophotometry of α -tocopherol

The α -tocopherol content was measured spectrophotometrically. The freeze-dried materials before and after storage were reconstituted to the original weight and vortexed for 30 s at high speed for mixing. Aliquots of 1 ml of the reconstituted emulsions were transferred into test tubes (20 ml) and destabilized by ethanol (3 ml). Ascorbic acid solution (5%, w/v, freshly made, 2 ml) was added to the mixes to prevent oxidation in the liquids. Separation of α -tocopherol (unsaponified fraction) from the oil (saponified fraction) was achieved by adding saturated KOH-methanol (1 ml) into the mixes and vortexing for 15 s, followed by holding at 45 °C in a waterbath for 30 min. After

cooling to room temperature, α -tocopherol was extracted three times with n-hexane (with 0.1% BHT, w/v, 2 ml), which was added into the mixes followed by vortexing for 30 s to extract α -tocopherol. The mixes were left to stand for 10 min for the separation of the organic layer containing α -tocopherol on top and the water layer on the bottom. The organic layer was removed carefully using a glass Pasteur pipette (9 inch Pasteur Pipets, Corning Incorporated, Corning, NY, U.S.A.) into a glass vial containing anhydrous Na₂SO₄ powder (about 0.5 g) which absorbed possible residual water (modified from Cornacchia and Roos, 2011c). After 1:10 dilution with n-hexane (with BHT), the extracts were transferred into cuvettes (semi-micro low form U.V. grade, Kartell, Italy), and the absorbance was measured at 297.7 nm using a spectrophotometer (Varian Cary 300, Bio UV-Visible Spectrophotometer, Agilent Technologies, Santa Clara, CA, U.S.A.). This wavelength was found to correspond to the maximum absorbance of α -tocopherol in n-hexane (with BHT) over the spectrum of wavelengths from 200 to 400 nm (Hewavitharana et al., 1996). A standard curve was obtained by measuring absorbance of α -tocopherol in n-hexane (with BHT) at various concentrations (0-125 μ g/ml). The amount of α -tocopherol in the olive oil was measured to adjust the actual amount of added α -tocopherol, but this was, however, undetectable.

4.2.6 Storage of freeze-dried materials and stability of α -tocopherol

To study the stability of α -tocopherol in different encapsulants, the freeze-dried materials in closed vials were stored in an incubator at 60 °C for 40 d. The α -tocopherol

content was measured at intervals during storage. To study the effect of water activity and structural changes on the stability of α -tocopherol, the freeze-dried materials in open vials were equilibrated for 5 d at room temperature (24 ± 1 °C) in evacuated desiccators over P_2O_5 and various saturated salt solutions (LiCl, CH_3COOK , $MgCl_2$, K_2CO_3 , $Mg(NO_3)_2$, $NaNO_2$, and NaCl), giving respective a_w of 0, 0.11, 0.23, 0.33, 0.44, 0.54, 0.65, and 0.76 at equilibrium, according to the water sorption results. The sample vials were closed manually with septa, sealed with parafilm, and then transferred into the incubator at 60 °C for 10 d. Due to the high porosity of the freeze-dried materials, the total volume of the glass vials (10 ml) was considered as the headspace volume during storage. The α -tocopherol content was measured after (i) equilibration and (ii) incubation, and the ratio [content after incubation/content after equilibration] * 100 calculated as % retention.

4.2.7 Statistics

All measurements carried out in this study were done in triplicate. The mean values of triplicate samples plus/minus one standard deviation (SD) are reported as results for water sorption, glass transition and crystallization, and the stability study.

4.3 RESULTS AND DISCUSSION

4.3.1 Water sorption and sorption isotherms

Water sorption of freeze-dried lactose-MPI-OO, lactose-SPI-OO, trehalose-MPI-OO, and trehalose-SPI-OO systems over various a_w conditions as a function of time was plotted, as shown in Figure 4.1. The final water contents are given in Table 4.1. At low water activities up to 0.44 a_w , sugar-protein systems showed the most rapid water sorption and the highest amounts of sorbed water, followed by sugar-protein-oil systems (Figures 4.1A and 4.1C).

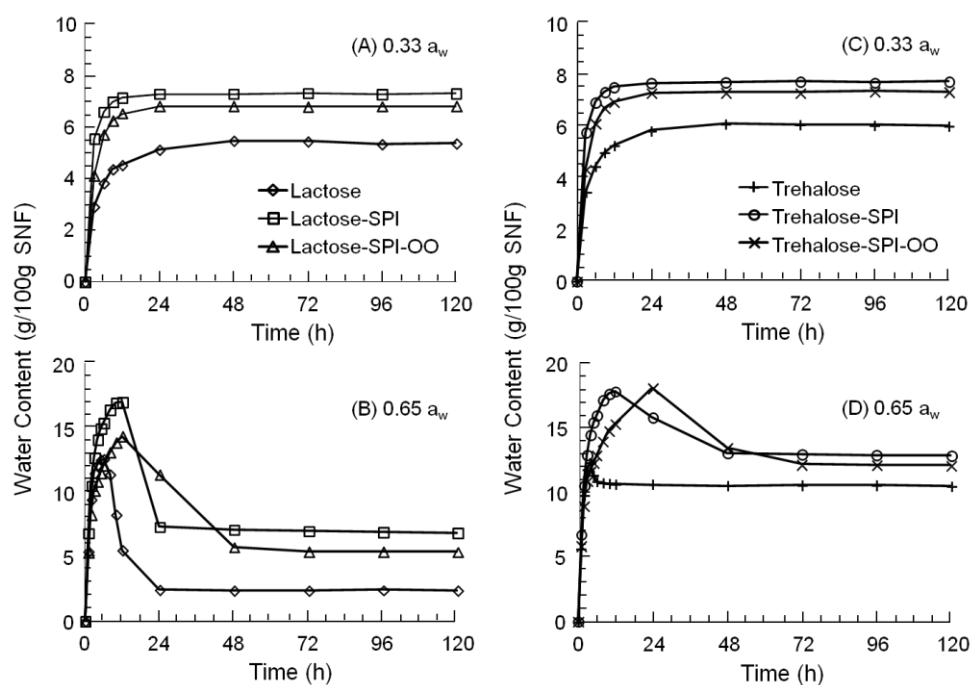


Figure 4.1 Water sorption (g/100g solid-non-fat) of freeze-dried lactose (Chapter 2), trehalose (Chapter 2), lactose-SPI (3:1) (Chapter 2), trehalose-SPI (3:1) (Chapter 2), lactose-SPI-OO (3:1:2), and trehalose-SPI-OO (3:1:2) systems at (A and C) 0.33 a_w and at (B and D) 0.65 a_w at room temperature (24 ± 1 °C). Loss of water at 0.65 a_w indicated sugar crystallization.

Table 4.1 Water content (mean values \pm SD) in freeze-dried carbohydrate-protein-oil (3:1:2) systems after equilibration at various water activities (a_w) for 5 d at room temperature (24 ± 1 °C).

Systems	Water content (g/100g SNF)							
	0.00 a_w	0.11 a_w	0.23 a_w	0.33 a_w	0.44 a_w	0.54 a_w	0.65 a_w	0.76 a_w
Lactose-MPI-OO	0.00 \pm 0.00	3.44 \pm 0.03	5.45 \pm 0.02	7.00 \pm 0.01	9.61 \pm 0.03	12.62 \pm 0.04	5.58 \pm 0.06	8.21 \pm 0.04
Lactose-SPI-OO	0.00 \pm 0.00	3.29 \pm 0.04	5.39 \pm 0.01	6.85 \pm 0.02	9.18 \pm 0.02	11.90 \pm 0.08	5.39 \pm 0.09	7.78 \pm 0.05
Trehalose-MPI-OO	0.00 \pm 0.00	3.66 \pm 0.02	5.82 \pm 0.07	7.48 \pm 0.04	10.28 \pm 0.04	14.27 \pm 0.06	12.61 \pm 0.02	14.23 \pm 0.11
Trehalose-SPI-OO	0.00 \pm 0.00	3.57 \pm 0.03	5.76 \pm 0.02	7.34 \pm 0.07	9.93 \pm 0.01	13.78 \pm 0.03	12.08 \pm 0.03	13.07 \pm 0.02

Less water sorption in sugar-protein-oil systems compared with sugar-protein systems was possibly because of hydrophobic interactions between proteins and oils at the interface. This decreased the quantity of proteins in the sugar-protein rich continuous phase. Sugar crystallization was found at 0.54 a_w and above for lactose and trehalose (Chapter 2). Delayed sugar crystallization occurred in sugar-protein and sugar-protein-oil systems as a result of interference with mobility of lactose and trehalose molecules and possible interactions between sugars and proteins (Figures 4.1B and 4.1D), e.g., by hydrogen bonding between sugars and proteins. A limited amount of hydrogen bonding between sugars and proteins, above which, sugars and proteins exist as free components without interaction has been reported, although the components were not necessarily completely immiscible, i.e. phase-separated but forming a homogeneous bulk (Imamura et al., 2001). Our earlier studies showed that at 3:1 ratio sugars and proteins existed as phase-separated, largely immiscible glass formers (Silalai and Roos, 2010; Chapter 2) which excluded major molecular interaction effects on sugar crystallization. At 0.65 a_w , lactose crystallization was found after 6 h, 12 h and 12 h for lactose, lactose-SPI, and lactose-SPI-OO systems, respectively. It appeared that lactose crystallization responsible for changes in sorbed water contents in lactose-SPI-OO system (Figure 4.1B) proceeded more slowly at a lower water content than in lactose-SPI system. Trehalose crystallization was found after 4 h, 12 h, and 24 h in trehalose, trehalose-protein, and trehalose-protein-oil systems, respectively (Figure 4.1D). Trehalose crystallization was less rapid in the sugar-protein-oil systems than in the sugar-protein systems. We assume that the dispersed oil phases with protein interfaces disturbed the continuous hydrophilic sugar-protein phase and hindered the movement of sugar molecules to form crystals. The molecular assemblies of the components occur in

emulsification prior to freezing (protein-oil) and as a result of freeze-concentration (protein-sugar). The protein molecules are likely to become covered by sugar molecules during freezing and this structure can be retained to the freeze-dried systems. Diffusion of the sugar molecules at the molecular surfaces of proteins and the hydrophobic environment of oil droplets can reduce their nucleation and crystal growth rates.

The GAB model was fitted to the water sorption data. Sugar-protein systems at the low experimental a_w range showed the sigmoid sorption isotherms and highest water sorption, followed closely by sugar-protein-oil systems and then by pure sugar systems (Figure 4.2).

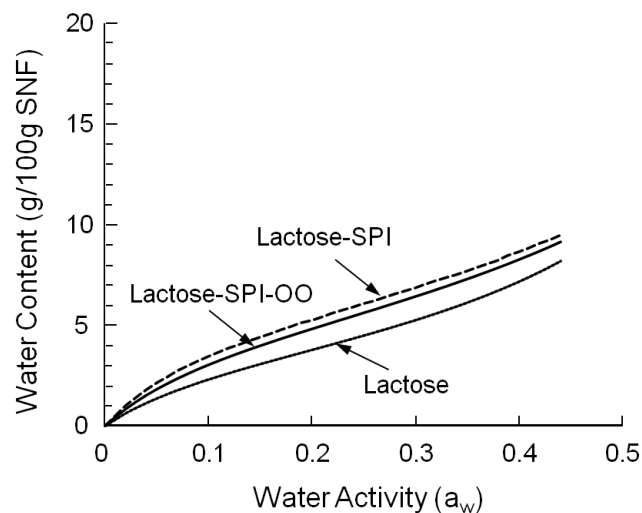


Figure 4.2 Water sorption isotherms of freeze-dried lactose (Chapter 2), lactose-SPI (3:1) (Chapter 2), and lactose-SPI-OO (3:1:2) systems. The isotherms were modeled using the GAB relationship with experimental data.

The lower amount of sorbed water in the nonfat solids of systems containing oil at each a_w conditions could be due to the hydrophobic interactions between protein and oil, which decreased the amount of protein in the sugar-protein phases and their hydrogen

bonding with water. The monolayer water contents (m_m , g/100g solid-non-fat) were slightly different, which were 4.96, 5.51, 5.30, and 5.57 g/100g of solid-non-fat for lactose MPI-OO, lactose-SPI-OO, trehalose-MPI-OO, and trehalose-SPI-OO systems, respectively, but similar corresponding a_w values (0.21-0.23) were obtained for all systems.

4.3.2 Glass transition and instant sugar crystallization

The glass transition and sugar crystallization for anhydrous and humidified lactose-MPI-OO, lactose-SPI-OO, trehalose-MPI-OO, and trehalose-SPI-OO systems were measured and the glass transition temperatures and instant sugar crystallization temperatures were read from the DSC thermographs.

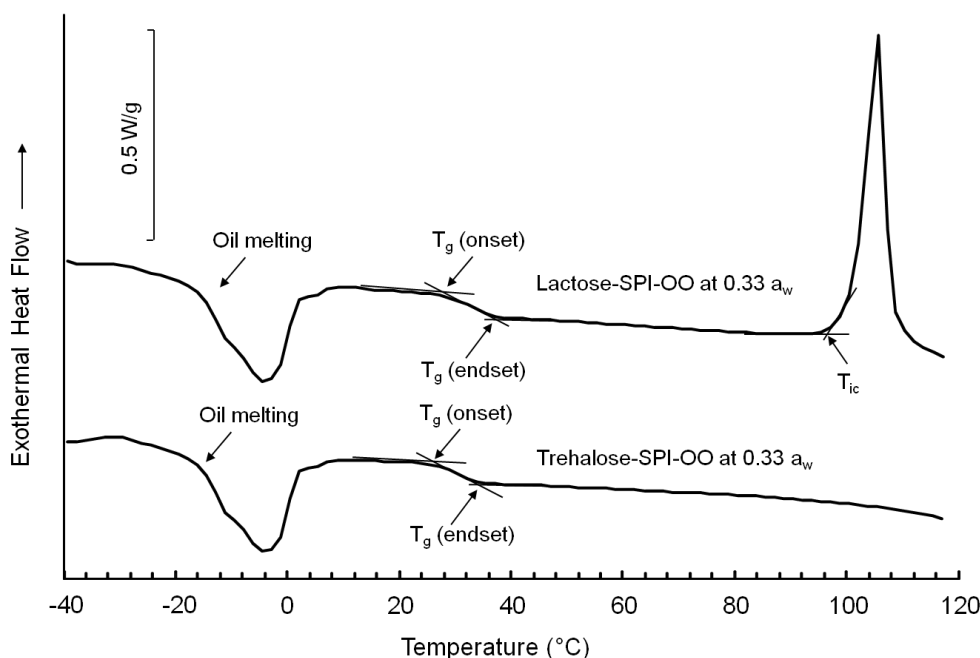


Figure 4.3 The DSC thermographs of lactose-SPI-OO and trehalose-SPI-OO at 0.33 a_w , showing oil melting, glass transition, and sugar crystallization. The thermographs were taken from the 2nd heating scans (heating rate at 5 °C/min).

The 2nd heating scans of DSC thermographs for lactose-SPI-OO and trehalose-SPI-OO systems at 0.33 a_w are given in Figure 4.3 as examples, in which oil melting occurred and was followed by a step endothermal change for glass transition; an exothermal peak, representing sugar crystallization, was observed only for lactose-containing systems at a_w above zero. The T_g of all systems, as shown in Table 4.2, was depressed as a result of water-plasticization (Roos and Karel, 1990; Slade and Levine, 1991).

Table 4.2 Onset and endset temperatures of glass transition (T_g , °C) at various water activities (a_w) for freeze-dried lactose-MPI-OO (3:1:2), lactose-SPI-OO (3:1:2), trehalose-MPI-OO (3:1:2), and trehalose-SPI-OO (3:1:2) systems.

Systems		T_g^a , °C				
		0.00 a_w^b	0.11 a_w^c	0.23 a_w^d	0.33 a_w^e	0.44 a_w^f
Lactose-MPI-OO	onset	101	52	35	27	15
	endset	111	60	44	34	24
Lactose-SPI-OO	onset	106	50	37	29	16
	endset	118	59	45	37	25
Trehalose-MPI-OO	onset	111	53	33	25	14
	endset	119	60	42	33	21
Trehalose-SPI-OO	onset	116	49	38	28	15
	endset	124	58	47	35	23

^a $T_g \pm 1^\circ\text{C}$

^b DSC method: (i) 25 °C to 150 °C at 5 °C/min, (ii) 150 °C to -50 °C at 10 °C/min, and (iii) -50 °C to 200 °C at 5 °C/min.

^c DSC method: (i) 25 °C to 90 °C at 5 °C/min, (ii) 90 °C to -50 °C at 10 °C/min, and (iii) -50 °C to 150 °C at 5 °C/min.

^d DSC method: (i) 10 °C to 70 °C at 5 °C/min, (ii) 70 °C to -50 °C at 10 °C/min, and (iii) -50 °C to 140 °C at 5 °C/min.

^e DSC method: (i) 0 °C to 60 °C at 5 °C/min, (ii) 60 °C to -50 °C at 10 °C/min, and (iii) -50 °C to 130 °C at 5 °C/min.

^f DSC method: (i) -10 °C to 50 °C at 5 °C/min, (ii) 50 °C to -50 °C at 10 °C/min, and (iii) -50 °C to 120 °C at 5 °C/min.

The T_g values of anhydrous lactose-MPI-OO and lactose-SPI-OO were similar to that of pure lactose. The T_g values of anhydrous trehalose-MPI-OO and trehalose-SPI-OO were slightly higher than that of pure trehalose, suggesting a possible better compatibility of trehalose with proteins, which may also contribute to the excellent

protecting effects of trehalose on protein structures (López-Díez and Bone, 2004). Proteins may affect the T_g of anhydrous systems by hydrogen bonding to sugar molecules, depending on the type of proteins and sugars and the amount of proteins in the sugar-protein phase after emulsification, and self-assembly of proteins at the oil droplet interfaces. The hydrogen bonding between sugars and proteins may be diminished in the presence of water. The plasticizing effect of water was dominant at increasing a_w , and in humidified systems, the T_g values were dependent on the a_w and the component sugar (Figure 4.4B) rather than water content (Figure 4.4A), regardless of the presence of protein and oil.

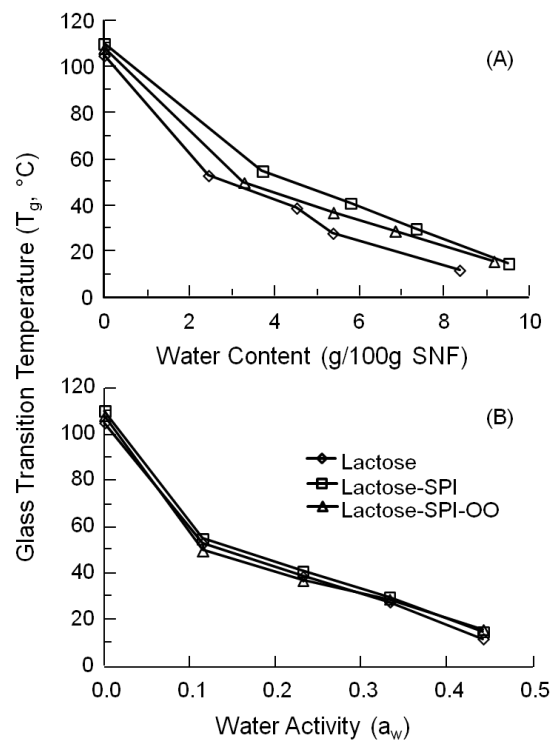


Figure 4.4 Effects of (A) water content (g/100g solid-non-fat) and (B) water activity (a_w) on the onset temperature of glass transition (T_g , °C) in freeze-dried lactose (Chapter 2), lactose-SPI (3:1) (Chapter 2), and lactose-SPI-OO (3:1:2) systems.

As shown in Figure 4.4, it should be noted that the glass transition occurred only in the miscible nonfat solids components and the T_g values at varying a_w followed closely those of the component sugars (Chapter 2). This confirmed that the protein and carbohydrate components were largely phase separated and the T_g values corresponded to those of carbohydrates at most a_w , i.e., the presence of protein affected the quantity of sorbed water but the T_g corresponded to that of the carbohydrate at any constant $a_w > 0$.

Table 4.3 The onset temperature of crystallization (T_{ic} , °C) in freeze-dried lactose-MPI-OO (3:1:2) and lactose-SPI-OO (3:1:2) systems.

Systems	T_{ic}^a , °C				
	0.00 a_w	0.11 a_w	0.23 a_w	0.33 a_w	0.44 a_w
Lactose-MPI-OO	N/O ^b	124	108	91	83
Lactose-SPI-OO	N/O ^b	124	107	94	75

^a $T_{ic} \pm 1^\circ\text{C}$

^b Not observed

The instant crystallization at T_{ic} , showing rapid amorphous lactose crystallization, occurred in lactose-MPI-OO and lactose-SPI-OO systems at 0.11-0.44 a_w (Table 4.3) but no T_{ic} was found for anhydrous systems. Our earlier studies reported that lactose alone crystallized at 174 °C at zero a_w , but no T_{ic} was observed for anhydrous systems in the presence of other components, e.g., protein (Chapter 2) and hydrophilic vitamins (Chapter 3). These inhibiting effects of proteins and vitamins on sugar crystallization result from numerous factors including restricted diffusion and retarded arrangements of sugar molecules to nucleate and form crystals. The T_{ic} decreased with increasing a_w as a result of water plasticization and confirmed phase separation of the sugar components. No instant crystallization of trehalose was found in trehalose-protein-oil

systems (Figure 4.3), probably because an insufficient amount of water for trehalose to form dihydrate crystals was present and the interactions between trehalose and other components inhibiting trehalose molecules to crystallize (Chapter 2).

4.3.3 Oil droplet size distribution

The oil droplet size distributions for the emulsified systems are given in Figure 4.5. The volume weight mean diameter, $D[4,3]$, and the median diameter, $D[v, 0.5]$, of emulsions are given in Table 4.4.

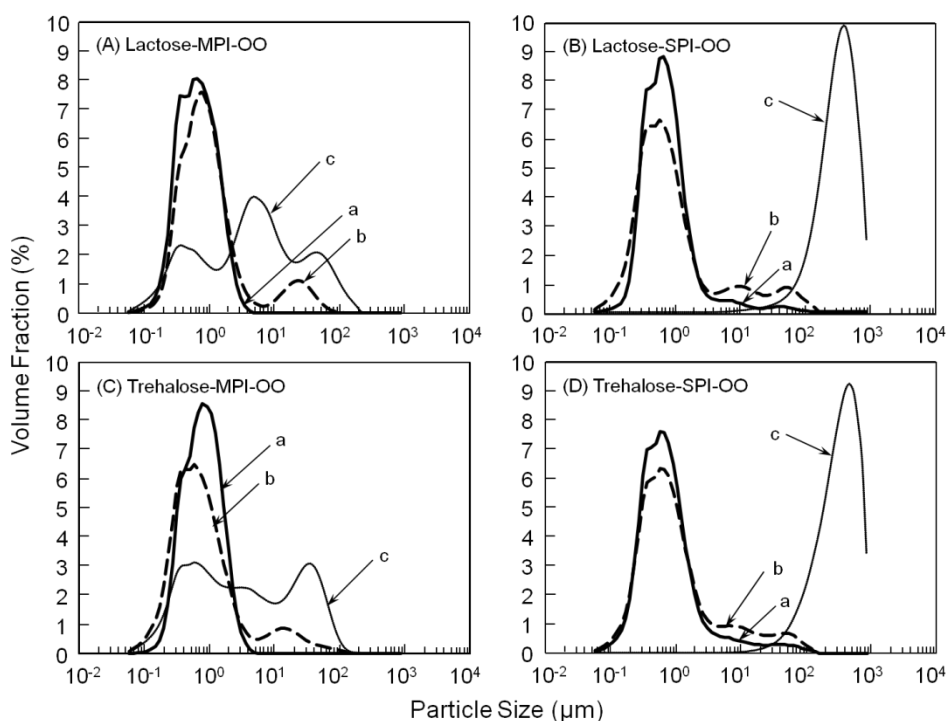


Figure 4.5 Emulsion droplet size distribution of (A) lactose-MPI-OO (3:1:2), (B) lactose-SPI-OO (3:1:2), (C) trehalose-MPI-OO (3:1:2), and (D) trehalose-SPI-OO (3:1:2) systems. The emulsion samples for each system were: (a) the fresh emulsions which were measured within 1 h after homogenization, (b) the freeze-dried materials which were reconstituted and measured, and (c) the freeze-dried materials which were stored at 0.76 a_w for 5 d, reconstituted and measured.

The fresh lactose-MPI-OO and trehalose-MPI-OO emulsions showed mono-modal distribution of droplets (Figures 4.5A-a and 4.5C-a, respectively), while tail distribution was found in lactose-SPI-OO and trehalose-SPI-OO systems (Figures 4.5B-a and 4.5D-a, respectively). During freezing, the oil droplets were immobilized and encapsulated in the maximally freeze-concentrated solutes. Freezing at $-35\text{ }^{\circ}\text{C}$ for 24 h and thawing at room temperature did not cause significant changes of the $D[4,3]$ and the oil droplet distributions (data not shown) in all systems, except in trehalose-SPI-OO system, which showed an increase of $D[4,3]$, but similar $D[v, 0.5]$, indicating the increase of tail distribution (Table 4.4). The structure of freeze-dried materials was determined by (i) the oil droplet size distribution (size and number) during homogenization; and (ii) the ice crystals (size and number) formed during freezing. After the sublimation of ice crystals, pores were left and a porous structure was obtained. Due to the low molecular mobility in the glassy matrices, the oil droplet size distribution was retained in the freeze-dried materials. Freeze-dried lactose-MPI-OO and trehalose-MPI-OO systems showed bi-modal distribution (Figures 4.5A-b and 4.5C-b, respectively) and lactose-SPI-OO and trehalose-SPI-OO showed increased tail distribution (Figures 4.5B-b and 4.5D-b, respectively) of oil droplets, which could be a result of the breakdown of the thin interface during reconstitution. After storage at $0.76\text{ }a_w$ for 5 d, a dramatic change of droplet size distribution was observed, corresponding to the crystallization of component sugar which caused a complete rupture of the interfaces between the continuous phase and dispersed phase. Oil droplets were excluded from the encapsulants and coalescence occurred.

Table 4.4 The volume weighted mean diameter, D[4,3] (mean \pm SD, μm) and 50% volume percentile of droplet size distribution, D[v, 0.5] (median mean diameter \pm SD, μm) of lactose-MPI-OO (3:1:2), lactose-SPI-OO (3:1:2), trehalose-MPI-OO (3:1:2), and trehalose-SPI-OO (3:1:2) systems.

Systems	Fresh emulsions ^a		Thawed emulsions ^b		Freeze-dried emulsions ^c	
	D [4,3] (μm)	D [v, 0.5] (μm)	D [4,3] (μm)	D [v, 0.5] (μm)	D [4,3] (μm)	D [v, 0.5] (μm)
Lactose-MPI-OO	0.75 \pm 0.00	0.60 \pm 0.00	0.88 \pm 0.10	0.72 \pm 0.01	3.26 \pm 0.63	0.77 \pm 0.01
Lactose-SPI-OO	1.82 \pm 0.03	0.59 \pm 0.02	1.95 \pm 0.20	0.62 \pm 0.01	5.35 \pm 0.15	0.62 \pm 0.01
Trehalose-MPI-OO	0.85 \pm 0.02	0.61 \pm 0.02	1.03 \pm 0.43	0.61 \pm 0.01	3.03 \pm 0.33	0.62 \pm 0.01
Trehalose-SPI-OO	2.53 \pm 0.16	0.60 \pm 0.02	3.92 \pm 0.70	0.63 \pm 0.01	5.47 \pm 1.27	0.67 \pm 0.02

^a Measurements were carried out within 1 h after homogenization (fresh emulsions).

^b Measurements were carried out after thawing of frozen emulsions. Fresh emulsions were frozen at -35 °C for 24 h then thawed at room temperature for 1 h.

^c Measurements were carried out after reconstitution of freeze-dried materials.

4.3.4 Stability of α -tocopherol as affected by water activity

The retention of α -tocopherol in the freeze-dried materials was measured right after freeze-drying, which were $94.8 \pm 0.8\%$, $93.9 \pm 1.5\%$, $95.1 \pm 1.6\%$, and $92.4 \pm 1.2\%$ for lactose-MPI-OO, lactose-SPI-OO, trehalose-MPI-OO, and trehalose-SPI-OO systems, respectively. These amounts of retained α -tocopherol were taken as 100 % for the storage study.

During 40 d of storage at 60 °C, rapid loss of α -tocopherol occurred in all anhydrous systems within 3 d of storage, followed by less rapid loss up to 25 d of storage. From 25 d to 40 d, constant retention of α -tocopherol was found, except for lactose-SPI-OO system in which α -tocopherol content decreased but at a lower rate (Figure 4.6). After 40 d of storage, lactose-MPI-OO and trehalose-MPI-OO systems retained $84.6 \pm 1.5\%$ and $82.8 \pm 1.2\%$ of α -tocopherol, respectively, while lactose-SPI-OO and trehalose-SPI-OO systems retained smaller amounts of α -tocopherol, which were $75.3 \pm 2.1\%$ and $78.3 \pm 1.7\%$, respectively.

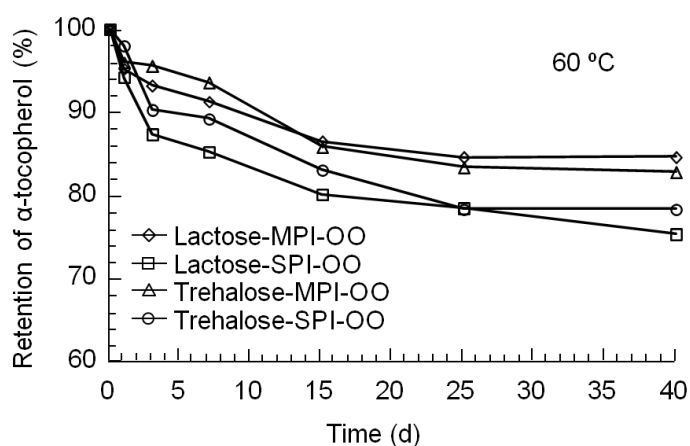


Figure 4.6 Retention (%) of α -tocopherol in anhydrous freeze-dried lactose-MPI-OO (3:1:2), lactose-SPI-OO (3:1:2), trehalose-MPI-OO (3:1:2), and trehalose-SPI-OO (3:1:2) systems during 40 d of storage at 60 °C.

The retention of α -tocopherol after 5 d of storage at various a_w conditions and the water contents of systems at corresponding a_w were plotted as a function of a_w (Figure 4.7).

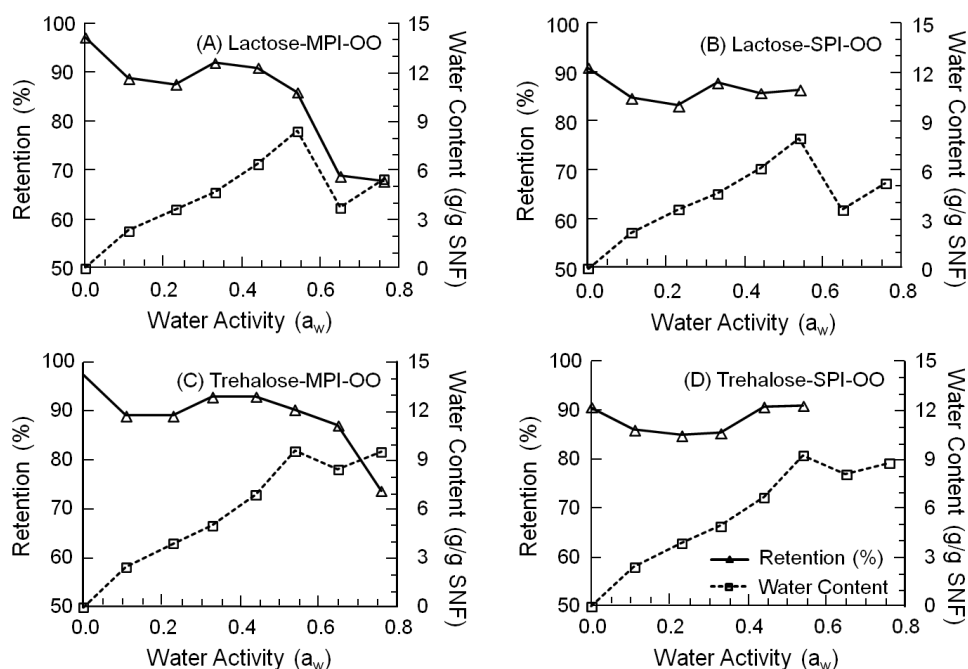


Figure 4.7 Retention (%) of α -tocopherol and water content (g/100g solid-non-fat) for freeze-dried (A) lactose-MPI-OO (3:1:2), (B) lactose-SPI-OO (3:1:2), (C) trehalose-MPI-OO (3:1:2), and (D) trehalose-SPI-OO (3:1:2) systems after storage at various a_w (0.0-0.76) for 5 d.

The α -tocopherol was the most stable at zero a_w . MPI-stabilized systems showed higher retention. This high retention of α -tocopherol confirmed our hypothesis that α -tocopherol did not show good antioxidant activity in anhydrous systems, which could be similar to bulk oil systems, and the stability of α -tocopherol was assured by its immobilization in the glassy solid matrices. α -tocopherol is a hydrophobic compound but contains a hydrophilic OH group, which is surface active to be oriented in the oil-water interface to protect oil against oxidation (Frankel et al., 1994). During freezing, water molecules formed ice crystals and the glassy solids with α -tocopherol at

interfaces were formed. Freeze-drying removed ice crystals by sublimation and retained the structures formed during freezing explaining a relatively high stability of α -tocopherol at low a_w . The α -tocopherol showed highest stability at zero a_w in all the systems. A minimum retention of α -tocopherol was found at 0.11-0.23 a_w (at 0.11-0.33 a_w for trehalose-SPI-OO system), which agreed with rapid lipid oxidation at low a_w (Labuza, 1980). At increasing a_w (0.33-0.44 a_w for trehalose-SPI-OO system and from 0.23-0.33 a_w for all other systems from), the retention of α -tocopherol increased showing that the loss of hydrophobic α -tocopherol coincided with oxidation of the oil (Widicus et al., 1980; Labuza, 1980; Widicus and Kirk, 1981). At higher than 0.54 a_w , loss of α -tocopherol was concomitant to component sugar crystallization. The reasons for the loss of α -tocopherol could be (i) exclusion of oil droplets from the matrices causing loss of protection; (ii) increased availability of oxygen from the environment; and (iii) increased mobilization of α -tocopherol at the interfaces and its consumption as antioxidant. Some differences in α -tocopherol stability at crystallizing conditions may also relate to higher solubility of trehalose and retention of a protective trehalose 'syrup' on entrapped oil particles. SPI-containing systems at $a_w > 0.54$ showed a difficulty in reconstitution of freeze-dried materials and therefore a difficulty in the extraction of α -tocopherol, possibly due to the gelation of SPI with sufficient amount of water, which was released from sugar crystallization. Extraction of oil from such systems, however, was technically difficult and data at higher a_w values were not included.

Materials equilibrated at various a_w (referring to a_w at room temperature) were transferred to 60 °C and kept for 10 d. At 60 °C, systems with T_g above (zero a_w) and

around (0.11 a_w) the storage temperature retained α -tocopherol in the glassy structures, indicating that the glassy state protected α -tocopherol. Loss of α -tocopherol occurred at 0.23 a_w and above, at which the heat-induced plasticization depressed the T_g of the systems to below the storage temperature, followed by component sugar crystallization (Figure 4.8). Lactose crystallization had more severe effect on the loss of α -tocopherol compared with trehalose crystallization. Trehalose crystallized to a lesser extent as a dihydrate and retained a higher amount of water in the crystals. The higher solubility of trehalose dihydrate also allowed trehalose to dissolve in water and form trehalose syrup, which possibly protected the sensitive compounds (Chapter 2). The rapid loss of α -tocopherol at sugar crystallization further suggested that a relative large quantity of α -tocopherol could be located at the oil-water interface.

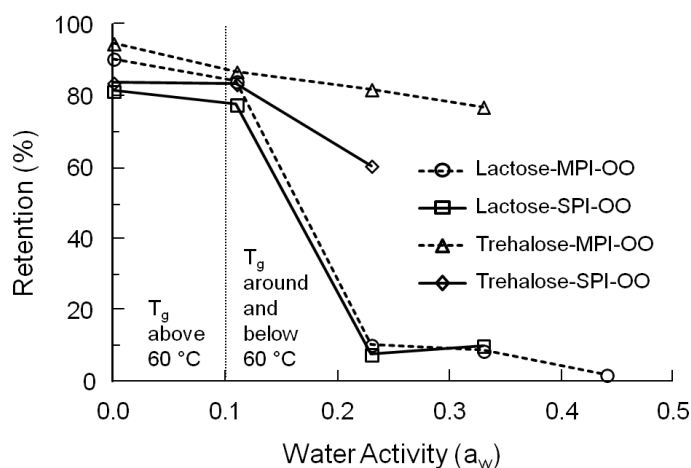


Figure 4.8 Retention (%) of α -tocopherol for freeze-dried lactose-MPI-OO (3:1:2), lactose-SPI-OO (3:1:2), trehalose-MPI-OO (3:1:2), and trehalose-SPI-OO (3:1:2) systems after storage at 60 °C for 10 d. The materials were equilibrated to various a_w (0.0-0.44) for 5 d before transportation to 60 °C.

Significant color changes (browning) were visually observed at $a_w \geq 0.23$ after storage at 60 °C for lactose-containing systems; slight color changes were found in trehalose-

containing systems at $a_w \geq 0.65$ after storage at 60 °C, which could be due to the presence of traces of reducing-sugars in proteins. SPI-containing systems at $a_w > 0.33$ in storage at 60 °C showed a difficulty in reconstitution of freeze-dried materials, which was due to the possible gelation of SPI at these conditions.

4.3.5 Matrices structure and stability of α -tocopherol

Schematic diagrams of the structure formation during processing and structural changes during storage for model systems are shown in Figure 4.9. Homogenization broke down the oil phase into small droplets and stabilized the dispersed phase in the water phase by the amphiphilic proteins (McClements, 2004) (Figures 4.9A and 4.9B).

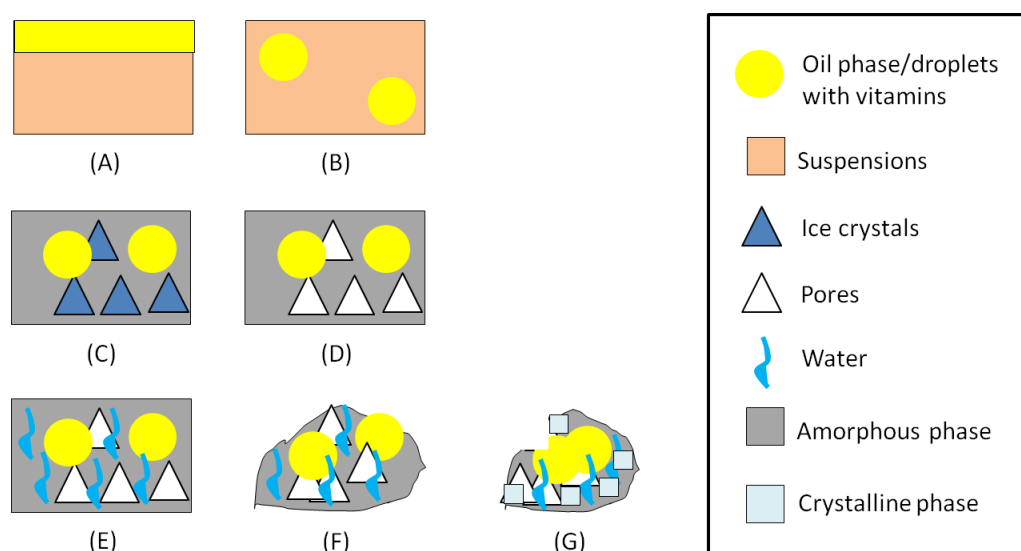


Figure 4.9 Diagrams of the model systems before (A) and after (B) homogenization, frozen (C), and freeze-dried (D). During storage, water-plasticization (E), and collapse (F) occurred due to water sorption. Crystallization of sugars may lead to exclusion and coalescence of the oil droplets (G). The symbols do not represent the real size of components.

During freezing, ice crystals were formed and the solutes (sugar-protein) were freeze-concentrated. The oil droplets were immobilized and encapsulated in the continuous unfrozen solute phase (Figure 4.9C). Pores were left after the sublimation of ice crystals, and the size of ice crystals formed during freezing determined the porosity of the freeze-dried materials. The oil droplets were encapsulated in the matrices, although partial exposure to the pores was possible (Figure 4.9D). During storage at various a_w conditions, water was sorbed by the amorphous solutes due to the high hygroscopy and porosity of the freeze-dried materials (Figure 4.9E). Labuza (1980) has found that at zero and low a_w , lipid oxidation occurred rapidly. At increasing a_w , water exerted a protective effect, which attributed to the hydration of metal catalysts decreasing their effectiveness and hydrogen bonding to peroxides. This explained the low retention of hydrophobic α -tocopherol at low a_w . α -tocopherol could be consumed as antioxidant and showed lower retention, accounting for the decreased oxidation of the solvent lipid. In our study, the stability of α -tocopherol at zero a_w was possibly enhanced by partial immobilization at interfaces of the oil and the glassy matrices that could reduce antioxidant activity of α -tocopherol, i.e., corresponding lower consumption as antioxidant, at zero a_w . At water activities that depressed the T_g to below the storage temperatures (room temperature or 60 °C) and allowed the component sugar to crystallize time-dependently, the stability of α -tocopherol was no longer retained due to the increased exposure of lipids to surrounding atmosphere. Structural changes, e.g., collapse (Figure 4.9F) and sugar crystallization (Figure 4.9G), caused the exclusion of the oil droplets from the encapsulants to the environment and coalescence of the oil droplets, leading to losses of α -tocopherol (Chapter 3).

4.4 CONCLUSIONS

This study showed that stability of α -tocopherol in freeze-dried carbohydrate-protein-oil emulsions was affected by water plasticization and physical changes. This information contributes to the use of carbohydrate-protein systems as structure-forming matrices for stabilization of hydrophobic nutrients. Freezing and freeze-drying of emulsions encapsulated oil droplets in structure-forming sugar-protein matrices. Milk proteins and soy proteins showed good emulsifying properties, as well as contribution to the matrices properties. The structure of the systems was well retained during processing, although changes of oil droplet size distribution occurred due to the ruptures of the interfaces on reconstitution. The presence of oil slightly altered the water sorption behavior of the matrices, but reduced the crystallization rate of the component sugars at high water activity conditions. α -Tocopherol was probably immobilized at anhydrous conditions at interfaces and did not show antioxidant activity, and the stability of α -tocopherol was retained in anhydrous freeze-dried sugar-protein matrices. Water activity affected the stability of α -tocopherol by affecting the rate of lipid oxidation and the antioxidant activity of α -tocopherol. Water sorption- and thermal- induced crystallization of the component sugars caused dramatic structural changes of the matrices, which were believed to be the main cause of the loss of the stability of α -tocopherol. Depending on the properties (type of crystals and their solubility) of the component sugars, the effects of sugar crystallization differed. Since sugar crystallization is a time-dependent phenomenon above the T_g of the matrices, more studies are required to understand the changes above T_g of the systems and the effects of structural changes on the stability of encapsulated particles.

CHAPTER 5

Double interface formulation for improved α -tocopherol stabilization in dehydration of emulsions

Accepted in Journal of the Science of Food and Agriculture, Zhou and Roos, In Press

ABSTRACT

Encapsulation of hydrophobic nutrients can be achieved by freezing and freeze-drying of oil-in-water emulsions containing glass forming materials. The addition of a polyelectrolyte layer on the protein-stabilized oil droplets may provide better protection to the oil phase against external stresses. Soy protein-trehalose and whey protein-trehalose emulsions with (layer-by-layer, LBL) and without (single-layer, SL) ι -carrageenan were used as the delivery systems for olive oil with dissolved α -tocopherol. Emulsions containing 0.0125% proteins, 0.042% oil, and 15% trehalose with (LBL) or without (SL) 0.025% ι -carrageenan at pH 3 were frozen and freeze-dried and their state transitions were studied. The stability of α -tocopherol in freeze-dried systems at 0 and 0.33 water activity (a_w) during storage at 55 °C was followed. Loss of α -tocopherol was found in soy protein-stabilized SL systems at 0.33 a_w and this loss coincided with trehalose crystallization. The stability of α -tocopherol was retained in soy protein-stabilized LBL and whey protein-stabilized LBL and SL systems at all conditions. Trehalose crystallization-induced loss of structure was confirmed from changes of

emulsion properties and visual appearance. Component sugar crystallization contributed to the loss of sensitive compounds, but the stability of these compounds can be improved by the use of LBL emulsions.

Keywords: layer-by-layer emulsions, freezing and freeze-drying, SPI and WPI, ι -carrageenan, trehalose, α -tocopherol

5.1 INTRODUCTION

Protein-stabilized oil-in-water emulsions can be used as hydrophobic nutrient delivery systems. The efficiency of proteins as emulsifiers over a wide pH range supports their use as a primary layer with an oppositely charged interface stabilizer/polyelectrolyte. Proteins exhibit a positive (below the isoelectric point of protein, pI_{pr}) or negative (above pI_{pr}) charge at the protein-oil interface and the oppositely charged secondary layer accumulating on the primary interface further stabilizes emulsions (Dickinson and Pawlowsky, 1997; Moreau et al., 2003; Gu et al., 2004). The stability of emulsions with a proteins-polyelectrolytes interface is affected by the ionic strength of the continuous phase. The electrostatic interactions between a polyelectrolyte and a particle decrease as the ionic strength of the solution increases because of the accumulation of counter-ions around the surfaces. Such decrease of the net charges of particles is referred to as “electrostatic screening” (McClements, 2004). The concentration of polyelectrolytes is also critical, as a low concentration may allow bridging flocculation of protein-stabilized particles and depletion flocculation may occur at high polyelectrolyte

concentrations (Dickinson and Euston, 1991; Dickinson, 2003). Due to the charge heterogeneity of proteins, it is possible to have local negative charges of proteins at $\text{pH} < \text{pI}_{\text{pr}}$, and local positive charges of proteins at $\text{pH} > \text{pI}_{\text{pr}}$ (Park et al., 1992; Dickinson, 1998). Therefore, local interactions between protein and polyelectrolyte molecules, which could be weak, may be found at pH conditions where proteins and polyelectrolytes have the same net charges (Gu et al., 2004). κ -Carrageenan has a strong electrolytic character due to its sulphate groups, which explain its $\text{pK}_a \sim 2.0$ and a negative charge at both acidic and neutral pH systems (Bredy and Holum, 1993).

Freezing is common in the food industry, but factors such as fat crystallization, ice formation, freeze-concentration, interfacial phase transitions, and the presence of cryoprotectants affect emulsion stability (McClements, 2004; Cornacchia and Roos, 2011c). In freezing, the dispersed oil particles are forced closely to each other due to the reduced available volume of the unfrozen phase (Saito et al., 1999). The electrostatic repulsion between the charged particles might become less important because of the increase in ionic strength in the freeze-concentrated solute phase. The differences in the thickness and structure of the interface, which protects the particles against aggregation through steric repulsion, may become critical for stability of the frozen systems. Mun et al. (2008) found that β -lactoglobulin-pectin/carrageenan-stabilized oil-in-water emulsions. A layer-by-layer (LBL) emulsion showed improved resistance against freeze-thaw (-20°C to 30°C) cycling than emulsions stabilized by β -lactoglobulin. It was assumed that the ionic sides of pectin and carrageenan adsorbed to the surfaces of the β -lactoglobulin-stabilized particles, forming a thicker interface than the β -lactoglobulin alone. Pectin showed even better protection because of its non-ionic side

chains which protruded into the surrounding phase and produced thicker coatings than the carrageenan. Stability of both LBL and primary emulsions was further improved by maltodextrin, which increased the volume of unfrozen water phase available to the dispersed particles.

Freezing followed by freeze-drying produces amorphous, glassy solids that show limited molecular mobility and high chemical and microbiological stability (Labuza, 1980; Slade and Levine, 1991; Roos, 1995). The structure of freeze-dried materials is dependent on (i) the solids composition, which may show different delaying effects on ice formation and depression of the freezing point, as well as glass transitions, and (ii) the freezing temperature, which controls the number and size of the ice crystals and thereby the porosity of the freeze-dried materials (Roos, 1997; Harnkarnsujarit et al., 2012). Trehalose is a glass-forming disaccharide that is commonly used in food and pharmaceutical industries. Several researchers have reported the effects of amorphous state and crystallization behaviour of trehalose on the stability of sensitive components (Elizalde et al., 2002; Cerdeira et al., 2005). Our earlier study found that loss of the stability of α -tocopherol in freeze-dried sugar-based matrices coincided with sugar crystallization (Chapter 4).

The present study used oil-in-water emulsions with LBL stabilization by a soy protein isolate (SPI) or a whey protein isolate (WPI) as the emulsifier and ι -carrageenan as the polyelectrolyte. The objectives were to characterize the primary emulsions prepared at various protein:oil ratios, to study differences in freezing and freeze-drying behaviour of LBL emulsions as compared to corresponding protein-stabilized primary emulsions,

and to investigate stability of α -tocopherol in the oil phase of these freeze-dried emulsions for nutrient delivery applications during storage at various conditions.

5.2 MATERIALS AND METHODS

5.2.1 Materials

Soy protein isolate (SPI, PRO-FAM891, Archer Daniels Midland, Decatur, IL, U.S.A.) or whey protein isolate (WPI, Isolac, Carbery Food Ingredients, Balineen, Ireland) were used as emulsifiers (the primary layer). ι -Carrageenan (ι -CAR, Sigma-Aldrich, St. Louis, MO, U.S.A.) was used as a polyelectrolyte (the secondary layer). Trehalose dihydrate (Cargill Inc., Minneapolis, MN, U.S.A.) was used as a glass former in freezing and freeze-drying. Olive oil (OO, Extra-Virgin Olive Oil, Don Carlos, Hacienda Don Carlos, Spain) was used as the lipid phase and the solvent for the hydrophobic α -tocopherol (Sigma-Aldrich, St. Louis, MO, U.S.A.). Other chemicals were all purchased from Sigma-Aldrich (Sigma-Aldrich, St. Louis, MO, U.S.A.).

5.2.2 Preparation of emulsions

5.2.2.1 *Preparation of primary emulsions*

Primary emulsions were prepared with 1, 2, 3, 4, and 5% dry solids of SPI or WPI and 10% oil (500g, w/w), i.e., at 1:10, 1:5, 3:10, 2:5, and 1:2 protein:oil ratios. SPI or WPI

were suspended in deionised water and allowed to hydrate at room temperature under stirring for 2 h, the suspensions were then adjusted to $\text{pH } 3.00 \pm 0.03$ with a series of HCl solutions (1M, 0.5M, 0.01M, 0.001M). The hydrated SPI and WPI suspensions were further hydrated at pH 3 for 1 h, and the weight was adjusted to 450 g with a pH 3 HCl solution (prepared from 1M HCl and deionised water). α -tocopherol (5%, w/w) was mixed with olive oil, which naturally contained a smaller amount of α -tocopherol than other oils (Contreras-Guzmán and Strong III, 1982), under stirring in dark (i.e., the beaker was wrapped by aluminium foil) for 1 h. The oil phase (50 g) and water phase (450 g) were mixed, pre-homogenized using Ultra-Turrax (T25 Digital, Staufen, Germany) at 10,000 rpm for 30 s, and immediately homogenized at room temperature (APV-1000 High-Pressure homogenizer, Wilmington, MA, U.S.A.) at 24 MPa (two stages, 20 and 4 MPa) for three cycles. The protein-stabilized primary emulsions were characterized for emulsion droplet size and charge.

5.2.2.2 *Preparation of layer-by-layer (LBL) emulsions*

Solution of ι -carrageenan (ι -CAR, 0.1%, w/w, 150g) was prepared in deionised water at 70 °C for at least 30 min under stirring and cooled to room temperature. The pH of the ι -CAR solution was adjusted to $\text{pH } 3.00 \pm 0.03$ using a series of HCl solutions. The primary emulsions at each protein:oil ratio were diluted with pH 3 HCl solution to give final concentrations of 0.05% protein and various oil contents. The diluted SPI- or WPI-stabilized emulsions and ι -CAR solution were mixed at 1: 1 (v/v) ratio to form the layer-by-layer (LBL) emulsions with protein:carrageenan ratio of 1:2. The pH of the LBL emulsions was checked and adjusted to pH 3 when necessary. These LBL emulsions were characterized for particle size and charge.

5.2.2.3 Preparation of emulsions with sugar

Trehalose solution (30%, w/w) was prepared in deionized water and the pH of trehalose solutions was adjusted to 3.00 ± 0.03 with a series HCl solutions. The primary emulsion at 3:10 protein:oil ratio was used to prepare LBL and single layer (SL) emulsions. The emulsions with a composition of 0.025% protein, and 0.083% oil with (LBL) or without (SL) 0.05% ι -CAR was mixed with the trehalose solution (1:1, v/v) to obtain emulsions with the final compositions of 0.0125% protein, 0.042% oil, and 15% trehalose with (ST-LBL and WT-LBL, representing SPI-trehalose-LBL and WPI-trehalose-LBL systems, respectively) or without (ST-SL and WT-SL, representing SPI-trehalose-SL and WPI-trehalose-SL systems, respectively) 0.025% ι -CAR. The pH of the final emulsions was measured and adjusted to pH 3 when necessary.

5.2.3 Characterization of emulsions

The particle size (zeta-average, Z; polydispersity index, PDI; peak mean diameter, Peak) and particle charge (zeta-potential) were measured using Zetasizer (Zetasizer Nano ZS, equipped with 4mV 633nm He-Ne Laser, Malvern Instruments Ltd., Malvern, Worcestershire, U.K.). To measure the emulsion droplet size and charge, the emulsions were diluted with 1:1000 using pH 3 HCl solution to obtain the scattering from individual particle. The diluted emulsions were transferred to plastic cuvettes (Square cuvettes, PS, $10 \times 10 \times 45$ mm, SARSTEDT AG&Co., Nümbrecht, Germany) for particle size or to plastic capillary cells (Folded capillary cells, DTS 1061, Malvern Instruments Ltd., Malvern, Worcestershire, U.K.) for particle charge analysis at room

temperature. Triplicate injections were run for each emulsion, with at least 12 readings made for each sample. The average particle size and particle charge were reported.

5.2.4 Frozen state transitions

The onset temperature of glass transition of the maximally freeze-concentrated solutes, T_g' , and the onset temperature of ice melting of the maximally freeze-concentrated systems, T_m' , were measured for LBL-trehalose and primary-trehalose emulsions using differential scanning calorimetry (DSC, Mettler Toledo 821e with liquid N₂ cooling, Switzerland). To analyze the T_g' and T_m' values, 20-25 mg of the emulsions were transferred into 40 μ l preweighed DSC aluminum pans (Mettler Toledo, Switzerland). Pans with samples were hermetically sealed and weighed (Mettler Toledo AG245 balance). A sealed empty pan was used as a reference in all measurements. The T_g' and T_m' values of the maximally freeze-concentrated systems were analyzed according to Chapter 2 using STAR thermal analysis software, version 6.0 (Mettler Toledo, Switzerland). All measurements were carried out in triplicate.

5.2.5 Freezing profiles

The freezing profiles of LBL-sugar or primary-sugar emulsions were monitored using a data logger with temperature sensor probes (Squirrel SQ800, Grant Instruments Ltd., England). The emulsions (5 ml aliquots) were transferred using a pipette (Pipetman P5000, Gilson Inc., Middleton, WI, U.S.A.) into glass vials (Vials 10.00 ml Fiolax

Clear, SCHOTT forma vitrum, Müllheim, Germany) and sealed with parafilm (PM-992, Pechiney Plastic Packaging, Menasha, WI, U.S.A.). The temperature probes were punctured through the parafilm and placed in the centre of the emulsions. The emulsions in vials were placed on aluminium trays and frozen at -20 and -35 °C in laboratory chest freezers (Heto, Jouan Nordic A/S, Denmark). Temperature data were recorded at 10 s intervals for at least 3 h. The initial cooling rates were obtained from the slopes of the initial temperature decrease. The supercooling temperature, T_s , and freezing temperature, T_i , were read from the freezing curves. The average results of triplicate samples were reported. The emulsions after thawing were characterized for emulsion droplet size and charge.

5.2.6 Freezing and freeze-drying of emulsions

The emulsions (5 ml aliquots) with a composition of 0.0125% protein, 0.042% oil, 15% trehalose, and with (LBL-trehalose) or without (primary-trehalose) 0.025% ι -CAR were transferred using a pipette (Pipetman P5000, Gilson Inc., Middleton, WI, U.S.A.) into glass vials (Vials 10.00 ml Fiolax Clear, SCHOTT forma vitrum, Müllheim, Germany), frozen using laboratory chest freezers (Model HLLF-240, Heto, Jouan Nordic A/S, Denmark) at -20 or -35 °C for 24 h, and subsequently transferred to a -80 °C freezer (Icebird/Mini Freeze 80, Heto, Jouan Nordic A/S, Denmark) for 5 h to decrease temperature and avoid ice melting during transfer to a freeze-dryer (Lyovac GT2, STERIS, Hürth, Germany). Frozen samples in glass vials with semi-closed rubber septa were freeze-dried at < 0.1 mbar ($T < -40$ °C) for ≥ 72 h in dark (i.e., the drying chamber

of the freeze-dryer was wrapped using aluminium foil). All vials were hermetically closed in the freeze-dryer using rubber septa prior to breaking the vacuum with ambient air. The emulsion droplet size and charge for freeze-dried materials were characterized on reconstitution as described above.

5.2.7 State transitions of freeze-dried materials

The state transitions of freeze-dried LBL-trehalose or primary-trehalose emulsions, including glass transition, trehalose crystallization, and melting of trehalose crystals, were studied using DSC. The freeze-dried materials were powdered in vials by a spatula and transferred (10-15 mg) into preweighed DSC pans and equilibrated at 0.33 a_w over saturated $MgCl_2$ solution in an evacuated desiccator for 4 d. The pans were hermetically sealed, weighed, transferred to an incubator at 55 °C, and taken after 0, 1, and 2 d to measure the crystallization of trehalose during storage. The dynamic scans were run according to Chapter 2. All measurements were carried out in triplicate.

5.2.8 Storage of freeze-dried materials and stability of α -tocopherol

The freeze-dried materials were equilibrated at 0 and 0.33 a_w over P_2O_5 and saturated $MgCl_2$ solution, respectively, in evacuated desiccators in dark (i.e., desiccators were placed in a dark closed cabinet) for 4 d. The equilibrated samples in glass vials were sealed under vacuum. The vacuumized and sealed vials were packaged in plastic pouches (PA/PE 90, FISPAK, Leamore Warehouse, Dublin, Ireland) using a vacuum

sealing system (POLAR80, Henkelman vacuum systems, Hertogenbosch, The Netherlands), and stored in an incubator at 55 °C for 10 d. These conditions allowed no oxygen or water transfer with surroundings during storage. The α -tocopherol in freshly-prepared LBL-trehalose or primary-trehalose emulsions was extracted and measured at 297.7 nm using a spectrophotometer (Varian Cary 1E, UV-Visible Spectrophotometer, Agilent Technologies, Santa Clara, CA, U.S.A.) according to Chapter 4. Retention in fresh emulsions was considered as 100%. The retention of α -tocopherol in freeze-dried materials was measured on reconstitution after humidification and during storage.

5.2.9 Statistics

All measurements carried out in this study were done in triplicate. The mean values of data for triplicate samples plus/minus one standard deviation (SD) are reported as results for the characteristics of emulsions, physical properties of matrices, and the stability study. A one-way analysis of variance (ANOVA) was used to analyze the differences in data of emulsion properties and freezing profile at 95% confidence level with SPSS 20.0 for Windows (SPSS Inc., Chicago, IL, U.S.A.).

5.3 RESULTS AND DISCUSSION

5.3.1 Emulsion characteristics

The protein-stabilized primary emulsions with various protein:oil compositions were characterized for particle size and charge. Both SPI- and WPI-stabilized emulsions

showed monomodal particle size distribution. WPI-stabilized primary emulsions at pH 3 showed smaller peak mean particle diameter (i.e., the size at the peak of size distribution) than SPI-stabilized primary emulsions. Both emulsions showed a constant size at the peak of the size distribution regardless of the protein content (Figure 5.1A). A constant size at peak indicated there was sufficient coverage of the oil particles by proteins at all concentrations. The size difference of the SPI- and WPI-covered particles was possibly due to their molecular size difference and variation in molecular assembly at the interface (Dickinson, 2001; Keerati-u-rai et al., 2012).

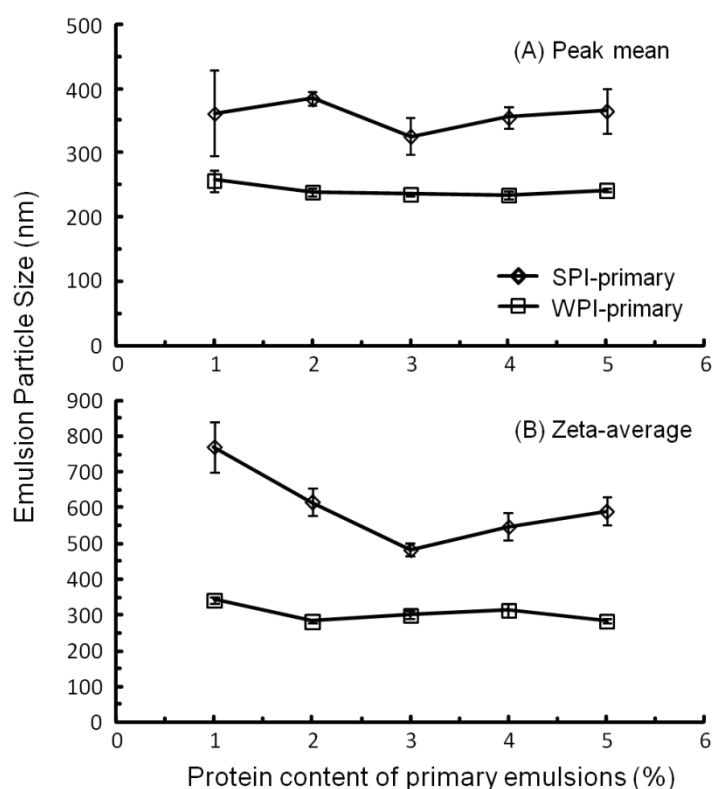


Figure 5.1 The peak mean diameter (nm) (A) and zeta-average (nm) (B) of SPI-primary and WPI-primary emulsions (O/W, 10% oil, 1-5% proteins) at pH 3.

Zeta-average is a statistically derived particle size using the refracted laser light intensity. The polydispersity index (PDI), indicating the distribution of the particle sizes, is also calculated from the intensity (Malvern Instrument Ltd., 2004). A decrease of PDI in systems with 1 to 3% proteins suggested the narrowing of the particle size distribution with increasing amount of SPI. SPI-stabilized primary emulsions showed a decreased zeta-average with increasing protein content to 3% (Figure 5.1B). At pH 3, the SPI- and WPI-stabilized particles were positively charged. The zeta-potential gave the net charge of the electrical double layer of the particles (Malvern Instrument Ltd., 2004). The particle charge caused electrostatic repulsion between individual particles corresponding to the stability of emulsions. The zeta-potential for SPI- and WPI-stabilized primary emulsions were between 30 to 40 mV and 40 to 45 mV, respectively, decreasing with increasing protein content, especially for SPI-stabilized emulsions (Figure 5.2). The particles of SPI-stabilized emulsions were more dependent on the protein content and had a smaller charge than those of WPI-stabilized emulsions. To ensure both of the protein-stabilized primary emulsions had a narrow size distribution, we used emulsions with 3% SPI or WPI and 10% oil in the freezing and freeze-drying experiments.

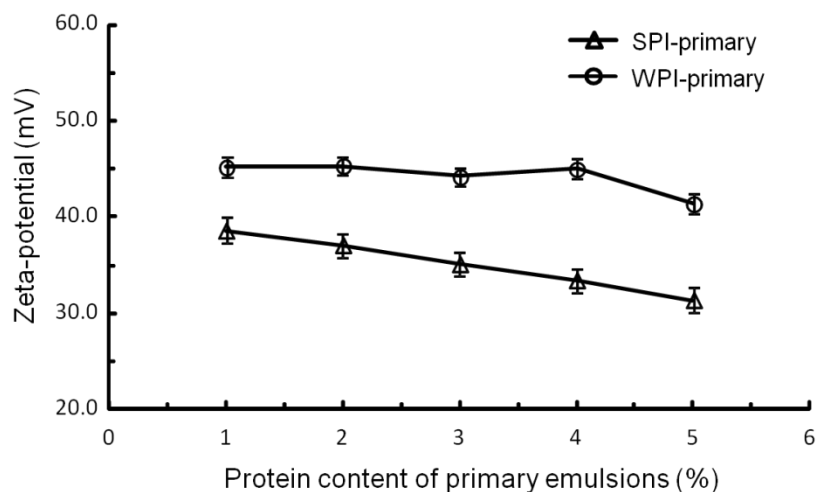


Figure 5.2 Effect of protein content on emulsion particle charge at pH 3.

ι -Carrageenan (ι -CAR) at pH 3 formed a second layer around the protein-stabilized oil particles (Gu et al., 2004), and the net charge became negative. Our preliminary tests showed that (i) the LBL emulsions only formed by dilute primary emulsions (0.01 to 0.1% protein), although at higher protein concentrations precipitation of protein-coated particles was immediate at the addition of the 0.05 to 0.1% ι -CAR solution; (ii) both the protein:oil ratio, that controlled the particle size, charge, and distribution, and the protein: ι -CAR ratio were important, especially in SPI-stabilized emulsions, as the LBL emulsions failed at 1:10 and 1:5 SPI:oil ratios with 1:0.5 and 1:1 SPI: ι -CAR ratios; and (iii) LBL emulsions with WPI-stabilized primary emulsions at 1:10 and 1:5 WPI:oil ratios were successful. For the primary emulsions at 3:10 protein:oil ratio, the addition of ι -CAR did not affect the peak mean particle diameter in comparison to the primary emulsions. However, there was an increase in the PDI and the zeta-average. The primary emulsions showed positive charges and the LBL emulsions showed negative charges at various ι -CAR contents. The distribution of particle charge changed from

monomodal to bi- or tri-modal at 1:4 and higher for i-CAR protein: ι -CAR ratios, indicating unevenly distributed charges at high ι -CAR concentrations.

Emulsions with trehalose showed decreased zeta-potential. This decrease was accounted for trehalose- ι -CAR (in ST-LBL and WT-LBL systems) or trehalose-protein (in ST-SL and WT-SL systems) interactions (McClements, 2002). The emulsion particle size and charge of fresh ST-LBL, ST-SL, WT-LBL, and WT-SL emulsions are given in Table 5.1.

Table 5.1 The zeta-average (Z-average, nm), peak mean diameter (Peak, nm), and zeta-potential (ζ , mV) of ST-LBL, ST-SL, WT-LBL, WT-SL. The emulsion droplet size and charge were measured for fresh emulsions, and emulsions thawed from -20 and -35 °C. Values shown were mean \pm SD of triplicate samples*.

Systems	Fresh			Thawed from -20 °C			Thawed from -35 °C		
	Z-average (nm)	Peak (nm)	ζ (mV)**	Z-average (nm)	Peak (nm)	ζ (mV)**	Z-average (nm)	Peak (nm)	ζ (mV)**
ST-LBL	800 \pm 78 (m)	286 \pm 43	-38.8 \pm 0.1 (b)	1015 \pm 265 (m)	293 \pm 58	-40.5 \pm 5.3 (t)	1014 \pm 106 (m)	333 \pm 39	-42 \pm 4.3 (b)
ST-SL	576 \pm 26 (m)	300 \pm 20	25.9 \pm 1.8 (m)	664 \pm 49 (m)	340 \pm 40	23.5 \pm 9.1 (m)	577 \pm 63 (m)	269 \pm 45	25.6 \pm 1.2 (m)
WT-LBL	610 \pm 35 (m)	308 \pm 25	-38.7 \pm 0.2 (m)	633 \pm 63 (m)	266 \pm 13	-34.7 \pm 3.7 (b)	639 \pm 26 (m)	287 \pm 15	-35.6 \pm 2.0 (b)
WT-SL	463 \pm 43 (m)	292 \pm 29	18.2 \pm 1.1 (m)	484 \pm 28 (m)	257 \pm 1	21.1 \pm 3.6 (m)	477 \pm 16 (m)	256 \pm 19	18.4 \pm 3.4 (m)

* No significant differences ($p \leq 0.05$) were found for the emulsion properties before and after freeze-thawing for each system.

**The small letter in brackets indicating the distribution: m=monomodal, b=bimodal, t=trimodal.

5.3.2 Freezing and freeze-drying

The onset temperature of glass transition and ice melting in maximally freeze-concentrated LBL-trehalose and primary-trehalose systems, T_g' and T_m' were -41 ± 1 °C and -31 ± 1 °C, respectively. No differences were found between SPI-stabilized and WPI-stabilized or LBL and primary emulsions. The freezing behavior of these systems was mainly that of trehalose, since trehalose content was $> 99\%$ of the solids.

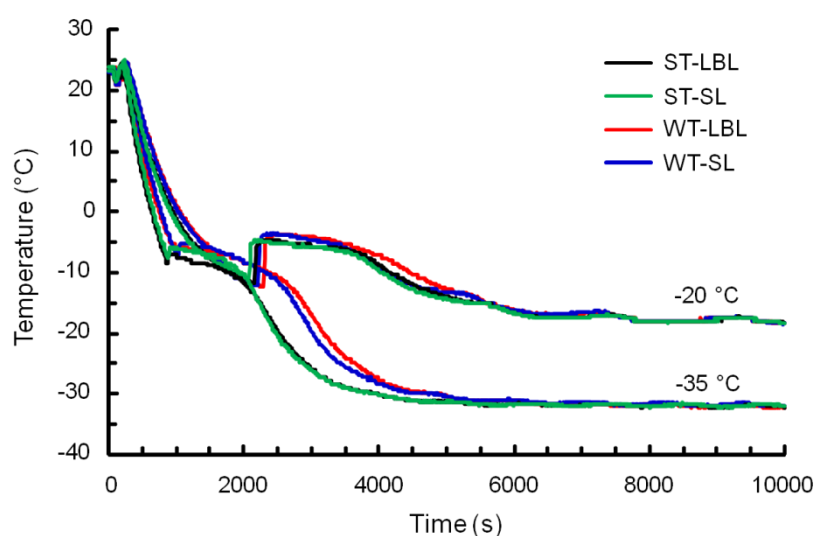


Figure 5.3 Freezing profiles of ST-LBL, ST-SL, WT-LBL, and WT-SL systems at freezing temperatures of -20 and -35 °C.

The freezing profiles of LBL-trehalose and primary-trehalose systems are shown in Figure 5.3. The initial supercooling temperature (T_s), the freezing temperature (T_i), and the initial cooling rate to T_s at -20 and -35 °C as determined from the cooling curves (Figure 5.3) are given in Table 5.2. All systems showed similar T_s and T_i values at each freezing temperature, while slightly higher T_s and lower T_i were found at -35 °C than at -20 °C. The initial cooling rate showed an increase as the freezing temperature was

decreased, which were 1.4 °C/min and 1.3 °C/min for SPI and WPI systems, respectively, at -20 °C and 2.3 °C/min and 2 °C/min for SPI and WPI systems, respectively, at -35 °C. The freezing process significantly affects the freeze-dried structure. The rate of nucleation of water molecules hence the number and size of ice crystals formed during freezing are mainly determined by the freezing temperature (or freezing rate) (Flink and Karel, 1970; Peterson et al., 1973; Harnkarnsujarit et al., 2012). Moreover, the formation of a maximally freeze-concentrated system could be obtained by annealing the system above the T_g' but below the T_m' (e.g., -35 °C in the present study) (Roos and Karel, 1991c).

Table 5.2 Freezing properties derived from freezing profiles: super-cooling temperature (T_s , °C) and freezing temperature (T_i , °C) of ST-LBL, ST-SL, WT-LBL, and WT-SL systems frozen at -20 and -35 °C prior to freeze-drying. Values shown were mean \pm SD of triplicate samples*.

Systems	-20 °C**		-35 °C***	
	T_s (°C)	T_i (°C)	T_s (°C)	T_i (°C)
ST-LBL	-12 \pm 0	-4 \pm 0	-8 \pm 0	-6 \pm 0
ST-SL	-11 \pm 1	-4 \pm 1	-8 \pm 2	-6 \pm 0
WT-LBL	-12 \pm 1	-5 \pm 2	-6 \pm 0	-5 \pm 0
WT-SL	-11 \pm 1	-4 \pm 0	-7 \pm 1	-5 \pm 0

*No significant differences ($p \leq 0.05$) were found for data in the same column.

** The initial cooling rates were calculated from the cooling curves, which were 1.4 °C/min for ST-LBL and ST-SL emulsions and 1.3 °C/min for WT-LBL and WT-SL emulsions.

***The initial cooling rates were calculated from the cooling curves, which were 2.3 °C/min for ST-LBL and ST-SL emulsions and 2 °C/min for WT-LBL and WT-SL emulsions.

Freezing at -20 or -35 °C followed by thawing at room temperature of each system was not found to significantly affect the peak mean diameter and zeta-average of emulsions, as given in Table 5.1. Constant peak mean diameter but slightly increased zeta-average

with high SD values were observed for ST-LBL systems after freezing and thawing, suggesting the possible changes of particle size distribution during freeze-concentration of ST-LBL system. The particle size data of ST-SL system showed that it was more stable than the ST-LBL system in freezing. Both WT-LBL and WT-SL systems showed constant particle size with small SD values, suggesting their good stability against freezing and thawing and their potential to retain the structure during freeze-concentration. The zeta-potential of ST-LBL system had bimodal distribution, while all other systems showed monomodal distribution of charges. No significant difference of zeta-potential of the systems was found before and after freezing and thawing (Table 5.1), however, the charges did become more unevenly distributed, e.g., from bimodal to trimodal for ST-LBL system (frozen at -20 °C) or from monomodal to bimodal for WT-LBL systems (frozen at both -20 and -35 °C). Both ST-SL and WT-SL systems retained the monomodal charge distribution. The appearance of the bimodal charge distribution indicated the damage of the LBL structure.

Freezing encapsulated the oil droplets in the freeze-concentrated solutes. Freezing temperature determined the size of ice crystals, which further determined the structure and porosity of freeze-dried materials after the removal of ice crystals by sublimation during freeze-drying (Roos, 1997). It was found that the freeze-dried carbohydrate-agar systems, which were frozen at higher temperature with smaller freezing rate, showed a more porous structure with thicker solute-wall membranes than systems frozen at lower temperatures (Harnkarnsujarit et al., 2012). Accordingly, systems frozen at -20 °C should show a smaller number of large pores distributed in continuous trehalose glass with dispersed oil particles stabilized by either LBL or SL interfaces. The structural

differences of the continuous phase as well as the interface composition of the systems could lead to different protection of the oil particles with consequent improvement of α -tocopherol stability. On the other hand, freeze-concentration followed by freeze-drying may also affect the properties of the dispersed oil particles by changing their local environment. Freeze-dried LBL and SL systems showed increased zeta-average on reconstitution as compared to fresh emulsions, while no changes were found for peak mean particle diameter. The particle charges were retained in reconstitution after freeze-drying (Table 5.3). These results suggested that reconstituted freeze-dried materials showed similar properties to the fresh emulsions.

Table 5.3 The zeta-average (Z-average, nm), peak mean diameter (Peak, nm), and zeta-potential (ζ , mV) of freeze-dried ST-LBL, ST-SL, WT-LBL, and WT-SL systems.

Systems	Freeze-dried (frozen at -20 °C)			Freeze-dried (frozen at -35 °C)		
	Z-average (nm)	Peak (nm)	ζ (mV)*	Z-average (nm)	Peak (nm)	ζ (mV)*
ST-LBL	865 ± 132 (m)	307 ± 35	-39.1 ± 5.8 (b)	882 ± 101 (m)	290 ± 47	-37.5 ± 0.1 (b)
ST-SL	750 ± 63 (m)	283 ± 28	23.6 ± 1.6 (m)	780 ± 19 (m)	314 ± 20	24.5 ± 0.8 (m)
WT-LBL	702 ± 69 (m)	259 ± 16	-42.0 ± 2.2 (b)	694 ± 85 (m)	272 ± 33	-35.3 ± 4.6 (b)
WT-SL	508 ± 15 (m)	250 ± 8	19.9 ± 1.2 (m)	445 ± 56 (m)	260 ± 27	18.0 ± 0.8 (m)

*The small letter in brackets indicating the distribution: m=monomodal, b=bimodal, t=trimodal.

5.3.3 State transitions of freeze-dried systems

Freeze-drying typically retains an amorphous state of solids. Storage of materials above their T_g may result in glass transition and cause time-dependent changes, e.g., collapse of structure. Sugar crystallization may occur at a rate controlled by the difference between storage temperature and the glass transition ($T-T_g$) (Chuy and Labuza, 1994; Roos, 1995; Bhandari et al., 1997; Silalai and Roos, 2010). Our earlier studies found that the loss of stability of vitamins coincided with lactose and trehalose crystallization (Chapter 3 and 4). The higher solubility of trehalose crystals than lactose reduced crystallization and it formed a viscous syrup, which provided protection to the particles and contributed to the better stability of vitamins in trehalose systems. Trehalose crystallizes mainly into dihydrate, which requires sufficient amount of water to form the hydrated crystals (Cardona et al., 1997; Miao and Roos, 2005a). At 0.33 a_w , all systems showed T_g (onset) around 30 °C, and no trehalose crystallization was found by DSC (Figure 5.4), suggesting there was an insufficient amount of water for trehalose to crystallize as dihydrate during a dynamic measurement (Chapter 2 and 3). After storage of the samples in sealed DSC pans at 55 °C for 1 d, $T-T_g = 25$ °C, glass transition of trehalose was present but at a higher temperature at about 43 °C. The glass transition was followed by an endothermic peak, which indicated melting of trehalose dihydrate crystals (Figure 5.4). A slightly higher T_g of 47 °C and larger endotherm were found after 2 d of storage (Figure 5.4). These data showed that some water in the amorphous phase was consumed to form trehalose dihydrate and trehalose remained partially amorphous with dispersed crystalline phases.

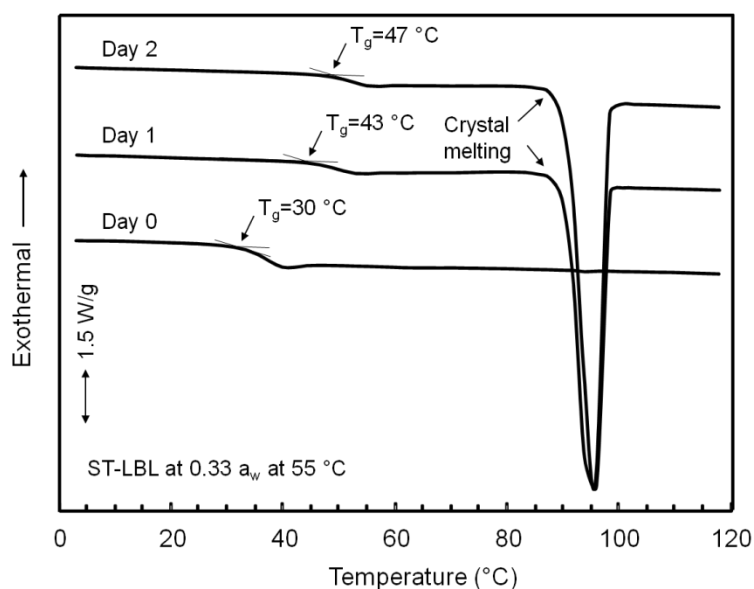


Figure 5.4 DSC thermograms of ST-LBL system equilibrated to 0.33 a_w room temperature during storage for 2 d at 55 °C, showing glass transition of amorphous trehalose and melting of trehalose dihydrate crystals. The thermograms are from the second heating scans (heating rate at 5 °C/min). The ST-LBL emulsion was frozen at -20 °C and freeze-dried.

Such crystallization of trehalose dihydrate reduced water content of the remaining amorphous phase and increased the T_g of the amorphous phase during storage, which were in agreement with the “partial desiccation effect” of trehalose as suggested by Aldous et al. and Schebor et al.. The increased T_g , giving a smaller $T - T_g$, slowed down trehalose crystallization. The results showed that crystal formation during the first day of storage was sufficient to stop further crystallization.

5.3.4 Stability of α -tocopherol and structural changes during storage

The retention of α -tocopherol in fresh and freeze-dried ST-LBL, ST-SL, WT-LBL, and WT-SL systems was measured and no loss was found after freezing and freeze-drying.

At $a_w=0$, all the systems were in the glassy state and the molecular mobility and chemical reactions were restricted in the trehalose glass. Full retention of α -tocopherol was found in all systems, regardless of the protein (SPI or WPI) and emulsion (LBL or primary) type (Figures 5.5Aa and 5.5Ba). At $a_w=0.33$, about 25% of α -tocopherol was lost within 1 d of storage of ST-SL systems (Figure 5.5Ab), which was possibly a result of structural changes induced by trehalose crystallization (Figure 5.4) and therefore exposure of the formerly-encapsulated oil particles to the surroundings (Elizalde et al., 2002; Cerdeira et al., 2005; Buera et al., 2005; Chapter 4). Surprisingly, ST-LBL systems showed full retention of α -tocopherol, although trehalose crystallization was also apparent. These results suggested that with SPI alone the oil droplets were well protected but the SPI layer was broken down as a result of trehalose crystallization. In the presence of ι -CAR, which formed a second layer around protein-stabilized oil particles, the particle structure was more resistant to trehalose crystallization. At $a_w=0.33$, both WT-LBL and WT-SL retained 100% α -tocopherol at all conditions (Figure 5.5Bb), suggesting that WPI alone was sufficient to protect oil particles against trehalose crystallization and the stability of the systems could be further improved in the presence of an ι -CAR layer.

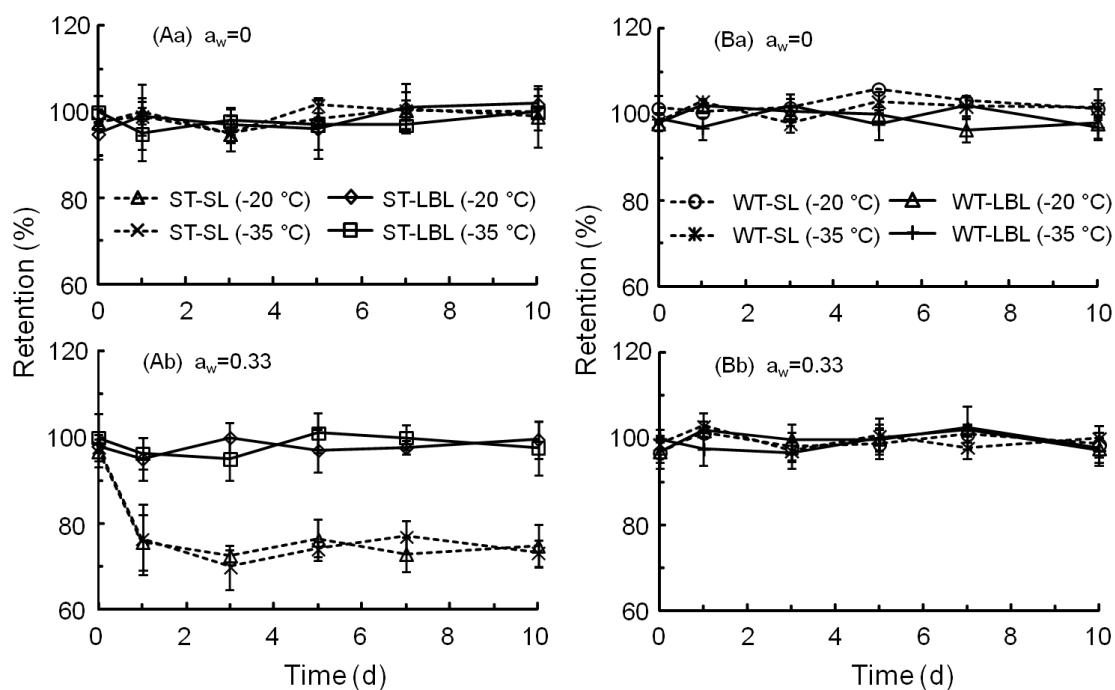


Figure 5.5 Retention (%) of α -tocopherol in freeze-dried ST-LBL and ST-SL systems at $a_w=0$ (Aa) and $a_w=0.33$ (Ab) during storage at 55 °C, and freeze-dried WT-LBL and WT-SL systems at $a_w=0$ (Ba) and $a_w=0.33$ (Bb) during storage at 55 °C. The freeze-dried materials were prefrozen at -20 °C or at -35 °C. The freeze-dried materials were vacuum sealed and packaged hermetically to anhydrous $a_w=0$ or $a_w=0.33$ prior to storage at 55 °C.

The mean diameter of the peak distribution of the particles showed very little changes during storage of all systems at both $a_w=0$ and 0.33 at 55 °C, while the zeta-average and PDI increased significantly for systems at $a_w=0.33$, especially for ST-LBL and WT-LBL systems, indicating that the particles became increasingly polydispersed.

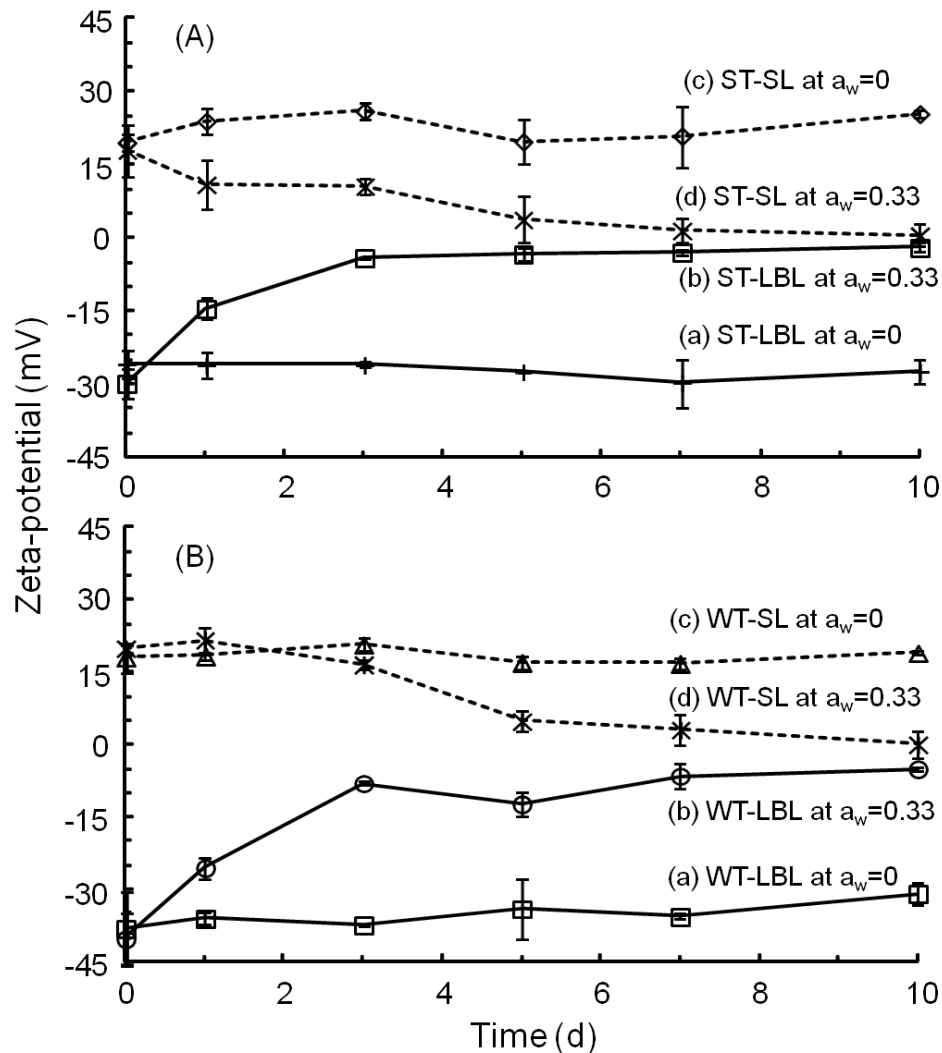


Figure 5.6 The zeta-potential (mV) of freeze-dried systems during storage at 55 °C. The systems were ST-LBL at $a_w=0$ (Aa) and $a_w=0.33$ (Ab), ST-SL at $a_w=0$ (Ac) and $a_w=0.33$ (Ad), WT-LBL at $a_w=0$ (Ba) and $a_w=0.33$ (Bb), and WT-SL at $a_w=0$ (Bc) and $a_w=0.33$ (Bd).

At $a_w=0$, a constant zeta-potential was found during 10 d of storage for ST-LBL (Figure 5.6Aa) and ST-SL (Figure 5.6Ac) systems at 55 °C. At $a_w=0.33$, both ST-LBL (Figure 5.6Ab) and ST-SL (Figure 5.6Ad) systems showed a decrease of zeta-potential approaching zero. The decrease of zeta-potential in ST-SL system during storage was possibly due to the breakdown of the protein layer around the particles as trehalose

crystallized (Figure 5.7B). In SPI LBL-trehalose systems, trehalose crystallization may only cause partial loss of ι -CAR layer and the droplets were still covered by proteins and some residual ι -CAR (Figure 5.7D). This hypothesis may explain the better stability of α -tocopherol in ST-LBL system than in ST-SL system at $a_w=0.33$ at 55 °C after trehalose crystallization (Figure 5.5B). The stability of α -tocopherol was retained in not only WT-LBL but also WT-SL systems after trehalose crystallization. The lower retention of α -tocopherol in ST-SL system was possibly because the bigger molecules of SPI assembled in a way that was more sensitive to sugar crystallization than the structure formed by small molecules of WPI at the primary layer.

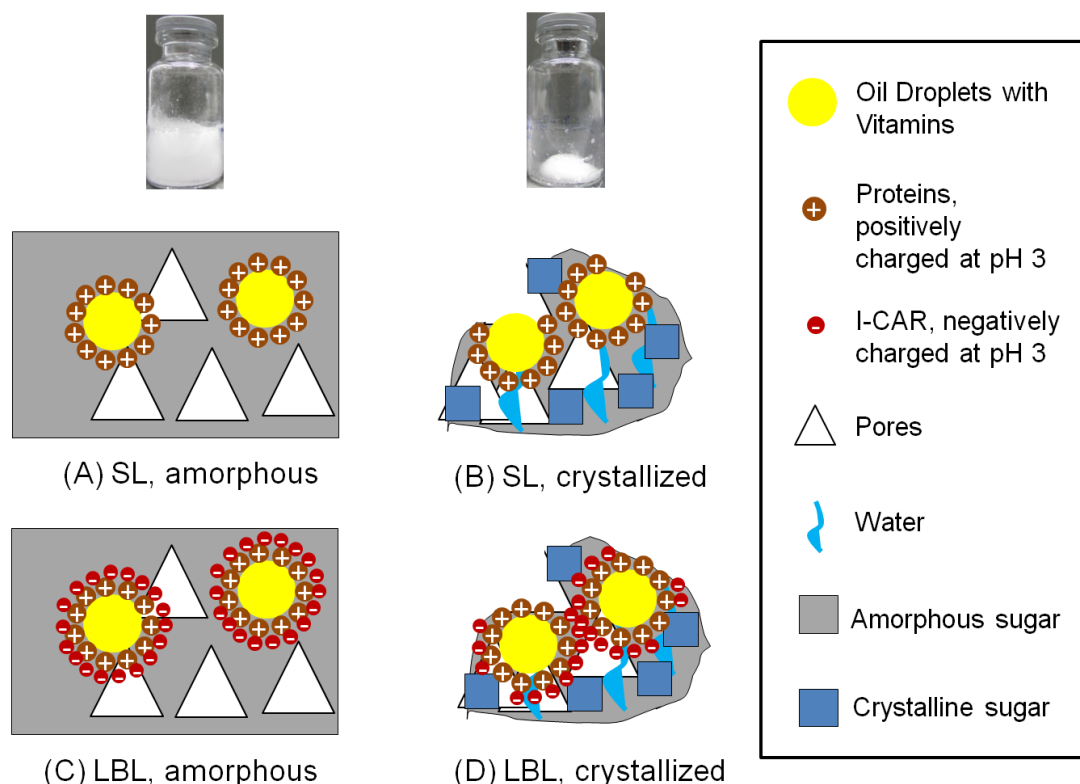


Figure 5.7 Schematic diagrams of protein-stabilized oil droplets in amorphous (A) and crystallized (B) trehalose matrices and protein- ι -CAR-stabilized oil droplets in amorphous (C) and crystallized (D) trehalose matrices. The amorphous matrices represent the freeze-dried materials at zero a_w at 55 °C and the matrices with crystallized trehalose represent the freeze-dried materials at $a_w=0.33$ at 55 °C. The inserted diagrams show the visual appearance of amorphous materials (left) and materials with crystallized trehalose (right).

5.4 CONCLUSIONS

The oil-in-water emulsions stabilized by SPI and WPI were made at various protein concentrations. Constant peak mean diameter of the particles with increasing protein contents was found for both SPI and WPI systems. SPI-stabilized particles showed bigger peak mean diameter possibly due to the larger molecular size of SPI than WPI. Layer-by-layer (LBL) emulsions were made at low protein concentration and 1:2 protein: α -CAR ratio. The properties of the primary (SL) emulsions were important in preparation of LBL emulsions. Similar freezing behavior was found for both SPI and WPI systems, but more delayed ice formation was found for WPI systems, especially at $-35\text{ }^{\circ}\text{C}$. The zeta-average of LBL systems were more sensitive to freeze-thawing than that of SL systems, while the peak mean diameter and zeta-potential of both LBL and SL systems were not significantly affected by freeze-thawing. Freeze-dried and reconstituted materials showed similar properties to the fresh emulsions.

Storage of freeze-dried ST-LBL, ST-SL, WT-LBL, and WT-SL systems at conditions that retained the glassy structures (at $a_w=0$ at $55\text{ }^{\circ}\text{C}$) resulted in full retention of α -tocopherol. At $a_w=0.33$ at $55\text{ }^{\circ}\text{C}$, which allowed the trehalose to crystallize, both WT-LBL and WT-SL systems retained 100% α -tocopherol; ST-SL system showed loss of α -tocopherol, but the stability was improved in the ST-LBL system. No differences were found between systems frozen at -20 and $-35\text{ }^{\circ}\text{C}$. Further studies are required to construct the LBL systems at higher concentration of oil. The use of other carbohydrates alone or in mixtures as structure forming materials with delayed sugar crystallization may reduce crystallization-induced structural changes and improve stability of sensitive compounds.

CHAPTER 6

General Discussion

6.1 FREEZE-DRYING OF SUGAR-BASED SYSTEMS

The present study investigated the entrapment of dispersed hydrophilic vitamins and the encapsulation of emulsified oil particles that contained hydrophobic vitamins in freeze-dried sugar-based matrices. Lactose and trehalose exist as amorphous glassy solids below their glass transition temperatures (T_g), which makes them potential glass formers in the entrapment/encapsulation of bioactive components. Freeze-drying produces amorphous sugars. Two processes are involved: (i) the pre-freezing of water and the entrapment/encapsulation of bioactive components in the solidified unfrozen solute phase (Figure 1.2A); and (ii) the retention of the solid state of the unfrozen phase with bioactive components during and after sublimation of ice crystals (Figure 1.2B). The unfrozen water during freezing or ice melting during drying may result in a water-plasticization and collapse of the structure (Roos, 1997), and possibly the release of bioactive components from the plasticized solids. A proper freeze-drying requires (i) the full solidification of the unfrozen phase, in other words, the systems need to reach a maximally freeze-concentrated state and (ii) the temperature of the solid phase should be lower than its glass transition to retain the structure during and after dehydration (Roos, 2010). For these reasons, the first parameters investigated in the present study were the glass transition temperature of the maximally freeze-concentrated sugar

solutes (T_g') and the ice melting temperature in the maximally freeze-concentrated systems (T_m'). As reported in Table 2.1, similar T_g' and T_m' were obtained for lactose and trehalose and these frozen state transitions were initial concentration-independent. Although a slightly lower T_g' was found in sugar-protein systems, the frozen state transitions in sugar-based systems were governed by the component sugars and not significantly affected by the presence of proteins (25%, w/w of total solids, Table 2.1) or hydrophilic vitamins (2.44%, w/w of total solids, Table 3.1). In the present study, maximum freeze-concentration was achieved by freezing and annealing the aqueous sugar-based systems at $-35\text{ }^\circ\text{C}$, which was below the T_m' ($-31 \pm 1\text{ }^\circ\text{C}$) but above the T_g' ($-41 \pm 1\text{ }^\circ\text{C}$) of lactose and trehalose. Freeze-drying was carried out at $p < 0.1\text{ mbar}$ with corresponding ice sublimation temperature, $T < -40\text{ }^\circ\text{C}$.

6.2 PHYSICAL PROPERTIES OF FREEZE-DRIED MATERIALS

6.2.1 Lactose and trehalose

In the present study, lactose and trehalose were used as the glass-forming materials. As pure sugars, lactose and trehalose showed similar water sorption and glass transition properties. The glass transition temperature, T_g , for anhydrous trehalose ($111\text{ }^\circ\text{C}$) was higher than that for anhydrous lactose ($105\text{ }^\circ\text{C}$), but the T_g of lactose and trehalose agreed at corresponding water activities (a_w) ranging from 0.11 to 0.44 (Table 2.4). The main difference of the sugars was their crystallization behavior. At $\geq 0.44\text{ } a_w$ at room temperature ($24 \pm 1\text{ }^\circ\text{C}$), crystallization occurred in both lactose and trehalose as indicated by sorbed water contents. Trehalose crystallized more rapidly than lactose

(Figure 2.3). The leveling off water contents after crystallization were about 3% for lactose and 10% for trehalose respectively, suggesting the formation of different types of crystals independently of a_w . These results were in agreement with Haque and Roos (2005a) for lactose and Miao and Roos (2005a) for trehalose. Haque and Roos (2005a) and Miao and Roos (2005a) confirmed using X-ray diffraction that lactose crystallized as a mixture of monohydrate and α - and β -anhydrides, but trehalose crystallized as dihydrate although the formation of anhydrate was also possible. Instant crystallization (T_{ic}) was found for lactose at 0-0.44 a_w by Differential Scanning Calorimetry (DSC). The T_{ic} decreased with increasing water content and a_w (Table 2.5). However, instant trehalose crystallization was found only at 0.44 a_w , showing lower T_{ic} than that for lactose at corresponding a_w , and no instant crystallization was present at $a_w \leq 0.33$ (Table 2.5). The absence of instant trehalose crystallization at low a_w conditions was also reported by Cardona et al. (1997). As reported in Table 2.2, at $a_w \leq 0.33$, only 6% water or less was sorbed by trehalose, which was not sufficient for trehalose to form dihydrate (about 10%). These results confirmed that water content was critical for trehalose crystallization, and the presence of sufficient amount of water to form trehalose dihydrate was required (Cardona et al., 1997; Iglesias and Chirife, 1997).

6.2.2 Sugars in mixture systems

6.2.2.1 *Water sorption*

Water sorption occurs in the hydrophilic solids phase. Different water sorption was found for sugar-based mixture systems compared to pure sugars. For instance, water

sorption was faster and the amount of sorbed water was higher in sugar-protein (3:1, w/w) systems than in pure sugar systems at low a_w (Figure 2.2) as a result of the higher water sorption of proteins. The effects of proteins on water sorption could be decreased when oil was present in the mixture systems (Figure 4.1). Some of the proteins were located at hydrophilic-hydrophobic interfaces, which decreased the amount of proteins in the continuous hydrophilic sugar-protein phase. In sugar-vitamin (2.44% of hydrophilic vitamins, w/w), water sorption was faster but the amount of sorbed water was slightly lower than in pure sugar systems at corresponding a_w condition. This shift of water sorption could be attributed to the individual water sorption behavior of each component and/or the interactions between sugar and other components (Haque and Roos, 2005a).

6.2.2.2 *Glass transition*

Haque and Roos (2005a) used lactose-protein (3:1, w/w) and Silalai and Roos (2010) used milk powders (lactose-based systems with various contents of milk protein concentrate) to study the glass transition behavior of these mixture systems using DSC. It appeared that the lactose-based mixture systems showed higher T_g than that of pure lactose in anhydrous systems, suggesting some miscibility of lactose and proteins. This was confirmed in the present study as higher anhydrous T_g was found for both lactose-protein (3:1, w/w) and trehalose-protein (3:1, w/w) systems compared with the T_g of the corresponding sugar (Table 2.4). Moreover, the proteins with higher molecular weight (soy proteins) showed more effect than the proteins with lower molecular weight (milk

proteins) on the T_g of sugar-based mixture systems (Table 2.4 and Figure 2.1). However at $a_w > 0$, the lactose-protein and trehalose-protein systems showed similar T_g to that of corresponding sugar at each a_w condition and the effects of different proteins were negligible (Figure 2.5). It should be noted that the water contents of the sugar and sugar-based systems at each a_w differed as a result of differences in water sorption of the proteins (Table 2.2). That means the T_g for each mixture system at the same a_w corresponded to a different water content. This was also in agreement with results of Haque and Roos (2005a) and Silalai and Roos (2010) that in water-plasticized systems, the T_g of lactose-based mixture systems followed closely the T_g of pure lactose at all corresponding a_w conditions. This a_w -dependence of T_g in sugar-protein systems could be attributed to the dominant effect of sugar on the glass transition at each level of water plasticization in sugar-protein systems, as suggested by Silalai and Roos (2010). The effects of proteins on glass transition of sugars in anhydrous systems could be explained by the interactions between components at molecular level. There is intermolecular hydrogen bonding between the sugar molecules and proteins as found using Fourier transform infrared spectroscopy (FTIR) (Allison et al., 1999 and Souillac et al., 2002), but the amount of hydrogen bonding (level of interaction) between sugars and proteins is often limited, above which sugars and proteins exist as free components without interactions (Imamura et al., 2001). These results suggested a partial miscibility of lactose and trehalose with proteins. The variations of the anhydrous T_g in the presence of different proteins (milk proteins or soy proteins) indicated differences in miscibility with sugars. The minor effects of proteins on the glass transition of sugars in water-plasticized systems indicated that the interactions between sugars and proteins could be diminished in the presence of water. Since the glass transition occurred only in

the non-fat solids, the presence of oil particles was not found to affect the glass transition in mixture systems. In contrast, a system containing miscible components showed glass transition of the mixture and each component contributed to the T_g of the system, such as lactose-salt (Omar and Roos, 2007) and lactose (in milk solids)-maltodextrin (Silalai and Roos, 2011).

The present study also found that a level of 2.44% (w/w) vitamins in lactose and trehalose systems showed plasticizing effects on the anhydrous T_g of sugars (Table 3.5). However, this level of addition was relatively low, and the plasticizing effects of vitamins were diminished with increasing amount of water at 0.11 to 0.44 a_w (Table 3.5 and Figure 3.4) and the effects of water as a plasticizer (Slade and Levin, 1991) dominated at $a_w > 0$.

6.2.2.3 *Sugar crystallization in mixture systems*

Sugar crystallization in pure and mixture systems occurred during isothermal storage at $a_w \geq 0.44$ (Figure 2.3, Figure 3.2 and 3.3, Figure 4.1) as a result of water sorption, which depressed the T_g of the systems to below the ambient temperature. The rate of crystallization was suggested to follow the temperature difference between storage temperature and the glass transition ($T-T_g$) (Roos and Karel, 1990). That means the lower the T_g in systems at higher a_w resulted in a larger $T-T_g$ and faster sugar crystallization, as confirmed by the faster sugar crystallization at 0.76 a_w than at 0.65 a_w in the present study. However, the T_g was not the only factor controlling sugar crystallization, especially in mixture systems. Delayed sugar crystallization was found

in the presence of hydrophilic vitamins (Figure 3.2 and 3.3), proteins (Figure 2.3), and oil particles (Figure 4.1), although these sugar-based mixture systems showed similar T_g to that for pure sugars at the same a_w conditions as discussed above. A study by Mazzobre and Buera (1999) showed that the lower T_g in freeze-dried trehalose-salt systems than in pure trehalose system did not increase the rate of trehalose crystallization as expected and a delayed trehalose crystallization was observed in the presence of salts. These results suggested that components other than sugars restricted the diffusion of sugar molecules to nucleation and the crystal growth via direct interactions with sugars (hydrophilic vitamins and proteins) and/or the presence as physical barriers (proteins and oil particles). In the present study, the rate of sugar crystallization was different although the same amount of each vitamin was mixed with sugars (w/w) (Figure 3.2 and 3.3). We attributed the more delaying effect by ascorbic acid than by thiamine hydrochloride to the lower molar ratio between sugar and ascorbic acid (20:1; while 40:1 for thiamine hydrochloride), which means there were twice as many ascorbic acid in comparison to thiamine hydrochloride molecules per mole of sugar (Table 3.3). The effects of molar ratio were in agreement with the results by Barham et al. (2006b). They studied the crystallization of lactose in the presence of CaCl_2 at various lactose:salt ratio (2:1, 4:1, and 9:1) and the most delayed lactose crystallization was found in system at 2:1 ratio. As reported by Haque and Roos (2004b), lactose crystallization was delayed in the presence of various proteins and the delaying effects were $\text{WPI} < \text{albumin} < \text{gelatin} = \text{sodium caseinate}$. They suggested the more delaying effects of gelatin and sodium caseinate to the greater extent of interactions with lactose. In the present study, although trehalose as a pure sugar crystallized more rapidly than lactose, trehalose crystallization was more delayed than

lactose crystallization in the presence of proteins. This could be an indication of the possible interactions of sugars, especially trehalose, with proteins, since sugars were found to preserve the structure of proteins via hydrogen bonding and trehalose showed better preserving ability among all sugars (Crowe et al., 1993; Allison et al., 1999; Ohtake and Wang, 2011). However, the delaying effects of proteins on sugar crystallization were only partially due to sugar-protein interactions, because sugars and proteins were suggested to exist as free components (but not necessarily complete immiscible) without significant interactions at increasing a_w . The two types of proteins used in the present study differed significantly in molecular weight (Figure 2.1). The delaying effect was found to be more severe by low molecular weight proteins (casein) than high molecular weight proteins (soy proteins) (Figure 2.3). The most delayed sugar crystallization was found in sugar-protein-oil systems (Figure 4.1). This indicated that the delaying effects were not necessarily through direct interactions between components with sugars, as the presence of hydrophobic phase could also hinder the movement of sugar molecules by disturbing the continuous hydrophilic sugar-protein phase and change the environments around sugar molecules.

The delayed sugar crystallization could also be observed from the higher T_{ic} in the mixture systems (Table 2.5). It should be noted that although the amount of water was higher in trehalose-protein systems than in pure trehalose system and seemed sufficient for trehalose to crystallize as dihydrate, no T_{ic} was found for trehalose in mixture systems at any a_w condition. These results not only suggested the restricted trehalose movement in the presence of proteins, but also confirmed the individual water sorption behavior by each component in the mixture systems.

6.3 STABILITY OF BIOACTIVE COMPONENTS

6.3.1 Hydrophilic components

6.3.1.1 *Impact of a_w and T_g*

The hydrophilic ascorbic acid and thiamine hydrochloride existed as part of the hydrophilic phase and showed plasticizing effects on the sugar matrices in the present study. Stabilization of these hydrophilic particles by amorphous sugars could be a result of direct interactions between components. Bell and White (2000) found that both a_w and T_g appeared to affect thiamine stability in amorphous Polyvinylpyrrolidone (PVP) matrices and T_g showed a larger effect. The degradation of thiamine was not inhibited below the T_g but a reduction of degradation rate was observed above the T_g only if the collapse of structure was observed. Their results suggested that glass transition, particularly the glass transition-induced collapse phenomenon, should be considered in relation to the thiamine stability. In the present study, the stability of ascorbic acid and thiamine hydrochloride was evaluated as a function of a_w . However, the increase of a_w from 0 to 0.44 did not cause significant loss of vitamins in either lactose or trehalose matrices, although a minor increase of degradation rate was observed at 0.44 a_w , which was above the critical a_w and allowed the matrices to transform into rubbery state during storage (Figure 3.7).

6.3.1.2 *Impact of sugar crystallization*

Simultaneous loss of ascorbic acid was observed with lactose crystallization (Figure 3.6) and significant increase of degradation rate was found upon sugar crystallization at

higher a_w (Figure 3.7). As shown in Figure 3.8, sugar crystallization increased the interactions between sugar molecules and the interactions between hydrophilic vitamins and sugars could be diminished, resulting in the exclusion of vitamins from the sugar phase. While both lactose and trehalose crystallization caused loss of vitamin, trehalose always retained some of the stability even after crystallization (Figure 3.7). We attributed the differences to the different crystallization behavior between lactose and trehalose (Figure 3.2 and 3.3). The higher solubility of trehalose dihydrate than lactose anhydrate (Figure 3.1) should also be considered besides the crystallization behavior itself, since the protection by trehalose was still possible as a result of the re-dissolution of trehalose crystals and the formation of viscous trehalose syrup (Figure 3.8). These results suggested that state transitions, particularly sugar crystallization, were more important than a_w in relation to the stability of hydrophilic vitamins in sugar-based systems.

6.3.2 Hydrophobic components

6.3.2.1 *Impact of a_w and T_g*

Sugars did not directly interact with the hydrophobic α -tocopherol. The α -tocopherol dissolved in oil particles were coated by proteins, which existed at the hydrophilic-hydrophobic interfaces, and the stabilization was achieved via the interactions between the proteins at interfaces and the sugars in the continuous hydrophilic phase. The degradation of α -tocopherol was not completely inhibited in the glassy state of lactose- and trehalose-based systems (Figure 4.6 and 4.7) because of the possible diffusion of

small molecules (such as oxygen) in glasses (Tromp et al., 1997; Goubet et al., 1998; Schoonman et al., 2002). However, α -tocopherol was the most stable in the absence of water (Figure 4.7). In anhydrous systems, the stability of α -tocopherol was, however, enhanced in the absence of oxygen and light, since full retention of α -tocopherol was found in systems stored under vacuum in dark (Figure 5.5). Degradation in glassy matrices was also reported for β -carotene in trehalose-based (Elizalde et al., 2002), PVP-based (Prado et al., 2006), and maltodextrin-based (Ramoneda et al., 2011) systems. Several authors reported a shifted degradation rate when glass transition of the matrices occurred. Elizalde et al. (2002), Ramoneda et al. (2011), and Harnkarnsujarit et al. (2012) found an increase of β -carotene degradation rate in the rubbery state and attributed this to the increased matrix mobility and diffusion above the T_g . In the contrast, Prado et al. (2006) found the degradation rate of β -carotene became smaller in the rubbery state when collapse of the matrices was observed, which reduced the porosity of the matrices hence the reduced diffusion. In the present study, loss of α -tocopherol was affected by a_w and followed lipid oxidation (Figure 4.7) instead of being controlled by the glass transition at a_w ranging from 0.11 to 0.44.

6.3.2.2 *Impact of sugar crystallization*

Significant loss of α -tocopherol was observed upon sugar crystallization, for instance, during storage at $a_w \geq 0.54$ at room temperature (Figure 4.7), at $a_w \geq 0.23$ ($T_g \leq 35$ °C) at 60 °C (Figure 4.8), and 0.33 a_w (T_g around 30 °C) at 55 °C (Figure 5.5). The loss of hydrophobic components was also reported for β -carotene on trehalose crystallization

(Elizalde et al., 2002) and milk fat on lactose, sucrose, and trehalose crystallization (Cerqueira et al., 2005). Sugar crystallization caused the loss the matrix structure, which not only expelled the protein-coated oil particles from the continuous hydrophilic phase, but also possibly resulted in a damaged protein structure at the interfaces hence the exposure of oil particles to the surroundings. This structural change could be proved by the change of emulsion properties as reported in Figure 4.5 for the significant broadening/change of oil particle size distribution (Cerqueira et al., 2005), and in Figure 5.6 for the decrease of positive charges (at pH 3) around the protein-covered particles.

6.3.2.3 *Impact of interface composition*

Systems containing oil particles that were coated by proteins (single layer, SL) or by proteins as the first layer and ι -carrageenan as the second layer (layer-by-layer, LBL) were studied to investigate the impact of interface composition on α -tocopherol stability. Full retention of α -tocopherol was found in both SL and LBL systems at conditions that retained the glassy structures of trehalose (Figure 5.5). At conditions that allowed trehalose to crystallize, SL and LBL systems containing WPI retained 100% α -tocopherol. However, loss of α -tocopherol was found in SL systems containing SPI, but the stability was improved in LBL systems (Figure 5.5). These results suggested the significant importance of the interface composition on the stability of hydrophobic bioactive components in crystallizing systems: (i) WPI-coated oil particles were less susceptible to sugar crystallization than SPI-coated oil particles; (ii) double layers around the oil particles provided better protection to the hydrophobic

components upon sugar crystallization. The sugar crystallization-induced damage of interface structure was found in both SL and LBL systems as suggested by the shifted emulsion properties. Although the mean particle size of the peak distribution showed little changes, the increased zeta-average and polydispersity index (PDI) indicated the broadening of oil particle size distribution. At pH 3, the protein-coated oil particles were positively charged in SL systems; the particle charge became negative after the addition of ι -carrageenan layer around the protein-coated oil particles in LBL systems. Decreases of the positive charges in SL systems and the negative charges in LBL systems towards zero net charge were observed upon sugar crystallization (Figure 5.6). These results confirmed that sugar crystallization caused a breakdown of interface structure or a detachment of the molecules from the hydrophilic-hydrophobic interfaces around oil particles as illustrated in Figure 5.7. In SL systems, sugar crystallization-induced breakdown of the protein layer exposed oil particles to surroundings, while in LBL systems, the oil particles were still protected by the protein layer when the ι -carrageenan layer was damaged (Figure 5.7D). This could be accounted to the improved α -tocopherol stability in LBL systems upon sugar crystallization.

In conclusion, sugar crystallization was responsible to the loss of hydrophobic components in dehydrated sugar-based systems. However, the extent of destabilization differed depending on the formulation of the systems in the continuous phase and at the interfaces. First, lactose crystallization caused more severe loss of α -tocopherol in the system than trehalose crystallization (Figure 4.8). The stabilizing effects from the crystallized trehalose as a result of the high solubility of trehalose dihydrate and the

formation of viscous trehalose syrup have been discussed earlier for hydrophilic components. Second, the different retention of α -tocopherol in systems containing same matrix materials but different proteins at interfaces suggested that the resistance of proteins to sugar crystallization differed, although no direct measurement of the protein structure was made. MPI was more resistant to sugar crystallization than SPI in lactose- and trehalose-based matrices (Figure 4.8) and WPI was more resistant than SPI in trehalose matrices (Figure 5.5). Third, the addition of ι -carrageenan layer to protein-coated oil particles, especially SPI-coated oil particles, significantly improved the stability of α -tocopherol upon trehalose crystallization (Figure 5.5).

6.4 OVERALL CONCLUSIONS

The present study characterized the physical properties of sugar-based matrices that could be applied to nutrient delivery systems. Experimental evidence indicated that all components in the hydrophilic phase contributed to the water sorption behavior of the mixture systems. Although interactions between components were possible, each component showed individual water sorption. The glass transition of amorphous solids in mixture systems was governed by that of the component sugar, which was slightly affected by the presence of other hydrophilic components (such as proteins and hydrophilic vitamins) but the effects became negligible with increasing water content and a_w . Crystallization of amorphous lactose and trehalose resulted in the formation of different types of crystals, which was a mixture of monohydrate and anhydrides for lactose but mainly dihydrate for trehalose. The presence of sufficient amount of water to form dihydrate was required for trehalose crystallization. Delayed sugar

crystallization was found for both sugars in the presence of proteins, hydrophilic vitamins, and hydrophobic oil particles. This delaying effect was mainly a result of the interactions between the foreign components with sugar (proteins and hydrophilic vitamins) and/or the hindered molecular movements in the presence of physical barriers (proteins and oil particles).

The present study related the stability of hydrophilic and hydrophobic bioactive components to the physical properties of the matrix materials. Sugar crystallization was the main factor that was responsible for the loss of both hydrophilic (ascorbic acid and thiamine hydrochloride) and hydrophobic (α -tocopherol) bioactive components, although the mechanism of destabilization was different. Degradation of hydrophilic vitamins was enhanced by the loss of interactions between the vitamins with the sugars upon sugar crystallization that resulted in exclusion of vitamins from the crystalline sugar phase. Degradation of hydrophobic vitamins in oil particles was not only because of the exclusion of protein-coated oil particles from the continuous sugar-based phase, but also a result of the destroyed interfaces of the emulsion structure upon sugar crystallization. The effects of sugar crystallization on the stability of hydrophobic components could be improved by the careful design of the interface composition, for example the addition of ι -carrageenan layer to the protein layer around the oil particles.

The present study suggested the use of amorphous sugar-based matrices as entrapping/encapsulating materials for the delivery of hydrophilic and hydrophobic bioactive components. However, the physical properties of the sugars, particularly sugar crystallization behavior, could significantly affect the physical stability of the delivery systems and the chemical stability of the bioactive components. Understanding

the physical behavior of the encapsulating solids is required when designing delivery systems for bioactive components.

BIBLIOGRAPHY

Aldous BJ, Auffret AD, Franks F. 1995. The crystallization of hydrates from amorphous carbohydrates. *Cryo-letters* 16(3):181-186.

Allison SD, Chang B, Randolph TW, Carpenter JF. 1999. Hydrogen bonding between sugar and protein is responsible for inhibition of dehydration-induced protein unfolding. *Archives of Biochemistry and Biophysics* 365(2):289-298.

Angell CA. 2002. Liquid fragility and the glass transition in water and aqueous solutions. *Chemical Reviews* 102: 2627–2650.

Arrese EL, Sorgentini DA, Wagner JR, Añón MC. 1991. Electrophoretic, solubility, and functional properties of commercial soy protein isolates. *Journal of Agricultural and Food Chemistry* 39:1029-1032.

Barham AS, Haque MK, Roos YH, Hodnett BK. 2006a. Crystallization of spray-dried lactose/protein mixtures in humid air. *Journal of Crystal Growth* 295:231-240.

Barham AS, Omar AME, Roos YH, Hodnett BK. 2006b. Evolution of phases and habit during the crystallization of freeze-dried lactose/salt mixture in humid air. *Crystal Growth & Design* 6(8):1975-1982.

Bell LN, White KL. 2000. Thiamin stability in solids as affected by the glass transition. *Journal of Food Science* 65(3): 498-501.

- Berlin E, Anderson BA, Pallansch MJ. 1968. Water vapor sorption properties of various dried milks and wheys. *Journal of Dairy Science* 51(9):1339-1344.
- Beristain CI, Azuara E, Vernon-Carter EJ. 2006. Effect of water activity on the stability to oxidation of spray-dried encapsulated orange peel oil using mesquite gum (*Prosopis Juliflora*) as wall material. *Journal of Food Science* 67(1):206-211.
- Bhandari BR, Datta N, Howes T. 1997. Problems associated with spray drying of sugar-rich foods. *Drying Technology* 15(2):671-684.
- Bhandari BR, Howes T. 1999. Implication of glass transition for the drying and stability of dried foods. *Journal of Food Engineering* 40(1-2):71-79.
- Bizot H. 1983. Using the "G.A.B." model to construct sorption isotherms. In: Jowitt CR, Escher F, Hallström B, Meffert HFT, Spiess WEL, Vos G editors. *Physical properties of foods*. London: Applied Science Publishers p 43-54
- Bredy JE, Holum JR. 1993. *Chemistry*. John Wiley & Sons, New York, pp. 681-702.
- Brownley Jr. CA, Lachman L. 1964. Browning of spray-processed lactose. *Journal of Pharmaceutical Science* 53 (4):452-454.
- Brunauer S, Emmett PH, Teller E. 1938. Adsorption of gases in multimolecular layers. *Journal of American Chemistry Society* 60:309-319.
- Buera P, Schebor C, Elizalde B. 2005. Effects of carbohydrate crystallization on stability of dehydrated foods and ingredient formulations. *Journal of Food Engineering* 67:157-165.

Burton GW, Ingold KU. 1986. Vitamin E: application of the principles of physical organic chemistry to the exploration of its structure and function. *Accounts of Chemical Research* 19:194-201.

Cardona S, Schebor C, Buera MP, Karel M, Chirife J. 1997. Thermal stability of invertase in reduced-moisture amorphous matrices in relation to glassy state and trehalose crystallization. *Journal of Food Science* 62(1):105-112.

Carpenter JF, Crowe JH. 1989. An infrared spectroscopic study of the interactions of carbohydrates with dried proteins. *Biochemistry* 28(9):3916-3922.

Cerdeira M, Martini S, Herrera ML. 2005. Microencapsulating properties of trehalose and of its blends with sucrose and lactose. *Journal of Food Science* 70(6):E401-408.

Chen Y-H, Aull JL, Bell LN. 1999. Solid-state tyrosinase stability as affected by water activity and glass transition. *Food Research International* 32: 469-472.

Chuy LE, Labuza TP. 1994. Caking and stickiness of dairy-based food powders as related to glass transition. *Journal of Food Science* 59:43-46.

Contreras-Guzmán E, Strong III FC. 1982. Determination of total tocopherols in grains, grain products, and commercial oils, with only slight saponification, and by a new reaction with cupric ion. *Journal of Agricultural and Food Chemistry* 30:1109-1112.

Cornacchia L, Roos YH. 2011a. Solid-liquid transitions and stability of HPKO-in-water systems emulsified by dairy proteins. *Food Biophysics* 6:288-294.

Cornacchia L, Roos YH. 2011b. Lipid and water crystallization in protein-stabilized oil-in-water emulsions. *Food Hydrocolloids* 25:1726-1736.

Cornacchia L, Roos YH. 2011c. Stability of β -carotene in protein-stabilized oil-in-water delivery systems. *Journal of Agricultural and Food Chemistry* 59: 7013-7020.

Crowe JH, Crowe LM, Carpenter JF. 1993. Preserving dry biomaterials: the water replacement hypothesis. *Biopharmaceutics* 6:28-37.

Danviriyakul S, McClements DJ, Decker E, Nawar WW, Chinachoti P. 2002. Physical stability of spray-dried milk fat emulsion as affected by emulsifiers and processing conditions. *Journal of Food Science* 67(6):2183-2189.

Davies MB, Austin J, Partridge DA. 1991. Vitamin C. Its chemistry and biochemistry. The Royal Society of Chemistry.

Dennison DB, Kirk JR. 1978. Oxygen effect on the degradation of ascorbic acid in a dehydrated food system. *Journal of Food Science*. 43: 609-612, 618.

Dennison DB, Kirk JR. 1982. Effect of trace mineral fortification on the storage stability of ascorbic acid in a dehydrated model food system. *Journal of Food Science* 47: 1198-1200.

Dennison D, Kirk J, Bach J, Kokoczka P, Heldman D. 1977. Storage stability of thiamin and riboflavin in a dehydrated food system. *Journal of Food Processing and Preservation* 1(1):43-54.

Desai KGH, Park HJ. 2005. Recent development in microencapsulation of food ingredients. *Drying Technology* 23:1361-1394.

Dickinson E. 1992. Introduction to food colloids. Oxford, U.K.:Oxford University Press.

Dickinson E. 1998. Stability and rheological implications of electrostatic milk protein-polysaccharide interactions. *Trends Food Science & Technology* 9:347-354.

Dickinson E. 2001. Milk protein interfacial layers and the relationship to emulsion stability and rheology. *Colloids and Surfaces. B* 20:197-210.

Dickinson E. 2003. Hydrocolloids at interfaces and the influence on the properties of dispersed systems. *Food Hydrocolloids* 17:25-39.

Dickinson E, Euston SR. 1991. Stability of food emulsions containing both protein and polysaccharide, in *Food Polymers, gels and colloids*, ed. by Dickinson E. Royal Society of Chemistry, Cambridge, UK, pp. 132-146.

Dickinson E, Pawlowsky K. 1997. Effect of ι -carrageenan on flocculation, creaming, and rheology of a protein-stabilized emulsion. *Journal of Agricultural and Food Chemistry* 45:3799-3806.

Dinç E, Kökdil G, Onur F. 2000. A comparison of matrix resolution method, ratio spectra derivative spectrophotometry and HPLC method for the determination of thiamine HCl and pyridoxine HCl in pharmaceutical preparation. *Journal of Pharmaceutial and Biomedical Analysis* 22: 915-923.

Doyon L, Smyrl TG. 1983. Interaction of thiamine with reducing sugars. *Food Chemistry* 12:127-133.

Drusch S, Serfert Y, Heuvel AVD, Schwarz K. 2006. Physicochemical characterization and oxidative stability of fish oil encapsulated in an amorphous matrix containing trehalose. *Food Research International* 39:807-815.

Dziezak JD. 1988. Microencapsulation and encapsulated ingredients. *Food Technology* 42:136-151.

Elizalde BE, Herrera ML, Buera MP. 2002. Retention of β -carotene encapsulated in a trehalose-based matrix as affected by water content and sugar crystallization. *Journal of Food Science* 67(8):3039-3045.

Farias, MC, Moura ML, Andrade L, Leão MHMR. 2007. Encapsulation of the alpha-tocopherol in a glassy food model matrix. *Material Research* 10(1):57-62.

Fäldt P, Bergenståhl B. 1996a. Spray-dried whey protein/lactose/soybean oil emulsions. 1. Surface composition and particle structure. *Food Hydrocolloids* 10(4):421-429.

Fäldt P, Bergenståhl B. 1996b. Spray-dried whey protein/lactose/soybean oil emulsions. 2. Redispersibility, wettability and particle structure. *Food Hydrocolloids* 10(4):431-439.

Fennema OR. 1977. Loss of vitamins in fresh and frozen foods. *Food Technology* 31(12):32-36.

Flink JM. 1972. Retention of 2-propanol at low concentration by freeze-drying carbohydrate solutions. *Journal of Food Science*, 37:617-618.

Flink J, Karel M. 1970. Retention of organic volatiles in freeze-dried solutions of carbohydrates. *Journal of Agricultural and Food Chemistry* 18(2):295-297.

Flink J, Karel M. 1972. Mechanisms of retention of organic volatiles in freeze-dried systems. *Journal of Food Technology* 7:199-211.

Frankel EN, Huang S-W, Kanner J, German JB. 1994. Interfacial phenomena in the evaluation of antioxidants: bulk oils vs emulsions. *Journal of Agricultural and Food Chemistry* 42:1054-1059.

Gordon M, Taylor JS. 1952. Ideal copolymers and the second-order transitions of synthetic rubbers, I. Non-crystalline copolymers. *Journal of Applied Chemistry* 2:493-500.

Goubet I, Le Quere JL, Voilley AJ. 1998. Retention of aroma compounds by carbohydrates: influence of their physicochemical characteristics and of their physical state. A review. *Journal of Agricultural and Food Chemistry* 46:1981-1990.

Grattard N, Salaün F, Champion D, Roudaut G, Le Meste M. 2002. Influence of physical state and molecular mobility of freeze-dried maltodextrin matrices on the oxidation rate of encapsulated lipids. *Journal of Food Science* 67(8):3002-3010.

Green BK, Scheicher L. 1955. Pressure sensitive record materials. US Patent no. 2, 217, 507, Ncr C.

Gu YS, Decker EA, McClements DJ. 2004. Influence of pH and κ -carrageenan concentration on physicochemical properties and stability of β -lactoglobulin-stabilized oil-in-water emulsions. *Journal of Agricultural and Food Chemistry* 52:3626-32.

Hancock BC, Zografi G. 1997. Characteristics and significance of the amorphous state in pharmaceutical systems. *Journal of Pharmaceutical Science* 86 (1):1-12.

Haque K, Roos YH. 2004a. Water plasticization and crystallization of lactose in spray-dried lactose/protein mixtures. *Journal of Food Science* 69(1):23-29.

- Haque MK, Roos YH. 2004b. Water sorption and plasticization behavior of spray-dried lactose/protein mixtures. *Journal of Food Engineering* 69(8):384-391.
- Haque MK, Roos YH. 2005a. Crystallization and X-ray diffraction of spray-dried and freeze-dried amorphous lactose. *Carbohydrate Research* 340:293-301.
- Haque MD, Roos YH. 2005b. Crystallization and X-ray diffraction of crystals formed in water-plasticized amorphous spray-dried and freeze-dried lactose/protein mixtures. *Journal of Food Science* 70(5):359-366.
- Haque MK, Roos YH. 2006. Differences in the physical state and thermal behavior of spray-dried and freeze-dried lactose and lactose/protein mixtures. *Innovative Food Science & Emerging Technologies* 7(1-2):62-73.
- Harnkarnsujarit N, Charoenrein S, Roos, YH. 2012. Porosity and water activity effects on stability of crystalline β -carotene in freeze-dried solids. *Journal of Food Science* 77(11):E313-320.
- Hewavitharana AK, van Brakel AS, Harnett M. 1996. Simultaneous liquid chromatographic determination of vitamins A, E and β -carotene in common dairy foods. *International Dairy Journal* 6: 613-624.
- Hodge JE. 1953. Chemistry of browning reactions in model systems. *Journal of Agricultural and Food Chemistry* 1 (15): 928-943.
- Hunziker OF, Nissen BH. 1926. Lactose solubility and lactose crystal formation. *Journal of Dairy Science* 9 (6):517-537.

- Iglesias H, Buera MP, Chirife J. 1997. Water sorption isotherm of amorphous trehalose. *Journal of the Science of Food and Agriculture* 75:183-186.
- Imamura K, Iwai M, Ogawa T, Sakiyama T, Nakanishi K. 2001. Evaluation of hydration states of protein in freeze-dried amorphous sugar matrix. *Journal of Pharmaceutical Sciences* 90(12):1955-1963.
- Johari GP, Hallbrucker A, Mayer E. 1987. The glass-liquid transition of hyperquenched water. *Nature* 330:552-553.
- Jouppila K, Roos YH. 1994a. Glass transition and crystallization in milk powders. *Journal of Dairy Science* 77(10):2907-2915.
- Jouppila K, Roos YH. 1994b. Water sorption and time-dependent phenomena of milk powders. *Journal of Dairy Science* 77(7):1798-1808.
- Jouppila K, Kansikas J, Roos YH. 1997. Glass transition, water plasticization, and lactose crystallization in skim milk powder. *Journal of Dairy Science* 80(12):3125-3160.
- Kalichevsky MT, Blanshard JMV. 1993. The effect of fructose and water on the glass transition of amylopectin. *Carbohydrate Polymers* 20:107-113.
- Kamal-Eldin A, Mäkinen M, Lampi A-M, Hopia A. 2002. A multivariate study of α -tocopherol and hydroperoxide interaction during the oxidation of methyl linoleate. *European Food Research and Technology* 214:52-57.

- Kanner J, Hartel S, Mendel H. 1979. Content and stability of α -tocopherol in fresh and dehydrated pepper fruits (*Capsicum annuum* L.). *Journal of Agricultural and Food Chemistry* 27(6):1316-1318.
- Kaushik V, Roos YH. 2007. Limonene encapsulation in freeze-drying of gum Arabic-sucrose-gelatin systems. *LWT* 40:1381-1391.
- Kaushik V, Roos YH. 2008. Lipid encapsulation in glassy matrices of sugar-gelatin systems in freeze-drying. *International Journal of Food Properties* 11:363-378.
- Keerati-u-rai M, Miriani M, Iametti S, Bonomi F, Corredig M. 2012. Structural changes of soy proteins at the oil-water interface studied by fluorescence spectroscopy. *Colloids and Surfaces B* 93(1):41-48.
- King CJ. 1972. Freeze drying. In: *Food dehydration 2nd edn, Vol. 1*. Ed. By van Arsdel WB, Copley MJ, Morgon Jr AI. AVI Publ. Co., Westport, Conn.
- Kinsella JE. 1979. Functional properties of soy proteins. *Journal of American Oil Chemist's Society* 56:242-258.
- Labuza TP. 1968. Sorption phenomena in foods. *Food Technology* 22:263-272.
- Labuza TP. 1980. The effect of water activity on reaction kinetics in food deterioration. *Food Technology* 34(4):36-41.
- Labuza TP, Kaanane A, Chen JY. 1985. Effect of temperature on the moisture sorption isotherms and water activity shift of two dehydrate foods. *Journal of Food Science* 50:385-391.

Labuza TP, Kamman JF. 1982. Comparison of stability of thiamine salts at high temperature and water activity. *Journal of Food Science* 47:664-665.

Labuza TP, McNally L, Gallagher D, Hawkes J, Hurtado F. 1972. Stability of intermediate moisture foods. 1. Lipid oxidation. *Journal of Food Science* 37:154-159.

Labuza TP, Tannenbaum ST, Karel M. 1970. Water content and stability of low-moisture and intermediate-moisture foods. *Food Technology* 24(5):35-42.

Lai H-M, Schmidt SJ. 1990. Lactose crystallization in skim milk powder observed by hydrodynamic equilibria, scanning electron microscopy and ²H nuclear magnetic resonance. *Journal of Food Science* 55(4):994-999.

Laing BM, Schlueter DL, Labuza TP. 1978. Degradation kinetics of ascorbic acid at high temperature and water activity. *Journal of Food Science* 43:1440-1443.

Lammert AM, Schmidt SJ, Day GA. 1998. Water activity and solubility of trehalose. *Food Chemistry* 61 (1-2):139-144.

Lea CH, Ward RJ. 1959 Relative activities of the seven tocopherols. *Journal of the Science of Food and Agriculture* 10:537-548.

Lee SH, Labuza TP. 1975. Destruction of ascorbic acid as a function of water activity. *Journal of Food Science* 40:370-373.

Levi G, Karel M. 1995. The effect of phase transitions on release of n-propanol entrapped in carbohydrate glasses. *Journal of Food Engineering* 24:1-13.

Levine H, Slade L. 1986. A polymer physico-chemical approach to the study of commercial starch hydrolysis products (SHPs). *Carbohydrate Polymer* 6(3): 213-244.

Levine H, Slade L. 1988. Principles of “cryostabilization” technology from structure/property relationships of carbohydrate/water systems-A review. *Cryo-Letter* 9:21-63.

Livney YD, Schwan AL, Dalglish DG. 2004. A study of β -casein tertiary structure by intramolecular crosslinking and mass spectrometry. *Journal of Dairy Science* 87(11):3638-3647.

López-Díez EC, Bone S. 2004. The interaction of trypsin with trehalose: an investigation of protein preservation mechanisms. *Biochimica et Biophysica Acta* 1673:139-148.

Madene A, Jacquot M, Scher J, Desobry S. 2006. Flavour encapsulation and controlled release-a review. *International Journal of Food Science and Technology* 41:1-21.

Malvern Instrument Ltd.. 2004. Zetasizer Nano Series User Manual (MAN0317), Issue 2.1.

Mazzobre MF, Buera MDP. 1999. Combined effects of trehalose and cations on the thermal resistance of β -galactosidase in freeze-dried systems. *Biochimica et Biophysica Acta* 1473:337-344.

Mazzobre MF, Soto G, Aguilera JM, Buera MP. 2001. Crystallization kinetics of lactose in systems co-lyophilized with trehalose. Analysis by differential scanning calorimetry. *Food Research International* 34:903-911.

McClements DJ. 2002. Modulation of globular protein functionality by weakly interacting cosolvents. *Critical Reviews in Food Science and Nutrition* 42(5):417-471.

McClements DJ. 2004. Protein-stabilized emulsions. *Current Opinion in Colloid & Interface Science* 9(6):305-313.

McClements DJ. 2005. *Food emulsions: principles, practice, and techniques*. 2nd ed. Boca Raton, Fla.:CRC Press.

McClements DJ, Decker EA, Weiss J. 2007. Emulsion-based delivery systems for lipophilic bioactive components. *Journal of Food Science* 72(8):R109-124.

McClements DJ, Decker EA, Park Y, Wess J. 2009. Structural design principles for delivery of bioactive components in nutraceuticals and functional foods. *Critical Reviews in Food Science and Nutrition* 49(6):577-606.

Miao S, Roos YH. 2005a. Crystallization kinetics and X-ray diffraction of crystals formed in amorphous lactose, trehalose, and lactose/trehalose mixtures. *Journal of Food Science* 70(5):350-358.

Miao S, Roos YH. 2005b. Non-enzymatic browning kinetics in low-moisture food systems as affected by matrix composition and crystallization. *Journal of Food Science* 70(2):69-77.

Millqvist-Fureby A, Malmsten M, Bergenståhl B. 1999. Surface characterization of freeze-dried protein/carbohydrate mixtures. *International Journal of Pharmaceutics* 191:103-114.

- Moreau L, Kim H-J, Decker EA, McClements DJ. 2003. Production and characterization of oil-in-water emulsions containing droplets stabilized by β -lactoglobulin-pectin membranes. *Journal of Agricultural and Food Chemistry* 51:6612-6617.
- Mun S, Cho Y, Decker EA, McClements DJ. 2008. Utilization of polysaccharide coatings to improve freeze-thaw and freeze-dry stability of protein-coated lipid droplets. *Journal of Food Engineering* 86:508-518.
- Nasirpour A, Landillon V, Cuq B, Scher J, Banon S, Desobry S. 2007. Lactose crystallization delay in model infant foods made with lactose, β -lactoglobulin, and starch. *Journal of Dairy Science* 90:3620-3626.
- Ohtake S, Wang YJ. 2011. Trehalose: current use and future applications. *Journal of Pharmaceutical Sciences* 100(6):2020-2053.
- Omar AME, Roos YH. 2007. Glass transition and crystallization behavior of freeze-dried lactose-salt mixtures. *LWT* 40:536-543.
- O'Regan J, Mulvihill DM. 2010. Sodium caseinate-maltodextrin conjugate stabilized double emulsions: encapsulation and stability. *Food Research International* 43:224-231.
- Özkan N, Walisinghe N, Chen XD. 2002. Characterization of stickiness and cake formation in whole and skim milk powders. *Journal of Food Engineering* 55:293-303.
- Pachapurkar D, Bell LN. 2005. Kinetics of thiamine degradation in solutions under ambient storage conditions. *Journal of Food Science* 70 (7):423-426.

Park JM, Muhoberac BB, Dubin PL, Xia J. 1992. Effects of protein charge heterogeneity in protein-polyelectrolyte complexation. *Macromolecules* 25:290-295.

Petersen EE, Lorentzen J, Flink J. 1973. Influence of freeze-drying parameters on the retention of flavour compounds of coffee. *Journal of Food Science* 38:119-122.

Porter WL, Black ED, Drolet AM. 1989. Use of polyamide oxidative fluorescence test on lipid emulsions: contrast in relative effectiveness of antioxidants in bulk versus dispersed systems. *Journal of Agricultural and Food Chemistry* 37: 615-624.

Prado SM, Buera MP, Elizalde BE. 2006. Structural collapse prevents β -carotene loss in a supercooled polymeric matrix. *Journal of Agricultural and Food Chemistry* 54:79-85.

Proot P, de Pourcq L, Raymarkers AA. 1994. Stability of ascorbic acid in a standard total parenteral nutrition mixture. *Clinical Nutrition* 13:273-279.

Ramonedá XA, Ponce-Cevallos PAP, Buera MP, Elizalde BE. 2011. Degradation of β -carotene in amorphous polymer matrices. Effects of water sorption properties and physical state. *Journal of the Science of Food and Agriculture* 91:2587-2593.

Riejtens IMCM, Boersma MG, de Haan L, Spenkeliink B, Awad HM, Cnubben NHP, van Zanden JJ, van der Woude H, Alink GM, Koeman JH. 2002. The pro-oxidant chemistry of the natural antioxidants vitamin C, vitamin E, carotenoids and flavonoids. *Environmental Toxicology and Pharmacology* 11: 321-333.

Risch SJ. 1995. Encapsulation: overview of uses and techniques. In Encapsulation and controlled release of food ingredients. Ed. Risch SJ and Reineccius GA. American Chemical Society. Chapter 1, pp 2-7.

Roos YH. 1993. Water activity and physical state effects on amorphous food stability. *Journal of Food Processing and Preservation* 16:433-447.

Roos. YH. 1995. Phase transitions in foods. San Diego: Academic Press. 360p.

Roos YH. 1997. Frozen state transitions in relation to freeze-drying. *Journal of Thermal Analysis* 48:535-544.

Roos YH. 2003. Thermal analysis, state transitions and food quality. *Journal of Thermal Analysis and Calorimetry* 71:193-199.

Roos YH. 2010. Glass transition temperature and its relevance in food processing. *Annual Review of Food Science and Technology* 1:469-496.

Roos YH, Himberg M-J. 1994. Nonenzymatic browning behavior, as related to glass transition, of a food model at chilling temperatures. *Journal of Agricultural and Food Chemistry* 42:893-898.

Roos Y, Karel M. 1990. Differential scanning calorimetry study of phase transitions affecting the quality of dehydrated materials. *Biotechnology Progress* 6(2):159-163.

Roos YH, Karel M. 1991a. Applying state diagrams to food processing and development. *Food Technology* 45(12):66, 68-71, 107.

Roos YH, Karel M. 1991b. Water and molecular weight effects on glass transitions in amorphous carbohydrates and carbohydrate solutions. *Journal of Food Science* 56:1676-1681.

Roos YH, Karel M. 1991c. Nonequilibrium ice formation in carbohydrate solutions. *Cryo-letters* 12:367-376.

Roos YH, Karel M. 1991d. Plasticizing effect of water on thermal behavior and crystallization of amorphous food models. *Journal of Food Sciences* 56:38-43.

Roos YH, Karel M. 1991e. Phase transitions of mixtures of amorphous polysaccharides and sugars. *Biochemical Progress* 7(1):49-53.

Roos Y, Karel M. 1992. Crystallization of amorphous lactose. *Journal of Food Science* 57:775-777.

Roudaut G, Simatos D, Champion D, Contreras-Lopez E, Le Meste M. 2004. Molecular mobility around the glass transition temperature: a mini review. *Innovative Food Science & Emerging Technologies* 5:127-134.

Santivarangkna C, Aschenbrenner M, Foerst P. 2011. Role of glassy state on stabilities of freeze-dried probiotics. *Journal of Food Science* 76(8):152-156.

Saito H, Kawagishi A, Tanaka M, Tanimoto T, Okada S, Komatsu H, Handa T. 1999. Coalescence of Lipid Emulsions in Floating and Freeze-Thawing Processes: Examination of the Coalescence Transition State Theory. *Journal of Colloid and Interface Science* 219(1):129-134.

- Schebor C, Mazzobre MF, Buera MP. 2010. Glass transition and time-dependent crystallization behavior of dehydration bioprotectant sugars. *Carbohydrate Research* 345:303-308.
- Schoonman A, Ubbink J, Bisperink C, Le Mester M, Karel M. 2002. Solubility and diffusion of nitrogen in maltodextrin/protein tablets. *Biotechnology Progress* 18:139-154.
- Slade L, Levine H. 1991. Beyond water activity: recent advances based on an alternative approach to the assessment of food quality and safety. *Critical Reviews in Food Science and Nutrition* 30:115-360.
- Silalai N, Roos, YH. 2010. Roles of water and solids composition in the control of glass transition and stickiness of milk powders. *Journal of Food Science* 75(5):285-296.
- Silalai N, Roos YH. 2011. Mechanical α -relaxations and stickiness of milk solids/maltodextrin systems around glass transition. *Journal of the Science of Food and Agriculture* 91:2529-2536.
- Singh KJ, Roos YH. 2006. State transitions and freeze concentration in trehalose-protein-cornstarch mixtures. *LWT* 39:930-938.
- Singh KJ, Roos YH. 2007. Frozen state transitions in freeze-concentrated lactose-protein-cornstarch systems. *International Journal of Food Properties* 10:577-587.
- Souillac PO, Costantino HR, Middaugh CR, Rytting JH. 2002. Investigation of protein/carbohydrate interactions in the dried state. 1. calorimetric studies. *Journal of Pharmaceutical Science* 91(1):206-216.

- Surana R, Pyne A, Suryanarayanan R. 2004. Effect of aging on the physical properties of amorphous trehalose. *Pharmaceutical Research* 21(5):867-874.
- Taylor LS, Zografi G. 1998. Sugar-polymer hydrogen bond interactions in lyophilized amorphous mixtures. *Journal of Pharmaceutical Sciences* 87(12):1615-1621.
- Thanh VH, Shibasaki K. 1978. Major protein soybean seeds. Subunits structure of β -conglycinin. *Journal of Agricultural and Food Chemistry* 26(3):692-695.
- Thijssen HAC, Rulkens WH. 1968. *De Ingenieur*. 80(47):45.
- Thijssen HAC, Rulkens WH. 1969. In: *Symp. On Thermodynamic properties of freeze-drying*. International Institute of Refrigeration, Lausanne, Switzerland.
- Thijssen HAC. 1971. Flavour retention in drying pre-concentrated food liquids. *Journal of Applied Chemistry & Biotechnology* 21:372-377.
- Tromp RH, Parker R, Ring SF. 1997. Water diffusion in glasses of carbohydrates. *Carbohydrate Research* 303:199-205.
- Tsourouflis S, Flink JM, Karel M. 1976. Loss of structure in free-dried carbohydrate solutions: effect of temperature, moisture content and composition. *Journal of the Science of Food and Agriculture* 27:509-519.
- Ubbink J, Krüger J. 2006. Physical approaches for the delivery of active ingredients in foods. *Trends in Food Science & Technology*. 17:244-254.
- Uddin MS, Hawlader MNA, Ding L, Mujumdar AS. 2002. Degradation of ascorbic acid in dried guava during storage. *Journal of Food Engineering*. 51:21-26.

Valenzuela A, Sanhueza J, Nieto S. 2002. Differential inhibitory effect of α -, β -, γ -, and δ -tocopherols on the metal-induced oxidation of cholesterol in unilamellar phospholipid-cholesterol liposomes. *Journal of Food Science* 67(6):2051-2055.

Vanapalli SA, Palanuwech J, Coupland JN. 2002. Stability of emulsions to dispersed phase crystallization: effect of oil type, dispersed phase volume fraction, and cooling rate. *Colloids and Surfaces A* 204:227-237.

Vega C, Goff H, Roos YH. 2005. Spray drying of high-sucrose dairy emulsions: feasibility and physicochemical properties. *Journal of Food Science* 70(3):244-251.

Vega C, Goff HD, Roos YH. 2007. Casein molecular assembly affects the properties of milk fat emulsions encapsulated in lactose or trehalose matrices. *International Dairy Journal* 17:683-695.

de Vos P, Fass MM, Spasojevic M, Sikkema J. 2010. Encapsulation for preservation of functionality and targeted delivery of bioactive food components. *International Dairy Journal* 20:292-302.

White GW, Cakebread SH. 1966. The glassy state in certain sugar-containing food products. *International Journal of Food Science & Technology* 1(1):73-82.

Widicus WA, Kirk JR, Gregory JF. 1980. Storage stability of α -tocopherol in a dehydrated model food system containing no fat. *Journal of Food Science* 45:1015-1018.

Widicus WA, Kirk JR. 1981. Storage stability of α -tocopherol in a dehydrated model food system containing methyl linoleate. *Journal of Food Science*. 46:813-816.

Wilson N, Shah NP. 2007. Microencapsulation of vitamins. *ASEAN Food Journal*. 14:1-14.

Woychik JH. 1965. Preparation and properties of reduced κ -casein. *Archives of Biochemistry and Biophysics* 109(3):542-547.

Zingg J-M, Azzi A. 2004. Non-antioxidant activities of vitamin E. *Current Medical Chemistry* 11(9):1113-1133.

PUBLICATIONS

Journal Papers

1. Y Zhou, YH Roos. 2011. Characterization of carbohydrate-protein matrices for nutrient delivery. *Journal of Food Science*. 76(4): 368-376.
2. Y Zhou, YH Roos. 2012. Stability and plasticizing and crystallization effects of vitamins in amorphous sugar systems. *Journal of Agricultural and Food Chemistry*. 60(4):1075-1083.
3. Y Zhou, YH Roos. 2012. Stability of α -tocopherol in freeze-dried sugar-protein-oil emulsion solids as affected by water plasticization and sugar crystallization. *Journal of Agricultural and Food Chemistry*. 60(30):7497-7505.
4. Y Zhou, YH Roos. Double interface formulation for improved α -tocopherol stabilization in dehydration of emulsions. *Journal of the Science of Food and Agriculture*. In Press.

Conference Abstracts

1. Y Zhou, YH Roos. 2009. State transition and water sorption of freeze-dried protein-carbohydrate systems (Oral Presentation). 39th UCC Annual Conference, Cork, Ireland, September 3-4, 2009.
2. Y Zhou, YH Roos. 2009. State transition and water sorption of freeze-dried protein-carbohydrate systems (Poster). EFFoST 2009, New Challenges in Food Preservation, Processing, Safety and Sustainability, Hungary, November 11-13, 2009.
3. Y Zhou, YH Roos. 2010. Water sorption and crystallization effects on stability of ascorbic acid in freeze-dried lactose and trehalose systems (Poster). Institute of Food Technologists (IFT) Annual Meeting in Chicago, IL., USA, July 17-20, 2010.

4. Y Zhou, YH Roos. 2011. Stability of ascorbic acid in freeze-dried lactose and trehalose as affected by water sorption and sugar crystallization (Oral Presentation). 40th UCC Annual Conference, Cork , Ireland, March 31-April 1, 2011.
5. Y Zhou, YH Roos. 2011. Stability of α -tocopherol in amorphous freeze-dried carbohydrate-protein systems (Oral Presentation). 11th International Congress on Engineering and Food, Athens, Greece, May 22-26, 2011.
6. Y Zhou, YH Roos. 2011. Water sorption and physical changes affect stability of α -tocopherol in freeze-dried carbohydrate-protein-oil systems (Poster). Institute of Food Technologists (IFT) Annual Meeting in New Orleans, LA., USA, June 11-14, 2011.
7. Y Zhou, YH Roos. 2012. Stabilization of sensitive components in frozen and dehydrated food systems: formulation, processing, and storage (Oral Presentation). 6th European Workshop on Food Engineering and Technology, Nestlé PTC Singen, Germany, March 7-8, 2012.
8. Y Zhou, YH Roos. 2012. Water sorption, glass transition and crystallization of sugars as affected by protein and oil in freeze-dried systems (Oral Presentation). 11th International Hydrocolloids Conference, Purdue University, USA, May 14-18, 2012.
9. Y Zhou, YH Roos. 2012. Water sorption and water plasticization-induced structural changes affect stability of α -tocopherol in spray-dried and freeze-dried emulsions (Oral Presentation). 7th International Conference on Water in Food, Helsinki, Finland, June 3-5, 2012.
10. Y Zhou, N Potes, YH Roos. 2012. Structural relaxation times and stability of hydrophilic vitamins in water-plasticized lactose solids (Oral Presentation). 5th International Symposium on Spray Dried Dairy Products, Saint-Malo, France, June 19-21, 2012.
11. Y Zhou, YH Roos. 2012. Spray-dried and freeze-dried encapsulant characteristics in stabilization of α -tocopherol (Poster). Institute of Food Technologists (IFT) Annual Meeting in Las Vegas, NV., USA, June 25-28, 2012.

APPENDIX
